CHAPTER 11

Interactions Between Adsorbate Particles

T.L. EINSTEIN

Department of Physics
University of Maryland
College Park, MD 20742-4111, USA

Handbook of Surface Science
Volume 1, edited by W.N. Unertl

Contents

11.1. Introduction 589
11.2. General features of lateral interaction energies 581
11.2.1. Fundamental ideas 581
11.2.2. Electronic indirect interactions in simple tight-binding model 586
11.2.2.1. Model Hamiltonian 586
11.2.2.2. Calculation of change in one-electron energies using Green's functions 588
11.2.2.3. Simpler illustration: pairs on a ring 592
11.2.3. Multisite interactions 597
11.2.3.1. Three-adatom (trio) interactions 597
11.2.3.2. Complete overlayers 598
11.2.4. Coulombic effects: self-consistency and correlation, and other improvements 599
11.2.5. Lattice indirect interactions: phonons and elastic effects 601
11.2.6. Asymptotic form of the indirect interaction between atoms and between steps 607
11.3. Attempts to model real systems 611
11.3.1. Tight-binding, jellium, and asymptotic-ansatz 611
11.3.2. Embedded cluster model 613
11.3.3. Effective medium theory and embedded atom method — semiempiricism 615
11.3.4. Empirical schemes 619
11.3.5. Field-ion microscopy, modern tight-binding, and more on semiempiricism 620
11.3.6. Scattered-wave theory 628
11.4. Further implications of lateral interactions 631
11.4.1. Ordered overlayers and their phase Boundaries 631
11.4.2. Local correlations and effects on chemical potential 632
11.4.3. Surface states on vicinal and reconstructed fcc(110) surfaces 635
11.5. Discussion and conclusions 638
References 642

11.1. Introduction

Progress in computing the interactions between small numbers, even pairs, of chemisorbed atoms has been remarkably slow because of the very low symmetry of the problem. In contrast, the energetics of monolayers of adatoms, which have the full two-dimensional symmetry of the substrate, can now be characterized with impressive precision. However, even treatment of partially completed adlayers with (2×1) or $c(2\times2)$ symmetry doubles the size of the surface primitive cell, but quadruples the size of secular matrices, raising computer time requirements by a factor of order 4^3. At the other end of the scale, a single adatom (in a symmetric site) will at least have the point-group symmetry of the substrate. Associated with these symmetries are conserved quantities ("good quantum numbers") which make calculations simpler. As a result, a variety of elaborate many-body techniques have been applied successfully to these systems. For two adatoms on a surface, there is little or no symmetry, typically just a two-fold rotation or mirror plane (leading often to splittings of levels). Few systems have been treated in a satisfactory way. Sophisticated computations attempting to assess these interactions tend to resort to studies of ordered overlayers (Tománek et al., 1986). Desjonquères and Spanjaard (1993) signaled the difficulty of the problem by placing it as the final topic in their recent text. Reviews stressing various aspects of the problem have been presented by Einstein (1979a, 1991), Muscat (1987), March (1987, 1990), Braun and Medvedev (1989), Feibelman (1989a), and Nørskov (1993).

This chapter will explore the many mechanisms by which chemisorbed atoms interact with each other. To set the stage early, it is useful conceptually to distinguish between direct and indirect interactions. Direct interactions would occur even if there were no substrate; they are, thus, sometimes called "through-space". Examples include van der Waals, dipolar, and electronic hopping (between the adatoms). The substrate, however, will generally provide at least some degree of perturbation. The alternative is indirect interactions, in which to lowest order there would be no interaction without the substrate. The coupling can be by electronic states (usually predominant), elastic effects, or vibrational coupling (usually insignificant). Since the coupling to the substrate is crucial, these are sometimes called "through bond". Special emphasis will be given to the indirect electronic ("pair") interaction between two light gas or transition series atoms on a (transition) metal. Moreover, we thoroughly explore a simple model of these interactions. The motivation is not so much to explain specific data but rather to give a theoretical framework in which to understand the relative magnitudes and qualitative behavior of the interactions. Without this sort of picture, it is difficult to make sense of the results that emerge from more realistic attempts to describe the adsorption systems.

We also present a thorough summary of the methods that have been applied to make progress in understanding this general problem.

As we fix ideas, it may be helpful to describe our problem in oversimplified terms by speaking of three characteristic energies: (1) E_{as} is the *binding energy* of an isolated atom to the most attractive site on the surface. Typically this is a high-symmetry site; e.g., on a square lattice, such sites (cf. Fig. 1.12) can be called A (atop, or linear, or on-top, the latter two inconsistent with the abbreviation), B (bridge, between two substrate atoms), and C (centered, or hollow, above the middle of a square). Identical terminology applies to substrates with triangular symmetry. E_d denotes the diffusion barrier, due to variations in the adatom–substrate potential, between adjacent most-favored sites. Usually this is a saddle point in a potential energy surface; e.g., if the C site is most attractive, one might expect $E_d = E_C - E_B$, although substrate relaxation can sometimes lower this barrier significantly. The corrugation of the substrate potential provides an upper bound for E_d. Finally, E_{aa} is the magnitude of the characteristic energy of interaction between nearby atoms. In physisorption, E_{aa} is comparable to E_{as}, both being much greater than E_d. (For dense overlayers, the actual diffusion barrier increases significantly due to adatom–adatom effects.) In contrast, in chemisorption $E_{as} > E_d >> E_{aa}$. Thus, in this ideal scenario, adatoms all sit in the most favorable site; their lateral interactions are relatively small. In this case it is fruitful to couch the discussion in terms of a classical lattice gas picture. (Cf. Chapter 13 by Roelofs.)

In setting the stage for what we will find regarding electronic lateral interactions, it may be helpful to divide (somewhat artificially) the physics into a few regimes, depending on the separation between adsorbates. (1) In the near regime, the adatoms may be close enough to have non-negligible direct interactions. If not, they typically still "share" one or more substrate nearest neighbors, so that the bonding of one adatom to this substrate atom is strongly influenced by the presence of the second adatom. This regime is the most important for applications: in chemistry it determines the details of dissociative adsorption; in surface transport it enters problems of surface diffusion mechanisms. The strong impact of one adatom on the other may alter their binding sites, weaken bonding to the substrate, etc., as emphasized in a review by Feibelman (1989a). In short, in this regime E_{aa} may be comparable to E_{as}. (2) In the intermediate regime, these effects fade and the lattice-gas approximation improves. The individual-adatom adsorption process is largely immune to the interactions. Most of the interesting physics can be isolated in the question of how the disturbance produced by a point defect at some position propagates to another. All the occupied band states in the substrate are involved in a complicated way. This regime is important in describing the formation of ordered fractional monolayers of adsorbates and in characterizing the chemical potential and the correlation functions of these adsorbates, even at higher temperatures at which there is little order. Thus, these interactions play a role in understanding thermal desorption spectra, vibrational line shifts, etc. (3) The asymptotic regime is reached when the adatoms are several spacings apart. The interaction is dominated by the substrate Fermi surface. Analytic expressions, albeit complicated, can be derived. Until recently, there was little evidence of experimental impact of

this regime, but there may be implications for the interactions between steps on metal surfaces. We caution that as with most simple pictures of complicated phenomena, it is easy to point out ways in which the broad-brush rendition is oversimplified. For example, in the case of weak, non-directional bonding, the adatoms may slip out of high-symmetry binding sites even when a couple spacings apart, as suggested by Persson (1991) for some cases of CO adsorption. Moreover, for weak bonding, the Fermi-surface electrons may dominate at close spacings, inviting simple descriptions in terms of frontier orbitals (Hoffmann 1963, 1988).

A major motivation for studies of pair interactions is to understand the origin of the wide variety of ordered overlayers at fractional coverages on metal surfaces (see Chapter 13). These have been tabulated by Ohtani et al. (1987), Van Hove et al. (1989), Watson (1987, 1990, 1992), and Watson et al. (1993). Consider a $c(2\times2)$, i.e. a checkerboard pattern on a square lattice (Chapter 1, Fig. 1.1). This pattern could arise simply because of a strong nearest-neighbor repulsion: $E_1 > 0$ for an overlayer with about half the sites occupied. If additionally there is a next-nearest-neighbor attraction, one finds islands of adatoms with $c(2\times2)$ symmetry at low temperatures and coverages. Sometimes these lie at temperatures so low that the equilibrium local configuration is not attained during the time of an experiment, at most several hours. But when islands are present, they provide strong evidence of an attraction. There are many more complicated phases. The explanation of most of their ground-state energies in terms of pair interactions is fairly obvious (cf. Suzanne and Gay, Chapter 10, and Roelofs, Chapter 13), but for troublesome cases, exhaustive tabulations have been published by Kaburagi and Kanamori (1974, 1978) and Kaburagi (1978). By attraction or repulsion here, we mean that the lattice site is favorable or unfavorable. There is no implication about the direction of a force acting on an adatom sitting in a lattice site; in the lattice gas picture, this force is assumed to vanish. In the near region, this assumption may often be questionable, but in the intermediate region it should be reasonable.

Some experimental data on these systems appear in Chapters 10, 12 and 13 to which we shall refer. We will dwell mostly on theory. Progress in the field has come in the form of study of self-consistency and correlation effects (which seem to be less important than might be expected) and of multi-parameter-model attempts to describe real systems. Next we shall show in a single simple model how pair, three-adatom, etc., interactions combine to produce ordered overlayers. We will briefly consider changes in density of states (DOS) caused by two-adatom interactions from a similar viewpoint, and also show the more dramatic effects that arise when these combine to produce an ordered overlayer. In closing, we shall speculate on areas ripe for development.

11.2. General features of lateral interaction energies

11.2.1. Fundamental ideas

If chemisorbed atoms are sufficiently close to overlap each other, there will be a strong direct interaction. This interaction is essentially a chemical bond, compara-

ble in strength to the chemisorption bond. (There is interesting physics in the degree to which these bonds are not simply the equivalent of bulk bonds. We shall explore these effects further in later sections.) For larger lateral interadatom distance R, the interaction falls off exponentially along with the overlap so that for R more than a few Å, it is negligible. Most of the physics of this problem comes from the two adatoms and their substrate nearest neighbors; hence a cluster calculation can be appropriate. These interactions are important for supersaturated or even monolayer-covered surfaces. They also arise in the problem of dissociation and reassociation of adsorbing molecules (e.g., the question of whether there is an activation barrier) which has been studied both schematically and in great detail.

If the chemisorption bond involves charge transfer, electric dipole moments μ will develop. Kohn and Lau (1976) showed that the non-oscillatory part of the dipole–dipole interaction energy on metals behaves as

$$E_{\text{dip-dip}} \sim 2\mu_a\mu_b/4\pi\varepsilon_o R^3 \tag{11.1}$$

for large R. The novel aspect of this expression is the factor of 2, for which they give the following qualitative explanation: For either adatom, say a, μ_a is the product of the charge transfer q_a to the adatom and the distance z_a between the adatom and the surface/image plane, at which the induced charge of $-q_a$ lies. However, the potential experienced by a second adatom is determined by the first adatom and its image at $-z_a$, and so is $2\mu_a z_b(4\pi\varepsilon_o)^{-1}R^{-3}$. Hence, the work in bringing the second charge from $z = +\infty$ to $z = z_b$, and so $E_{\text{dip-dip}}$ contains the novel factor of 2. Inserting numbers, we find this interaction energy to be 1.25 eV times the two dipole moments in units of debyes divided by R^3 in Å^3.

Nørskov (1993) reviews the direct electrostatic interaction in some detail. The effect is generally larger for electropositive than electronegative adsorbates because the latter tend to bond closer to the substrate; consequently, they are better screened and so have a smaller dipole moment. For alkali adatoms, dipolar effects dominate the interactions which determine the 2D phase diagram (Bauer, 1983; Müller et al., 1989). Pre-adsorbed alkali–metal atoms increase both the binding energy and the dissociation rate of light gas dimers like CO, NO, N_2, or O_2 on metals, while preadsorbed electronegative atoms do the opposite: Typically adsorption of these dimers involves some charge transfer *to* them. (Back donation to the anti-bonding molecular orbital exceeds donation from the bonding orbital.) In the simplest approximation, the resulting energy is the product of the admolecule-induced dipole moment normal to the surface and the gradient of the electrostatic potential due to the preadsorbed atoms (or the extra charge times the potential itself). To support this picture, Nørskov et al. (1984/5) explored the form of this potential, for several different preadsorbed atoms on jellium, as a function of the height of the dimer above the surface. For the particular case of N_2 on Fe(111) with pre-adsorbed K, Nørskov (1993) finds an interaction of 0.08 eV, which can be used to account for most of the measured shift in adsorption energy due to predosing. The second-order correction, proportional to the square of the potential, is always attractive. Thus, for cases in which the charge transfer is *from* the dimer, he notes

that the long-range interaction with a pre-adsorbed alkali can be repulsive while the short-range interaction is attractive.

In addition to producing static repulsions, dipole–dipole interactions can raise the vibrational frequency of adsorbed molecules. For example, Scheffler (1979), using just dipole–dipole coupling, accounts for the coverage dependence of the shift of the C–O stretch frequency of CO on Pd(100) and Pt(111) measured by IR absorption reflection spectroscopy. In the process, he derives a coverage-dependent (as well as frequency dependent) effective polarizability which depends significantly on the distance of the dipole from the reference (image) plane of the metal (assumed to be jellium). In focusing on the cases of CO on Cu(100) and Ru(0001), Persson and Ryberg (1981) advanced the treatment of these questions by treating the adsorbate polarization as a single entity rather than trying to split it into admolecule and an image; they, furthermore, used the coherent potential approximation (CPA) (Soven, 1966) to consider interactions for a dense but not ordered overlayer. They find that the dipole–dipole interaction is enough to account for the coverage-dependent frequency shift for the Ru substrate, but that on Cu there is a counteracting chemical shift of nearly the same magnitude. Nørskov (1993) discusses the shifts of dimer vibrational frequencies due to interactions between pre-adsorbed (non-neutral) atoms and the dimer.

The van der Waals interaction always produces a weak attraction between two adatoms and is the dominant contribution in the case of physisorption. The leading term is the dipole–dipole contribution, which goes as $-C/R^6$; C in turn is proportional to the square of the polarizability. According to Hirschfelder et al. (1954), C is roughly 30 eV-Å^6 for Ar, N_2, and O_2, and five times as great for Xe. For physisorbed gases, this mechanism dominates the interaction, and hence the details of the interatomic potential have been studied extensively. To fit gas-phase data, one must go beyond a simple R^{-12} Lennard–Jones repulsion (to some exponential description) to avoid overestimating C by nearly a factor of two. Two higher-order gas-phase effects are non-negligible: (1) The R^{-8} dipole–quadrupole force which increases the depth of the well-minimum by roughly 10% and (2) the repulsive (in all important cases) R^{-9} triple–dipole (Axilrod-Teller (1943)–Muto (1943)) interaction, the magnitude of which is at most 3% (for Ar) to 5% (for Xe) of a pair interaction if all distances are set at their equilibrium values. While this effect is of little concern here, there have been interesting applications (Klein et al., 1986).

A variety of calculations of rare gas adsorption onto jellium (Sinanoglu and Pitzer, 1960), continuous dielectrics (McLachlan, 1964), Xe crystals (MacRury and Linder, 1971), and graphite (Freeman, 1975) all show that physisorption reduces the gas-phase pair attraction by roughly 20%. As an example of the state of the art in this refined subject, Barker and Rettner (1992) produce an accurate "empirical" (actually more semiempirical, in the language we will use later) potential for Pt(111)–Xe as a "benchmark." For the lateral interactions, they include, in addition to the van der Waals potential, the "nonadditive" McLachlan modification, the interaction of adsorption-induced and image dipoles, and the triple–dipole term, citing as reference Bruch's (1983) clear and comprehensive discussion of the significant contributions. (This classic review of lateral interactions in physisorption,

as well as of the single-atom holding potential, provides an account of the general features of this problem that is evidently still timely a decade later. March (1987, 1990) presents more recent reviews. Vidali et al. (1991) have produced a useful compilation of potentials for physisorption.) The substrate-mediated dispersion energy is the largest contribution to the lateral interaction at the intermediate separations of ordered overlayers, accounting for slightly over half the (repulsive) corrections to the gas-phase interaction for two sample Xe overlayers (Bruch, 1983). The effect of the substrate on the interadatom interaction was first tackled using perturbation theory by Sinanoglu and Pitzer (1960). McLachlan (1964) calculates in second-order perturbation theory the interactions of adatom dipoles and their images in the substrate, including a frequency-dependent response for the substrate. Explicit expressions for the substrate-mediated dispersion energy and tables of the attendant coefficients are given by Bruch's (1983) review; a key issue is determining the distance of the adatoms from the image plane. Freeman (1975) approaches the problem using the Gordon-Kim (1972) version of density functional theory (for Ar adatoms) and obtains fair agreement with the preceding formalism; similarly, Vidali and Cole (1980) apply both methods to He on graphite.

The next largest contribution to the substrate-related interaction, perhaps half the size of the preceding, is the interaction of adsorption-induced dipoles. The role of the surface was noted earlier in Eq. (11.1). Bruch (1983) reviews the many contributors to this subject. He and Phillips (1980) showed how to compute these effects for an overlayer lattice. Other effects include triple–dipole (Axilrod-Teller (1943)–Muto (1943)) interactions within the overlayer and changes in zero-point energy. In this framework, lateral interactions can be computed to an accuracy that makes those working on chemisorption truly envious. Nonetheless, there are some differences between calculations on particular systems, e.g. the above-mentioned benchmark (Müller, 1990; Gottlieb and Bruch, 1991; Barker and Rettner, 1992).

To apply the van der Waals perspective to chemisorption, we can invoke the surface molecule picture to posit that the interaction between, say, two chemisorbed O atoms (coupled to their substrate neighbors) is similar to that between two O_2 molecules (although now the molecules are oriented), i.e. roughly -25 eV-Å^6/(R[Å])^6. At second and third neighbor separations on Ni(100), for instance, this yields an interaction of -13 meV and -2 meV, respectively, which is usually negligible compared to the electronic indirect interaction. For heavy adsorbates (e.g., W or Re) these numbers could possibly be several times greater; no firm data exists. A curious application, to Ni(100)–O, of van der Waals ideas by Gallagher and Haydock (1979) suggested that by virtue of large overlap with the attractive Ni potential of the substrate, the O 2p orbitals become larger and far more polarizable, dramatically increasing the associated interaction. There has been little follow-up work on this viewpoint.

The first proposal that adatoms might interact indirectly was made by Koutecký (1958). The essence of this interaction is seen in Fig. 11.1, taken from the pioneering work by Grimley (1967) on this problem, which even now begins most discussions. Consider two atoms, each with an atomic potential producing some (relatively high-lying) bound state. In free space (and at moderate separation), each

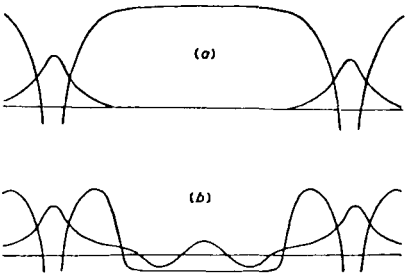

Fig. 11.1. Classic schematic of the indirect interaction between pairs of adatoms. (a) Potential and wave functions for two atoms in vacuum separated so far that there is no overlap and so no direct interaction. (b) The same atoms, now chemisorbed on a simple metal surface. From Grimley (1967a), with permission.

of the bound-state wavefunctions will remain confined near its atomic site; the vacuum barrier is insurmountable. If, alternatively, they are adsorbed onto (or absorbed into) a metal, both atomic wavefunctions can tunnel through the narrow potential barrier to the metal and couple with propagating metal wavefunctions. Figure 11.1b shows how both atomic wavefunctions might couple to one such background eigenstate. If the coupling places the two atomic wavefunctions in (out of) phase, the interaction is attractive (repulsive), lowering (raising) the energy of the participants. From the oscillatory nature of the intermediate wavefunction, the electronic indirect interaction should be oscillatory in sign as a function of interadatom distance. It should be (two-dimensionally) isotropic if and only if the (surface of the) metal background is. Such isotropy is expected only for substrates which can be well approximated by free-electron or jellium models. Furthermore, the two adatomic orbitals can couple through not just one, but any of the occupied states (including surface states). As adatom separation increases, fewer substrate wavefunctions will match well with the atomic orbitals, causing a rapid decay in magnitude of the interaction energy.

As discussed at the outset, our discussion assumes that $E_d >> E_{aa}$, which should be a good approximation for strong chemisorption at low to moderate coverage. Under these circumstances, the most favorable adsorption sites will be filled or vacant, and when nearby sites are filled, the associated interaction energy will modify the total energy of the system. In this lattice gas picture, the Hamiltonian of the adatoms takes the form:

$$H = E_1 \sum_{\langle ij \rangle_1} n_i n_j + E_2 \sum_{\langle ij \rangle_2} n_i n_j + \ldots$$
$$+ \sum_{T} E_T \sum_{\langle ijk \rangle_T} n_i n_j n_k + \sum_{Q} E_Q \sum_{\langle ijkl \rangle_Q} n_i n_j n_k n_l + \ldots \tag{11.2}$$

Each site of the net of most-favored substrate sites (labeled i) can be occupied ($n_i = 1$) or vacant ($n_i = 0$). Here the pair interaction energies are denoted E_m for mth

neighbors; E_T is the "trio" (three-adatom, non-pairwise) interaction energy, with the index running over the possible trimer configurations; E_Q is the "quarto" energy; and so forth. For this formulation to be useful, the pair energies should fall off relatively rapidly in magnitude with increasing m, so that only a few need be considered. Furthermore, the multisite terms should be small; at worst, only a small number of the most closely spaced multiadatom terms should contribute. We shall see that the pair interactions do decay rapidly. The multisite terms are smaller but not always negligible. Moreover, there may be several different configurations with comparable magnitude. Nonetheless, cancellations typically occur such that the energies of ordered submonolayer overlayers are often adequately described by the pair energy of the closest pair(s) found in the overlayer.

Before delving into specific simple models, it is worth stating the underlying philosophy motivating them.

11.2.2. Electronic indirect interactions in simple tight-binding model

To gauge roughly the relative magnitudes and general behavior of these interactions, it is convenient and customary to study a simple model, in this case a tight-binding model in which the substrate is a single-band, simple-cubic solid. (See LaFemina, Chapter 4, for a discussion of tight-binding models.) This model was adopted two decades ago (Einstein and Schrieffer, 1973) (hereafter ES) to embody the idea that the d-bands of the substrate were primarily responsible for the interactions and, unlike jellium, allowed one to consider the dependence of the interaction on the type of adsorption site in a simple way.

11.2.2.1. Model Hamiltonian

The model, as well as many subsequent discussions of interactions between adatoms, is couched in terms of an Anderson (1961) (magnetic) model in which the adatoms are represented as dilute impurities at sites $\boldsymbol{r}$ (= a,b for pairs) in an unperturbed host:

$$H = H^0_{\text{metal}} + \sum_r (H^0_r + H'_r) \tag{11.3}$$

The first term in the parentheses represents the atomic factors of adatom r, while the second is this atom's coupling to the metal. To include a direct interaction, one would add terms of the form H'_{ab} coupling atoms a and b. Until recently, most work on the problem has amounted to taking progressively more realistic expressions for various of these terms and solving the resulting system to varying levels of approximation. To simplify notation, we assume that the adatoms are identical. Over the last decade the coadsorption problem has attracted some interest; it is straightforward to extend the formalism. Some of the simplicity of the above ansatz comes from the use of an atomic orbital picture. While this formulation makes it easy to do initial calculations, it neglects such effects as orbital deformation and local distortion, which may often be important.

The adatom part of the Hamiltonian is

$$H_a^0 = \varepsilon_a^0 \sum_\sigma n_{a\sigma} + U n_{a\uparrow} n_{a\downarrow} \tag{11.4}$$

and similarly for H_b^0. This expression can be generalized to include degenerate orbitals, multiple levels, etc. As a first approximation, one might set ε_a^0 at the ionization level $-I$ of the adatom and take as U the difference between $-I$ and the affinity level. For greater accuracy, ε_a^0 should be raised and U reduced by correlation effects (screening and image charges). In a (restricted) Hartree–Fock approach, one neglects U entirely and replaces ε_a^0 by $\varepsilon_a = \varepsilon_a^0 + U\langle n_{a\sigma}\rangle$ where $\langle n_{a\sigma}$ is the mean occupation of the adatom for either spin direction. For neutral chemisorption, $\langle n_{a\sigma}\rangle$ is 1/2, suggesting ε_a be the (negative) average of the ionization and affinity energies, as in many chemical molecular orbital calculations (where this is called the Mulliken (1934) electronegativity) (cf., e.g., Pople and Beveridge, 1970) Using the idea of chemical transferability, Pandey (1976) adjusted the adatom and coupling parameters so that cluster computations of small molecules fit the levels found in photoemission experiments; presumably the same parameters carry over to the chemisorption system. Brenig and Schönhammer (1974), Hertz and Handler (1977), and Bell and Madhukar (1976) went beyond Hartree–Fock in the case of single atom adsorption. The first group also showed in the pair problem that correlation effects are relatively unimportant, compared to the single atom case, as we shall discuss below. On the other hand, using self-consistent Hartree–Fock and resorting to mean-field theory, Gavrilenko et al. (1989) explored the parametric conditions for magnetic ordering of the adatoms. Davydov (1978) considers a similar question, including direct interactions for a chain of adatoms.

The simplest approximation for the substrate assumes a single band of one-electron states with energy $\varepsilon_{\mathbf{k}}$. (A band index would also be needed if more than a single band were considered.) Many-body effects could also be included by putting a diagonal Coulomb term like U on each substrate site. Since only the component of crystal momentum parallel to the surface is conserved for a slab or semi-infinite crystal, $\boldsymbol{k}$ merely labels the states in some suggestive fashion. It is usually convenient to work in a mixed representation of $\boldsymbol{k}_\parallel$ and a layer index.

In general there can be a different coupling between each $\boldsymbol{k}$ state and the adatom. For most purposes, it is adequate to consider, in the case of bonding at an atop site, a single coupling constant V between adatom a (or b) and its nearest neighbor on the substrate:

$$H_{aS} = -V c_{a\sigma}^+ c_{o\sigma} + h{\cdot}c \tag{11.5}$$

where c^+ and c are creation and annihilation operators, respectively, for electrons in the state indicated by the substrate. For bonding in a bridge or centered site, $c_{o\sigma}$ is replaced by a symmetric normalized combination of c-operators for the number of substrate neighbors of the adatom. In principle this coupling should also consider an overlap term between atoms and metal. This question has been discussed at length by, among others, Schönhammer et al. (1975), Grimley (1974), and Einstein (1973). The usual approach is to "renormalize" previously stipulated natural orbitals (and resulting energies) with Löwdin (1950) or Gram–Schmidt (Birkhoff and MacLane, 1965) schemes.

11.2.2.2. Calculation of change in one-electron energies using Green's functions
Our goal is to find interaction energies between chemisorbed atoms, which in a one-electron framework can be expressed in terms of the associated change in density of states $\Delta\rho$:

$$\Delta W = 2\int_{-\infty}^{\varepsilon_F} (\varepsilon - \varepsilon_F)\,\Delta\rho(\varepsilon)\,d\varepsilon \tag{11.6}$$

The factor of 2 comes from spin degeneracy, and the use of $\varepsilon - \varepsilon_F$ rather than just ε indicates that the number of electrons rather than the chemical potential is being fixed (Grimley, 1967; Newns, 1969; ES). (The contribution due to the integral over $\varepsilon_F\Delta\rho(\varepsilon)$ is the result of an infinitesimal shift in the Fermi energy.)

In the calculation presented below, the essential idea is that the interaction between adsorbates can be obtained by finding the underlying shifts in the one-electron energies of the system. It is convenient to do so in terms of one-electron Green's functions. We present enough detail below to show that this procedure is not so daunting as novices might suspect. Nonetheless, we follow this subsection with an explicit simple illustration using a ring as the "substrate" and analyzing the results in terms of level shifts to make contact with those readers more comfortable thinking in terms of quantum chemical models.

To obtain the change in density of states $\Delta\rho$ needed so that the integral can be evaluated, we adopt a method used earlier in the theory of dilute alloys by Lifshitz (1964). Suppose the unperturbed ($H' \equiv H_{am} = 0$) and perturbed Hamiltonians, H^0 and $H \equiv H^0 + H'$, have eigenvalues ε_j and E_j, respectively. Then[1]

$$\Delta\rho = \sum_j \left[\delta(\varepsilon - E_j) - \delta(\varepsilon - \varepsilon_j)\right] \tag{11.7}$$

But this can be rewritten as

$$\begin{aligned}
\Delta\rho(\varepsilon) &= -\frac{1}{\pi}\,\mathrm{Im}\sum_j \left(\frac{1}{\varepsilon - E_j + i\delta} - \frac{1}{\varepsilon - \varepsilon_j + i\delta}\right) \\
&= -\frac{1}{\pi}\,\mathrm{Im}\sum_j \frac{\partial}{\partial\varepsilon}\Big(\ln(\varepsilon - H + i\delta) - \ln(\varepsilon - H_0 + i\delta)\Big) \qquad (11.8) \\
&= -\frac{1}{\pi}\,\mathrm{Im}\,\frac{\partial}{\partial\varepsilon}\,Ln\,\det\left(\frac{1}{\varepsilon - H_0 + i\delta}\right)(\varepsilon - H + i\delta) \\
&= -\frac{1}{\pi}\,\mathrm{Im}\,\frac{\partial}{\partial\varepsilon}\ln\det(1 - G^0\hat{V})
\end{aligned}$$

---

1 Remember that the units of a delta function are the inverse of its argument.

where G^0 is the unperturbed *retarded* Green's function $(\varepsilon - H_0 + i\delta)^{-1}$ and $\hat{V} \equiv H_{aS}$ was given in Eq. (11.5). (Since we choose here to follow convention by using retarded functions, the signs of all *imaginary* quantities will be the opposite of those appearing in ES and subsequent papers in that series, which used advanced Green's functions, with infinitesimals of the opposite sign.) In scattering theory $\det(1 - G^0\hat{V})$ is familiar as the Fredholm determinant (of the 0th partial wave) (Gottfried, 1966). Furthermore,

$$-\mathrm{Im}\ \ln \det(1 - G^0\hat{V}) = \eta(\varepsilon) \tag{11.9}$$

where $\eta(\varepsilon)$ is the s-wave phase shift. (This identification is perhaps clarified by the observation that "Im ln" is an arctangent, yielding an angle that amounts to a scattering phase shift.) This approach makes optimal use of the higher symmetry of the unperturbed system and the locality of the perturbation associated with adsorption. It is generalized in the scattering theory approach (Feibelman, 1989a). In terms of η, one writes the interaction energy simply as

$$\Delta W = -(2/\pi)\int_{-\infty}^{\varepsilon_F} \eta(\varepsilon)\, d\varepsilon \tag{11.10}$$

The Fredholm determinant contains a dense set of alternating poles and zeros, which turns into a branch cut in the continuum limit. Dreyssé and Riedinger (1983) pointed out that one can circumvent numerical difficulties with this sort of integral by adopting the contour-integration approach (in the $T = 0$ limit) developed for temperature-dependent fermion Green's function problems. The result is basically an integration of the real part of the analytic continuation of $\ln \det(1 - G^0\hat{V})$ from $\varepsilon_F + i0^+$ to $\varepsilon_F + i\infty$. This integration can be cast into a finite interval by making a substitution for the imaginary part of the energy integration variable (Liu and Davison, 1988).

To evaluate the phase shift for the two-adatom problem, we arrange the matrix so that the adatom sites (a and b) and the substrate nearest neighbors to which they couple (o and n) come first (o, a, n, b) and then all other substrate sites. The matrix $(1 - G^0 V)$ then differs from a unit matrix only in the upper left hand 4×4 block:

$$\begin{bmatrix} 1 & -G^X_{oo}V_{oa} & 0 & -G^X_{on}V_{nb} \\ -G^X_{aa}V_{oa} & 1 & 0 & 0 \\ 0 & -G^X_{no}V_{oa} & 1 & -G^X_{nn}V_{nb} \\ 0 & 0 & -G^X_{bb}V_{bn} & 1 \end{bmatrix} \tag{11.11}$$

The superscript X indicates that the substrate Green's functions can be easily generalized, for adsorption in B or C rather than A sites, to represent a (normalized) hybrid (cf. remarks after Eq. (11.5)) of substrate orbitals (Einstein and Schrieffer,

1973).[1] The major result coming from the possibility of coupling to combinations of orbitals is that G^B or G^C is generally very different from G^A, so that the pair interaction will depend very strongly on the adsorption site. This feature arises naturally in LCAO models, in contrast to the other simple starting point, jellium models (see below). (Braun (1981), however, argues that the effective ε_a becomes adsorption-site dependent, possibly mitigating the variation with site symmetry.) The determinant of this matrix can be written as

$$\det(1 - G^o\hat{V}) = (1 - G_{aa}G^X_{oo}|V_{oa}|^2)\,(1 - G_{bb}\,G^X_{nn}|V_{nb}|^2) - G_{aa}G^X_{on}G_{bb}G^X_{no}|V_{oa}|^2V_{nb}|^2 \tag{11.12}$$

It is noteworthy in this expression that the parentheses enclose the contribution to $\det(1 - G^0\hat{V})$ from the adsorption of an isolated adatom a at o (or b at n). Factoring out these terms, and assuming adatoms a and b are identical, as are sites o and n, we find

$$\det\,(1 - G^0\,\hat{V})_{\text{pair}} = \frac{\det\,(1 - G^0\,\hat{V})}{\left[\det\,(1 - G^0\,\hat{V})_{\text{single}}\right]^2} = 1 - (\bar{G}^X_{aa})^2\,(G^X_{on})^2\,V^4 \tag{11.13}$$

where $\bar{G}^X_{aa}$ is a Green's function for a single adatom renormalized to account for its adsorption:

$$\bar{G}^X_{aa} \equiv (1 - G_{aa}\,G^X_{oo}|V_{oa}|^2)^{-1}\,G_{aa} = [\varepsilon - \varepsilon_a - V^2\,G^X_{oo}(\varepsilon)]^{-1} \tag{11.14}$$

Because of the logarithm, the phase shift (and hence the changes in DOS and energy) characterizing the "pair" interaction of the adatoms can be obtained directly from the phase shift associated with $(1 - V^4(G^X_{aa})^2(G^X_{on})^2)$ rather than from explicitly subtracting twice the single-adatom-phase shift from the two-adatom shift. For any number of adatoms, the single adatom adsorption part factors out of the matrix (ES; Grimley and Walker, 1969). On the other hand, as shown below in Eq. (11.20), for more than two adatoms there is no way to factor out the pair effects from the higher order ones. (The feature that the single-adatom part factors out is a pleasant convenience, but with modern computational power it does not produce a significant improvement in numerical results, except perhaps in the asymptotic regime.)

---

[1] Explicitly, $G^A_{on} = \sum_j \dfrac{\cos(\boldsymbol{k}^j \cdot \boldsymbol{R}_n)}{\varepsilon - \varepsilon_j + i\delta}$, where $\boldsymbol{R}_n$ is the vector in the surface plane from site o to site n, ε_j denotes the eigenvalues of H_o, and the notation on the wavevector reflects the fact that only crystal momentum in the surface plane is a good quantum number. If a single adatom sits in a bridge site between surface atoms 0 and 1, then $G^B_{oo} = G^A_{oo} + G^A_{o1}$. If a second adatom sits between n and $n+1$ (assuming all four sites colinear for simplicity, then $G^B_{on} = G^A_{on} + (1/2)(G^A_{o,n+1} + G^A_{o,n-1})$. To complete the description, one must make some statement about how the adatom–substrate hopping depends on the adsorption site, which will involve some at-least-implicit assumption about dependence on bond angles, bond lengths, local relaxations, etc. The parameter V that appears in the formalism corresponds to $\sqrt{z}$ times the hopping parameter between the adatom and *one* of the z members of the hybrid to which it couples.

In the LCAO framework, the formula for the pair interaction energy E_n between the adatoms adsorbed on sites o and n (which we identify as nth nearest neighbor sites on the surface) is, from Eqs. (11.9), (11.10), and (11.13),

$$E_n = \frac{2}{\pi} \int_{-\infty}^{\varepsilon_F} \mathrm{Im} \ln \left[1 - (\bar{G}^X_{aa}(\varepsilon))^2 \, (G^X_{on}(\varepsilon))^2 \, V^4 \right] \mathrm{d}\varepsilon \tag{11.15}$$

To gain some understanding of this interaction, we first expand the logarithm and consider the lowest order term (Kim and Nagaoka, 1963), which becomes a good approximation for weak coupling (small V) or large separation (small G_{on}):

$$E_n = -\frac{2}{\pi} \mathrm{Im} \int_{-\infty}^{\varepsilon_F} V^4 \, (\bar{G}^X_{aa}(\varepsilon))^2 \, (G^X_{on}(\varepsilon))^2 \, \mathrm{d}\varepsilon \tag{11.16}$$

If $\bar{G}$ is neglected (which is generally a poor approximation at small separations), expression (11.16) is just the RKKY interaction energy (Ruderman and Kittel, 1954; Yosida, 1957), in which two localized spins (here localized defects) interact via coupling to a *bulk* conduction electron sea. If this sea is viewed as a free-electron gas, the propagator G_{on} reduces to a continuum $G(|\boldsymbol{R}|;\varepsilon)$, where $\boldsymbol{R}$ goes from one bulk spin/defect to the other. This bulk interaction is proportional to $(x \cos x - \sin x)\, x^{-4}$, where $x = 2k_F|\boldsymbol{R}|$. It is thus oscillatory in R and decays asymptotically as R^{-3}, characteristic of Fermi surface domination. We shall discuss the decay on surfaces in the section on asymptotics.

A physical interpretation of Eq. (11.15) is that an electron in an occupied state starts at one adatom, hops back and forth to the substrate many times, then propagates to the second adatom, hops back and forth again for a while, then propagates back to the starting site. Alternatively, one can describe the process as a particle and a hole propagating from one adsorption site to the other (Zangwill, 1988). While Eq. (11.16) suggests that the interaction is proportional to V^4, such behavior only obtains in the limit of weak coupling. For stronger coupling, the V-dependence in $\bar{G}$ eventually cancels the leading V^4. This strong-adsorption case is the limit of the "surface molecule", in which the adatom and its substrate partner form a dimer which rebonds perturbatively (with the bulk coupling strength) to the substrate. The interaction between the adatoms then comes from the interference between the two dimers in the rebonding process, which does not depend on V.

Grimley (Grimley, 1967; Grimley and Walker, 1969) was the first to apply the Anderson model to chemisorption, using as a substrate a semi-infinite single-band crystal with a phenomenological surface reactivity. This adjustment highlights a problem with free-electron gas substrates, namely how to allow coupling with adatoms. If the adatom sits beyond an infinite barrier, e.g., there will be no coupling whatsoever. To avoid this problem, to put in site specificity in a natural way, and to reflect the belief that the d-bands were primarily responsible for the lateral interactions, ES modified Grimley's model by using as the substrate the (100) face

of a single-band simple cubic crystal ("simple cubium") in the nearest-neighbor tight-binding approximation. Eq. (11.15) was then evaluated numerically.

Table 11.1 capsulizes the results of ES. The energies are measured in units of one-sixth of the bandwidth (i.e., twice the hopping parameter). For the typical transition metal d-band being modeled, this unit is of order 1 to 2 eV. The Fermi energy and adatom level are measured relative to the center of the band. As the table illustrates, the pair interaction is highly anisotropic, oscillatory in sign, and rapidly decaying. At close separations the decay is precipitous, more exponential than inverse power like, dropping roughly by 1/5 with each lattice spacing, while asymptotically it decays as R^{-5}. While asymptotic behavior is discussed in more detail in § 11.2.6, we note here that it is characteristic of dominance by a single $\boldsymbol{k}$-state on the Fermi surface. The more complicated behavior at shorter range shows that many electronic states participate in the pair interaction. The pair interaction is comparatively insensitive to changes in ε_a and V, somewhat more sensitive to shifts in the Fermi energy (especially for larger interadatom separation), and very sensitive to the adatom binding site. Typical values of the magnitude of the nearest, next nearest, and third nearest pair energies are 1×10^{-1}, 2×10^{-2}, and 8×10^{-3} units, although each of these can vary over a range of an order of magnitude.

As presented here, this formalism implies that the substrate is essentially rigid during the adsorption process. In fact local distortions certainly do occur. Feibelman (1987, 1989, 1990) has emphasized that these distortions can play a crucial role, particularly at near-neighbor spacings. At farther separations, it does not seem unreasonable to believe that the distortions essentially renormalize $\overline{G}^X_{aa}$ while leaving G_{nn} relatively unaffected. Thus, over this range, the distortions might be taken into account by tuning the atomic and coupling parameters.

11.2.2.3. Simpler illustration: pairs on a ring

Many of the ideas in the preceding section may be couched in a (Green's functions) language unfamiliar to some readers. In an attempt to make the key ideas clearer to people more comfortable with the language of quantum chemistry, we present in this section results of an explicit calculation, done with *Mathematica*™, in which the substrate is taken to be a ring of 50 atoms. For a system of such limited size, we can keep explicit track of what happens to all of the molecular orbitals. While 1D models are a typical starting point in similar studies (Hoffmann, 1988; Whitten, 1993), we caution that consequently they contain some anomalous features which are not characteristic of most 3D substrates. In attempting to keep the following discussion uncluttered, we do not dwell on such unpleasantries as the inevitability of split-off states (due essentially to the divergence of the density of states at the band edge) and the anomalously slow decay of the interaction with separation. After exploring interaction energies from the perspective of shifting molecular orbitals, we show how the problem can be recast in the Green's function formalism presented above.

The Hamiltonian of the ring itself (H^0_{metal} of Eq. (11.3)) can be represented by a 50×50 matrix with non-zero entries (taken as −1/2) only along the two diagonals next to the main diagonal (i.e. entries $\{n, n\pm1\}$) and at the corners ($\{1,50\},\{50,1\}$) to close the chain into a ring. By analogy, e.g., to benzene rings, it is well known

Table 11.1

Display of the pair interaction energy E_n suggesting the sensitivity of adatom arrays to changes in the Fermi level, the hopping potential V, the adatom energy level ε_a, and the binding-site symmetry A, C, B, and BP. (For bridge-site adsorption, there are two nearest-neighbor configurations: in B, the vector $\boldsymbol{R}$ between adatoms is in the plane formed by the adatom and its two substrate neighbors; in BP, $\boldsymbol{R}$ is perpendicular to it. Note that, e.g., for E_2 there is no difference between B and BP.) One adatom sits at the origin "0"; the pair energy is for a second adatom at the nth nearest-neighbor site. The magnitude of the number given is 10 plus the common logarithm of the magnitude of the interaction. A plus (minus) sign indicates that the interaction is repulsive (attractive). Thus, table entries of +8.9, –7.7, and –6.6 represent interactions of $+8\times10^{-2}$, -5×10^{-3}, and -4×10^{-4}, respectively. The energy unit is one-sixth the substrate band width, roughly 1–2 eV.

Each chart is labeled by the symmetric adlayer pattern predicted. Adapted from Einstein and Schrieffer (1973) and Einstein (1979).

Binding site	A			C						B			BP		
n =	3	4	5	3	4	5				3	4	5	3	4	5
	1	2	4	1	2	4				1	2	4	1	2	4
	0	1	3	0	1	3	6	9	13	0	1	3	0	1	3
ε_F = 1.2	-7.7	-7.5	+7.5	-8.3	+7.1	-7.4				+8.4	+8.3	-6.1	-7.9	-7.4	-6.1
ε_a = -0.3	+8.9	-8.1	-7.5	-9.0	-8.0	+7.1				-9.3	-8.4	+8.3	+8.2	-8.4	-7.4
V = 3/2	0	+8.9	-7.7	0	-9.0	-8.3	-6.6	+6.1	+4.6	0	-9.3	+8.4	0	+8.2	-7.9
		c (2 x 2)			(1 x 1)						(1 x 1)			c (2 x 2)	
ε_F = 1.2	-7.8	-6.7	+7.4	-8.6	-6.2	-7.8				+8.7	+8.1	-7.6	+7.6	+7.0	-7.6
ε_a = 0.0	+8.8	-8.4	-6.7	-9.4	-8.6	-6.2				-9.3	-8.3	+8.1	+9.0	-8.3	+7.0
V = 3/2	0	+8.8	-7.8	0	-9.4	-8.6	+7.7	-5.8	+5.3	0	-9.3	+8.7	0	+9.0	+7.6
		c (2 x 2)			(1 x 1)						(1 x 1)			c (2 x 2)	
ε_F = 1.2	-7.7	+7.7	+6.9	+8.5	-7.5	+7.8				+8.5	-7.9	-7.8	-7.8	+6.9	-7.8
ε_a = -0.3	+8.6	-8.6	+7.7	-9.3	-8.4	-7.5				-9.1	+7.5	-7.9	+9.1	+7.5	+6.9
V = 2	0	+8.6	-7.7	0	-9.3	+8.5	+7.6	-6.1	+4.9	0	-9.1	+8.5	0	+9.1	-7.8
		c (2 x 2)			(1 x 1)						(1 x 1)			(2 x 2)	
ε_F = 0.9	-7.5	+7.7	-7.0	+8.1	-7.9	+7.7				+8.4	-7.7	-7.7	+6.3	+7.8	-7.7
ε_a = -0.3	+8.5	-8.5	+7.7	-9.3	-8.4	-7.9				-9.2	-7.1	-7.7	+9.0	-7.1	+7.8
V = 3/2	0	+8.5	-7.5	0	-9.3	+8.1	+7.5	-6.3	+4.7	0	-9.2	+8.4	0	+9.0	+6.3
		c (2 x 2)			(1 x 1)						(1 x 1)			c (2 x 2)	
ε_F = 1.5	-6.7	-7.8	+4.4	-7.3	+5.8	-6.8				-8.4	-7.7	+7.0	+6.7	-7.0	+7.0
ε_a = -0.3	+8.7	+8.3	-7.8	+6.2	-7.2	+5.8				-8.9	+6.2	-7.7	-8.7	+6.2	-7.0
V = 3/2	0	+8.7	-6.7	0	+6.2	-7.3	-6.3	+5.5	+4.5	0	-8.9	-8.4	0	-8.7	+6.7
		c (4 x 2)			c (2 x 2)						(1 x 1)			(1 x 1)	

that the 50 eigenstates are traveling waves with wavevectors $k = n\pi/25a$, where a is the nearest-neighbor spacing. There are just 26 distinct eigenenergies $-\cos(ka)$; all but two (viz. 1 and -1) are doubly degenerate (due to the symmetry of clockwise and counterclockwise travel). The bandwidth in these units is, thus, 2, and the band is centered about 0.

The prescription in this Hückel model for adding extra atoms essentially follows that in the tight-binding model. An adatom having energy ε_a (i.e. $-\alpha'$ in Hückel language; $\alpha = 0$) couples, via the hopping parameter $-V$ (i.e. $-\beta'$ in Hückel language; recall $\beta = 1/2$) to an orbital of the ring (as in atop bonding). Consequently, one adds a row and column to the 50×50 matrix. The diagonal entry $\{51,51\}$ is ε_a; the only other non-zero entries are pairs of $-V$'s at $\{1,51\}$ and $\{51,1\}$. For simplicity, to retain symmetry in ε and to focus on covalent effects, we take $\varepsilon_a = 0$. As might be expected, the computed eigenvalues move away from $\varepsilon_a = 0$, by an energy $\propto V^2$ in the perturbative regime. (Actually, this interaction splits the degeneracies of the ring. The combination of the two eigenstates with an antinode at the adsorption site gets shifted, while the other combination with a node keeps its original value of $-\cos(ka)$.) This downward shifting of orbitals increases the adsorption energy (absolute value of the change in total energy due to adsorption) as the Fermi energy approaches $\varepsilon_a = 0$; thereafter, the adsorption energy decreases, eventually reaching zero (as particle-hole symmetry demands).

To assess pair interactions, we add a second adatom n sites away from the first.[1] The matrix becomes 52×52, with $\varepsilon_a = 0$ at $\{52,52\}$ and $-V$ at $\{n+1,52\}$ and $\{52,n+1\}$. To compute the pair interaction at close spacings, we compare the eigenvalues when the adatoms are at neighboring or next-nearest neighbor sites with those when they are at opposite sides of the ring. To make sense of these results, we first consider the situation of adatoms at opposite sides of the ring. For an infinitely large ring one would expect results to be similar to the single-adatom case, but with shifts twice as large. For the finite case here, we note that this will occur only for states with an even number of nodes, so that the ring eigenstates to which the adatoms couple will have the same amplitudes on the two adsorption sites.

The pair interaction arises from the shifts in the energy levels when the above widely-separated pair of adatoms are moved to nearby sites.[2] We expect that the

---

1 Note that on the ring, there is really a second pair interaction over separation $(50-n)a$. Because of the periodic boundary conditions used in the previous section, this effect exists implicitly in the formalism developed there. For a large ring, this second interaction is negligible, but this effect prevents us from using a small ring. The alternative of using a chain rather than a ring is undesirable because the "substrate" sites are inequivalent.

2 There are alternative definitions. Burdett and Fässler (1990) start with ligands (viz. CO) attached to 1, 2, or 3 metal atoms, using the extended Hückel model, and seek to explain the structure of the ligand "pair potential" for a monolayer. Since it is impossible to move ligands far apart, they define the pair energy as the sum of the energy of the system with both ligands present and the energy with both absent, minus twice the energy with just one ligand attached. Some thought shows that this definition is equivalent to the one we use, assuming that our adatoms are far enough apart that they do not interact. While this perspective may be appealing, it is a chore to keep track of the electrons as they are added, and tricky to trace the evolution of the levels.

eigenenergy will decrease (become more energetically favorable) if the coupling is in-phase and increase if it is out-of-phase. More explicitly, we consider the eigenvectors of the antecedent of each energy level, from the original ring (without adatoms). If the eigenvector has the same sign on the two nearby sites, we expect the shift to be attractive (i.e. the level lowers in energy when the adatoms are brought to the nearby sites). The pair interaction comes from the shift of the *occupied* levels. How many levels are occupied is, of course, determined by the Fermi level. We generally expect that near the bottom of the band, the shifts will be attractive (negative) because the adatoms couple in phase. As the Fermi energy increases, more-rapidly oscillating eigenstates become involved.

To plot and thereby analyze this behavior, we do the following: Along the horizontal axis we use the energy of each of the levels of the ring with the adatoms at opposite sides. Thus, as we set the Fermi energy further to the right along this axis, more levels become filled. At each of these 52 discrete energies, we plot as the vertical coordinate the *shift* of the level when the adatoms are brought to nearby sites. It is these shifts, due to the "interference" of the proximate adatoms, which in the weak-V limit tend to scale as V^4 (cf. Eqs. (11.15) and (11.16)), i.e. as a next-order effect after taking into account the V^2 shifts due to adsorption. The *sum* of these shifts, for the *occupied* levels, is the pair interaction.[1] Thus, what we have plotted is the *integrand* in Eq. (11.15), essentially the phase shift η. Near the bottom of the band, the integrand is, as noted above, generally negative, but with increasing energy, it begins to oscillate in sign. (The closer the adatoms, the larger is the energy between sign changes.) In performing this analysis, the shifts alternate between the expected behavior and a much weaker shift of the uninteractive ring eigenstates. Thus, in Fig. 11.2 we combine pairs of shifts, plotting their sum vs. the average of their (unshifted) energies (from the case of adatoms at opposite sides).

We now seek to show that these results offer a decent finite-size approximation of the quasi-continuous behavior considered in the previous section. For an infinitely long chain, one can derive the analytic expression (cf., e.g., Economou (1979) or Davison and Steslicka (1992) for background information, or Kalkstein and Soven (1971), with no intralayer hopping):

$$G_{on}(\varepsilon) = \frac{-i}{\sqrt{1-\varepsilon^2}}\left[-\varepsilon + i\sqrt{1-\varepsilon^2}\right]^n \tag{11.17}$$

inside the band ($|\varepsilon| < 1$); outside the band $\sqrt{1-\varepsilon^2} \rightarrow i \cdot sgn(\varepsilon)\sqrt{\varepsilon^2 - 1}$ and G_{on} is pure real (Ueba, 1980). For the 50-atom ring, the substrate Green's functions can be computed numerically as

$$G_{on}(\varepsilon) = \frac{1}{50}\sum_{k} \frac{\cos(\boldsymbol{kna})}{\varepsilon + \cos(\boldsymbol{ka}) + i\delta} \tag{11.18}$$

---

1 Actually, it is half of the interaction, since we have been neglecting the factor-of-2 spin degeneracy in this section.

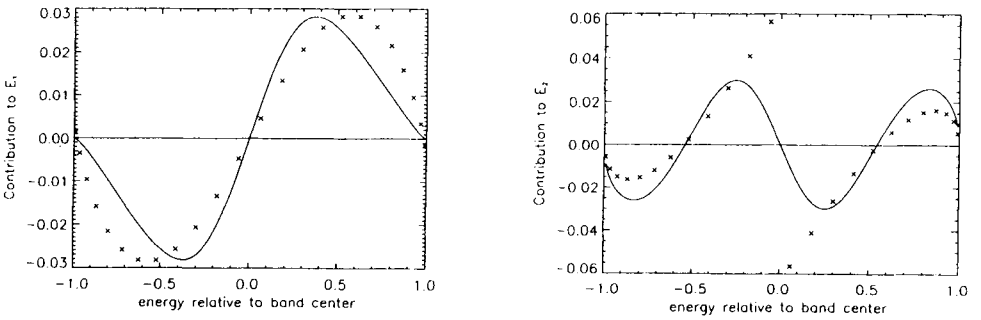

Fig. 11.2. Integrand used to compute pair interaction energy for adatoms at nearest-neighbor and next-nearest-neighbor sites on a ring. Solid curve: continuum limit, as described in § 11.2.2.2. ×: shifts of pairs of eigenvalues vs. average of their unshifted energy for a ring of 50 atoms. See text for discussion.

setting the infinitesimal at a value of, say, 0.1.[1] While these Green's functions have many secondary oscillations, their overall behavior is rather similar to the analytic infinite-length Green's functions of Eq. (11.17). In any case, inserting the analytic form into Eq. (11.15), we produce the integrand (without the factor of 2) and coplot it in Fig. 11.3. We see that the couple-dozen pairs of levels from the ring provides a decent accounting for the results of an infinite ring in a form that may be more transparent.

Our exercise further supports the idea that the pair interaction is a delicate mix of the couplings to *all* the occupied levels (or at least the half of them which are symmetric with respect to the inversion about the midpoint of the adsorption sites). Thus, a discussion in terms of HOMO (highest occupied molecular orbital) and LUMO (lowest unoccupied molecular orbital), i.e. frontier orbitals (Hoffmann, 1963, 1988) will not capture all the physics of the problem. On the other hand, with increasing separation there are more oscillations in sign as a function of ε_F. In the limit of large separations, reminiscent of stationary-phase problems, the interaction energy will be dominated by the endpoint of the integration, namely the behavior at ε_F, making a frontier-orbital approach appropriate, if one has some grasp of the long-range behavior of wavefunctions at this energy. (In the section on asymptotics, we shall explore this problem further.) More importantly, in the limit of small V, the shifts and hence the interaction are quite small except when ε_F is close to ε_a. In the limit of *weak* chemisorption, then, the HOMO/LUMO viewpoint may well offer a fruitful perspective on pair interactions. Burdett and Fässler (1990), for example, in modeling CO adsorption find the interaction is strong only when ε_F is near a large HOMO–LUMO gap.

Before closing, we mention, for those particularly interested, some details skirted above. In Fig. 11.3 only 24 pairs of levels are included. In addition, there

1 The size of δ in this discussion should be large enough so that the spiked distribution due to the discrete levels is smoothed but not so large that it is completed washed out. This parameter broadens the levels, a common way to represent a large system by a much smaller one with a limited set of eigenenergies.

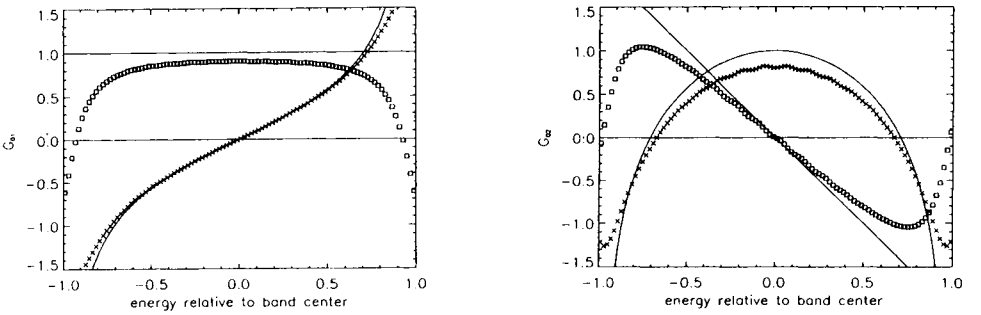

Fig. 11.3. Off-diagonal Green's functions G_{01} (nearest-neighbor) and G_{02} (next-nearest-neighbor) for a ring of 50 atoms (setting $\delta = 0.1$) compared with the continuum form (solid curves), computed exactly. ×: imaginary parts; □: real parts.

are pairs above and below the band, corresponding to what have been called "split-off" states (ES) and amount to localized levels outside the substrate band (where Im G vanishes). As one might guess from Eq. (11.12), they are the solutions $\varepsilon_\pm$ of the equation

$$\varepsilon - \varepsilon_a - V^2(\text{Re } G_{oo}(\varepsilon) \pm \text{Re } G_{on}(\varepsilon)) = 0 \tag{11.19}$$

For the case of isolated adatoms at opposite ends of the chain, the ± term is absent and the solutions ε_0 are doubly degenerate. The eigenenergies of the 52×52 matrices correspond virtually identically to the solutions of these equations, which use the quasicontinuum Green's functions. For 3D substrates, these states typically occur only for strong coupling (large V) but in 1D they are always present, formally due to divergent van Hove singularities in Re G at the band edge, physically because of the large number of states near the band edge in 1D models. From the figures in ES[1], one sees that $\varepsilon_+ + \varepsilon_- - 2\varepsilon_0$ is positive. This initially counterintuitive result can be derived analytically or graphically from the generic form of the Green's functions. The fact that ε_+ shifts down from ε_0 less than ε_- shifts up corresponds to the relative decrease in shifts in the levels as one gets farther from the band and ε_a. The split-off state involves fully in-phase hopping around the ring. Perhaps when the adatoms are close to each other, the electrons get somewhat concentrated in the region near the adatoms, so that they cannot take full advantage of the hopping all around the ring. In any case, this result leads to the spikey behavior with the unexpected sign near the band edge.

11.2.3. Multisite interactions

11.2.3.1. Three-adatom (trio) interactions

In general there will be several adatoms in close proximity. Eq. (11.2) anticipated the possibility of multiadatom interactions. The expectation of ES is that overlayer

1 Beware some misleading analysis in § II.B.3 of ES.

electronic energies are overwhelmingly dominated by nearest pair interactions. To evaluate multisite interactions, and thereby check this idea, it is straightforward (Einstein, 1979a,b) to enlarge the matrices needed to compute the phase shift in Eqs. (11.9) and (11.10). If the sites to which the adatoms bind are lth, mth, and nth nearest neighbors, we find

$$E_{T=lmn} \equiv -\frac{2}{\pi}\int_{-\infty}^{\varepsilon_F} \mathrm{Im}\,\ln(\Delta)\mathrm{d}\varepsilon - E_l - E_m - E_n \tag{11.20}$$

where

$$\Delta \equiv 1 - V^4\,\bar{G}_{aa}^2\,(G_{ol}^2\,G_{om}^2\,G_{on}^2) - 2V^6\,\bar{G}_{aa}^3\,G_{ol}\,G_{om}\,G_{on} \tag{11.21}$$

As indicated in § 11.2.1, Eq. (11.21) does not factor, making an explicit subtraction of pair energies necessary.

There are two parts of this new interaction: (1) a new triangular path, represented by the $G\,G\,G$ term; and (2) an "incompleted cubic" term, marked by the absence of V^8 and V^{12} terms that would be present in $E_l + E_m + E_n$ if their logarithms were merged. Trial calculations using just the "triangle path", with moderate V appropriate to chemisorption, reproduce the full interaction at least qualitatively.

Computations of trio energies using Eq. (11.20) suggest that their magnitudes are determined primarily by the two closest (strongest) pairs. In explicit comparisons (Einstein, 1979a,b) of $E_{lmn} = E_{223}$, E_{225}, E_{238}, and E_{335}, for typical V and ε_a, for all possible substrate fillings, the first two have the strongest trio interaction energy. E_{223}, which has a 3rd neighbor spacing as its third side, is somewhat the larger, and is nearly as strong as E_3. The other two are smaller by at least half an order of magnitude. With increasing adatom separation the trio energies fall off rapidly, much like the pair energies.

11.2.3.2. Complete overlayers

While quartets and higher-order terms could be calculated, numerical noise problems from successive cancellations would become troublesome. Starting from the other extreme, one can easily show (Einstein, 1977) that the indirect interaction energy per adatom for a complete (1×1) adlayer of N_a adatoms is

$$-\frac{2}{\pi N_{\|}}\sum_{k_{\|}}\int_{-\infty}^{\varepsilon_F} \mathrm{Im}\,\ln\left\{[1 - V^2 G_{aa}(\varepsilon)\,G(k_{\|},\varepsilon)\,/\,[1 - V^2 G_{aa}(\varepsilon)\,G_{oo}(\varepsilon)]\right\}\mathrm{d}\varepsilon$$

$$= -\frac{2}{\pi N_a}\sum_{k_{\|}}\int_{-\infty}^{\varepsilon_F} \mathrm{Im}\,\ln\left[1 - V^2\,\bar{G}_{aa}\{G(k_{\|},\varepsilon) - G_{oo}(\varepsilon)\}\right]\mathrm{d}\varepsilon \tag{11.22}$$

where the summation goes over the surface Brillouin zone (SBZ), containing $N_{\|}$ (the number of adsorption sites) points. $G(k_{\|},\varepsilon)$ can be computed analytically (Kalkstein and Soven, 1971), rather like a semi-infinite chain.

For a real monolayer, direct interactions between the closely-spaced adsorbates are likely to produce an interaction energy quite different from that predicted from Eq. (11.22). Not only does the direct interaction make a great difference for individual pairs (Burke, 1976), but it often leads to the formation of two-dimensional adlayer bands which overshadow any indirect effects (Liebsch, 1978). Therefore, we focus on the $c(2\times2)$ overlayer. Since the real space unit cell area is doubled, the SBZ is halved, most naturally taking the form of an inscribed "diamond" (square rotated by 45°). Points outside the new SBZ get folded back in, giving doubling of the (highly blurred) two-dimensional band-structure. The upshot is that for a $c(2\times2)$ adlayer, $G(k_{\|},\varepsilon)$ in Eq. (11.22) is replace by (Einstein, 1977, 1979a) and $N_a = N_{\|}/2$

$$\left\{G(k_{\|},\varepsilon) + G(\pi(1,1) - k_{\|},\varepsilon)\right\}/2 \tag{11.23}$$

Based on these ideas, one can compare (Einstein, 1977, 1979a) the indirect interaction energy (per adatom) for a full $c(2\times2)$ overlayer with an explicit sum over the pair energies for all pair configurations arising in a $c(2\times2)$ pattern — only the five shortest contribute significantly — weighting them according to the number per adatom existing in the pattern: two for pairs along the <10> and <11> mirror axes, four otherwise. Overall, this curve does a good job of reproducing the $c(2\times2)$ plot. Trio interactions can also be included in the sum and help make up differences between the overlayer calculation and the explicit sum. Their contribution generally is important only near energies corresponding to the Hartree–Fock bonding and antibonding resonances in the DOS. In short, multisite interaction energies are not too important in total overlayer energies, although they may play a role in other circumstances.

The other way to approach dense monolayers is to invoke results from the theory of alloys (Ehrenreich and Schwartz, 1976). Perhaps the simplest such scheme is the average T-matrix approximation (ATA) (Korringa, 1958), which assumes that adatoms are randomly distributed over the lattice sites. Urbakh and Brodskii (1984, 1985) work out the formal expression for $\Delta\rho(\varepsilon)$ and apply it to Pt(111)–H (cf. § 11.4.2.). The next level of sophistication is CPA, in which the self-energy of the "effective medium" of the alloy is calculated self-consistently; an application by Persson and Ryberg (1981) was noted in § 11.2.1.

11.2.4. Coulombic effects: self-consistency and correlation, and other improvements

The issue of self-consistency has pervaded most subsequent efforts to apply tight-binding methods to the pair problem. The inability to resolve this problem in a satisfactory way is one of the greatest difficulties in extending this approach to quantitative investigations. In the LCAO framework, since the electron orbitals are fixed at the outset, self-consistency is discussed in terms of the Friedel (1958) sum rule — which in this case requires charge neutrality within some finite range of an adatom — rather than Poisson's equation (Appelbaum and Hamann 1976). Typically, ε_a is adjusted (making it a derived rather than a free parameter) (Allan 1970, 1994). The energies of nearest neighbor(s) on the surface may also be altered, thereby inviting new surface states (Kalkstein and Soven, 1971; Allan and Lenglart, 1972). Sometimes off-diagonal Coulomb terms are also included in various ways

(Rudnick and Stern, 1973; Leynaud and Allan, 1975), meaning that changes in charge on a site affect the potential of its neighbors. Generally neutrality is required either at each site or just in the surface cluster consisting of the adatom and its nearest neighbor(s), excluding any longer-range oscillations. The quantitative results are rarely compelling. The qualitative results (Einstein 1975, 1979a) are plausible.

A second approach assumes that in a strongly chemisorbed system, the essence of the pair interaction lies in a surface molecule. A small cluster is treated carefully, gaining an improved description of local Coulomb effects at the expense of any background effects from the substrate. From studies of W_2H and W_3H_2, for example, Grimley and Torrini (1973) conclude that H atoms at nearest neighbor sites on W(100) will be unstable, the repulsive energy being of order 200 meV. This method is not extended readily to more widely separated pairs, since the distance from the adatom to the edge of the cluster should presumably be at least as large as its distance from the other adatom. Since the "substrate" wavefunctions — via which the pair interacts — are sensitive to the details of the cluster, matching conditions to the background must be adjusted carefully. Moreover, in cases where adatoms bond to a common substrate atom, some anomalous structure may arise which should not be generalized (ES; Einstein et al., 1990). The best hope for cluster approaches is to embed them in well-characterized semi-infinite substrates (Grimley, 1976). Grimley and Pisani (1974) have taken this approach for clusters containing single adatoms and calculated in a SCF–LCAO–MO scheme.

The embedded cluster technique has indeed flourished (cf. NATO conference proceedings in Pacchioni et al. (1992)). Most of the applications are to monomer adsorption, but the dissociation of (gas) dimers is also often considered (e.g. Cremaschi and Whitten (1981), Madhavan and Whitten (1982)). As noted, it is hard to imagine applying the method to larger pair separations. Feibelman (1989a) provides a lucid critique of this approach, questioning typical choices of bases and treatment of background effects. Also, since correlation is typically considered only in the cluster region, he wonders how much of the adsorbate binding energy actually comes from allowing substrate correlations in the bonding region.

Grimley and Walker (1969) observe that while sizeable charge transfer might take place during chemisorption, little more should happen as a function of the relative placement of the adatoms. If energies in simple models could be determined in some plausible way, the pair interaction should work out satisfactorily even if the single-adatom results are somewhat inadequate. Moreover, the pair interaction is a rather insensitive function of ε_a, as suggested by Table 11.1 and shown more convincingly by Fig. 11 of ES.

Schönhammer et al. (1975) studied carefully the correlation effects in indirect pair interactions. Using a (100) cubium substrate with parameters appropriate to H on Ni, Schönhammer (1975) had previously shown from a variational approach that the single adatom binding energy is roughly 1/3 stronger than in Hartree–Fock (although the two curves did have the same structureless shape as a function of ε_F). They find that this correlation energy, 1/4 the binding energy, roughly cancels out when the pair interaction energy is computed. Although this cancellation is reported to be less complete for other parameters, the qualitative behavior holds for V's of

order the "critical hopping" (below which Hartree–Fock local moments arise). In addition to confirming the anisotropic, oscillatory behavior of the pair interaction, Schönhammer et al. (1975) corroborate the roughly exponential fall-off with separation (for interadatom distances of order 1 to 4 lattice constants). The implication of this work is that correlation effects (in the form of careful treatments of the Anderson Coulomb term), while important for single adatom effects, can (to a reasonable approximation) be neglected in computing pair (and higher order) effects. Later studies discussed below (§ 11.3.5) cast doubt on how well this result generalizes to models treating the d-band aspects of the substrate.

Over the last decade or more, research in chemisorption theory has stressed generation of numerical results to fit quantitatively data from UV photoemission, ion neutralization spectroscopy, low-energy-electron-diffraction (LEED), and scanning tunneling microscopy (STM) experiments. The primary object has been to compute the spatial and energy distribution of the electron density near the surface region and to find exact locations of surface states. For these applications self-consistency (here in a Poisson's equation sense) is crucial. The first attempts to gauge the role of such effects considered the adsorption of single adatoms on jellium. In semiconductors it is difficult to propagate electrons from one adsorption site to another, from a physics viewpoint because the Fermi energy lies in the band gap, from a chemical perspective because electrons are relatively localized in covalent bonds. (Some implications are discussed in the next section.) Tosatti (1976) has considered the interaction between adatom pairs on Si(100)(2×1), assuming a short-range defect potential for the adatoms and linear response by the surface electrons. His pair interaction is always repulsive, oscillatory (in strength) with separation, but with an exponentially decaying envelope (due to trying to propagate electrons in the gap).

Realistic slab calculations for transition and noble metals began appearing about a decade ago and are becoming more or less routine for flat surfaces. They are discussed at length in volume 2 of this handbook. Nonetheless, even today most total energy self-consistent calculations consider only a (1×1) overlayer, with the full symmetry of the substrate.

11.2.5. Lattice indirect interactions: phonons and elastic effects

To check whether there were significant interactions mediated by phonon rather than electronic degrees of freedom of the substrate, Cunningham, Dobrzynski, and Maradudin (1973) studied the contribution to the free energy of the interaction between two identical adatoms via the substrate phonon field. In their model, the adatoms sit in the atop position on the (100) face of cubium. Results are computed as a function of the three dimensionless quantities: adatom mass over substrate mass, adatom–substrate coupling over substrate–substrate coupling, and inter-adatom separation R (in lattice constants). They find that the zero-point energy is invariably attractive and that it decreases monotonically in strength with R, going like R^{-7} for large R. The attraction is at most $10^{-4}\hbar\,\omega_L$ (where ω_L is the maximum phonon energy) or of order 10^{-6} eV, and thus nearly always negligible.

Given these negative results, little further work was done on this problem. However, beginning half a decade later, considerable interest has been paid to elastic interactions on surfaces. When electronic interactions play a significant role, it is generally not just difficult but artificial to try to isolate elastic effects from other electronic effects. However, for non-metallic substrates, where there are no electrons near the Fermi energy, focus on elastic interactions may often be a fruitful perspective. Also, in the asymptotic region, the elastic interaction generally dominates for large enough separation. In this section we first give a chronological account of studies of this interaction between adatoms. We then discuss in more detail, via a few examples, the interplay between elastic and electronic effects on metal substrates, and why this perspective is often not fruitful at close range.

Lau and Kohn (1977) investigate the long-range interaction between two adatoms due to classical elastic distortion of an isotropic semi-infinite substrate, finding:

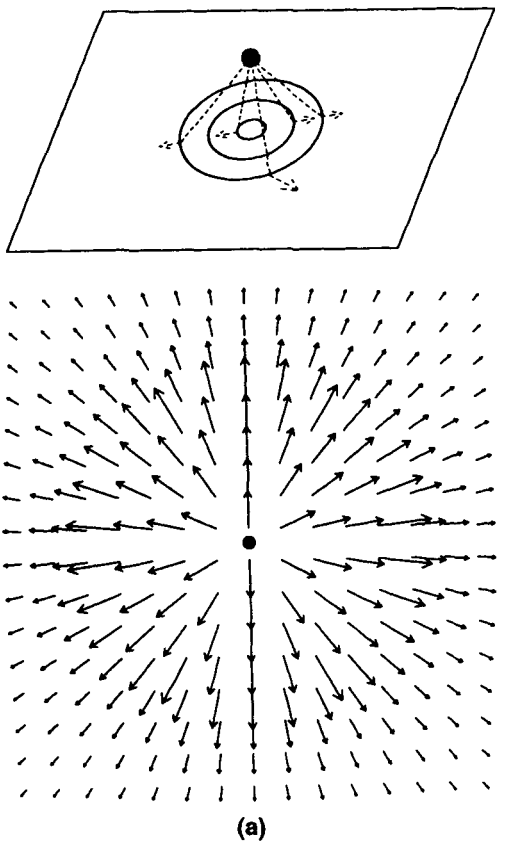

Fig. 11.4. Schematic of the origin of the elastic repulsion between like atoms on an elastically isotropic substrate. (a) Response of the substrate to a single atom. Here the displacement is taken to be away from the adsorbate, though it is more likely to be toward the adatom. (b) When two adatoms are present, substrate atoms between them cannot relax fully.

$$E^{\text{elas}}(R) = \frac{1-\sigma}{4\pi\mu}\frac{\Lambda_a\Lambda_b}{R^3}, \quad \Lambda_a = \sum_j \boldsymbol{F}_j^a \cdot (\boldsymbol{R}_j - \boldsymbol{R}_a) \tag{11.24}$$

where $\boldsymbol{F}_j^a$ is the force exerted by adatom a at $\boldsymbol{R}_j$, σ is the Poisson ratio, and μ the shear modulus. For identical atoms, this interaction is always *repulsive*, due to frustrated relaxation of substrate atoms between the two adatoms, as illustrated in Fig. 11.4. Taking $\sigma \approx 1/2$ and $\mu \approx 10^{-3}$ atomic units as typical, they estimate this repulsion to be of order 0.1 eV at $R = 10$ a.u. ≈ 5 Å. (If the adatom–substrate coupling on a triangular surface has the form $-3\gamma R_0^{-6}$, where $R_0 = |\boldsymbol{R}_j - \boldsymbol{R}_a|$ is the spacing between the adatom and one of its 3 substrate neighbors, then the "virial" (Stoneham, 1977) $\Lambda = -6\gamma a^2 R_0^{-8}$.) For different adatoms, the elastic interaction can have either sign. Its R^{-3} decay is reminiscent of the dipole–dipole repulsion. Inserting reasonable numbers for Xe pairs on Au, Lau and Kohn find at $R = 10$ a.u. that

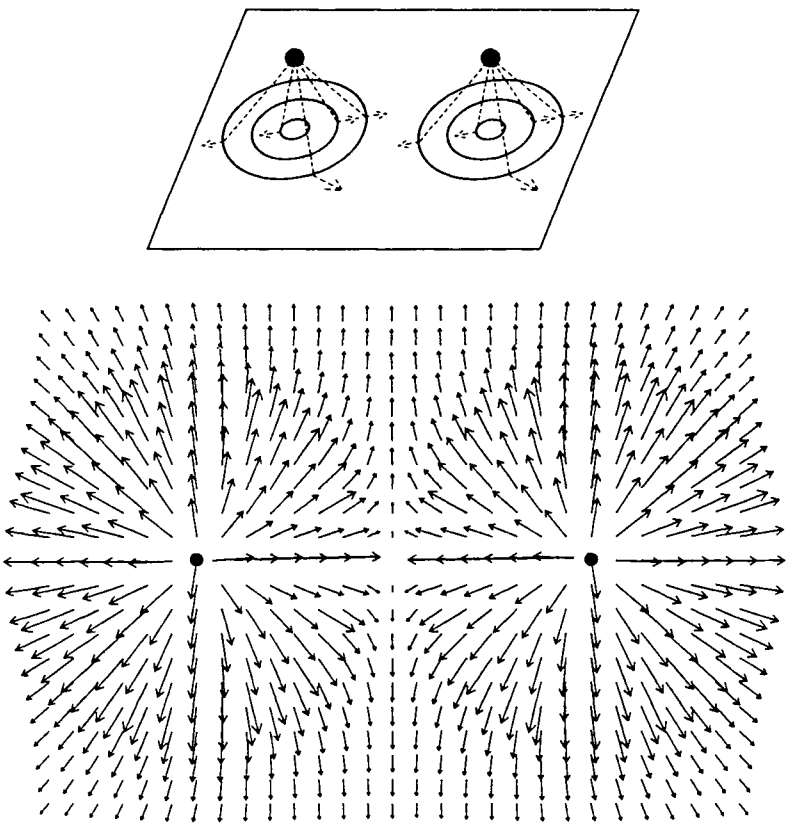

(b)

Fig. 11.4 (continued). Caption opposite.

the elastic repulsion is 0.53 meV, compared to their dipole repulsion of 1.1 meV, i.e., about half as large. On the other hand, at nearest neighbor sites it is three or four orders of magnitude greater than the phonon-mediated attraction just discussed; in essence Cunningham and coworkers' calculation (Cunningham et al., 1973) gives the leading quantum correction to the classical distortive effects.

Varying the vertical position of the adatoms relative to the isotropic substrate, Maradudin and Wallis (1980) also find the R^{-3} decay but find that the interaction is attractive if the average distance below the surface is greater than $R/2\sqrt{2}$.

Stoneham (1977) shows that if the substrate or the adatom–substrate coupling is anisotropic, then the elastic interaction between like adatoms can again be attractive. He estimates that the magnitude of interaction of neighboring bridge-bonded H on W is of order 0.1 eV, large enough to account for some measured interactions without recourse to electronic effects. He also considers additional elastic effects due to clusters of adsorbates.

Lau (1978) in turn considers anisotropic substrates with hexagonal or cubic symmetry. Using Green's functions derived by Dobrzynski and Maradudin (1976) and by Portz and Maradudin (1977), he works out explicit formulas. For Xe pairs on graphite, separated by 5 Å, he finds a repulsion of 0.18 meV. On Au (100), with pairs of Xe again 5 Å apart, he finds an attraction of 0.30 meV along the cube axis and a repulsion of 1.73 meV at 45°. He expects this anisotropic behavior to be fairly general. While these energies are quite small, he expects elastic effects to become stronger and play a significant role in distortive phase transitions.

Kappus (1978) rederives the previous results on isotropic and cubic substrates, finding again the possibility of homonuclear pair attractions on anisotropic substrates. Between clusters a repulsive barrier arises, proportional to the product of the areas of the clusters, even in directions in which the long-range interaction is attractive. Kappus (1980) extends this work to consider an anisotropic force dipole tensor, which enters the calculation of the virials, but restricts the substrate to be elastically isotropic, a reasonable approximation for W. Again there is the possibility of elastic attractions between like adatoms. The formalism is applied to explain the ordered $p(2\times1)$ phase of O on W(110) (Engel et al., 1975; Wang et al., 1978). He obtains "reasonable qualitative agreement" with the pair interactions used by Williams et al. (1978) in a Monte Carlo simulation of this system. However, since they do not lead to the $p(2\times1)$ superstructure, Kappus (1981) generalizes the model to include a nearest neighbor interaction, an electric dipole repulsion caused by adatom dipoles normal to the surface, and another long-range part coming from elastic dipoles of nearest-neighbor pairs of adatoms. This third energy leads to multisite interactions. Nonetheless, with an E_2 interaction, he cannot stabilize the $p(2\times1)$ superstructure; such an interaction could, of course, arise from the electronic indirect mechanism, from small anisotropy in the elastic constants, or from a breakdown in the continuum approximation.[1]

---

1 This system has proved quite challenging. Rikvold et al. (1984) used a model with $E_1 < 0$, $E_2 > 0$, E_3, and trio interactions, and still found that an attractive E_5 1% of E_1 could introduce pronounced first-order behavior at both low and high coverages.

Theodorou (1979) proposes an intriguing approach to the overlayer structure of W(110)–O. He noticed that on a rigid substrate the W–O–W angle of bridge-bonded O was 102.2° rather than the ideal 90°. Presumably, then, these two W's would be drawn toward each other; there are two other W's, at the far ends of the "diamond" at the center of which the O sits, which are repelled by a lesser amount. From this perspective, he estimated energies per O of isolated atoms, the chain constituent of the $p(2\times1)$, the $p(2\times1)$ itself, and a full (1×1) to be 0.15 eV, 0.05 eV, 0.15 eV, and 0.29 eV, respectively. In terms of interactions, he essentially finds an attraction $E_1 = -0.10$ eV which duly produces chains. A repulsion in a different direction keeps the chains apart. Unfortunately, some more distant (second-neighbor in some direction) interaction between chains is also repulsive, preventing the $p(2\times1)$ from forming. He speculates about what other interactions might overcome this repulsion, noting that the small work function change suggests that dipolar interactions are insignificant. Apparently no resolution of this problem was ever achieved and the paper seemingly has had little impact on research in adsorbate interactions, though perhaps it influenced thinking about strained superlattices in heterostructures (Tserbak et al., 1992).

Tiersten et al. (1989) note that Kappus (1978) smoothly truncates 2D integrals over the surface Brillouin zone with a cutoff parameter of order the inverse lattice constant and that his interaction energies between adatoms separated by less than a few lattice spacings depends sensitively on this cutoff. Thus, they conclude that a lattice-dynamics analysis of the substrate is needed in the non-asymptotic range instead of the continuum elasticity approach. Working in a mixed representation (cf. just above Eq. 11.5) they find an expression for the pair interaction energy in terms of (Fourier-transformed) local force vectors associated with each adatom and a substrate propagator between the sites. This propagator they take to be essentially the inverse of the dynamical matrix. (In elasticity theory, the propagator is an angular-dependent term divided by the magnitude of the 2D wavevector; one then readily recovers the R^{-3} decay.) Tiersten et al. (1989) apply their formalism to As dimers on Si(100). They plot the interaction along the three principal directions, finding that it (1) can change sign with increasing R, (2) is highly anisotropic, (3) is rather small, less than 10 meV (often much less) once $R \geq 8$ Å. They also look at interactions between H pairs on reconstructed W(100). Again they find that the interaction can be attractive or repulsive, that it depends on the direction, and is at most about 3 meV for the shortest R's, and becomes less than an meV quickly with increasing R. Presumably electronic effects are much larger for this case. In both cases the sign of the interaction at small separations can usually be understood in terms of the dominant forces on the substrate atoms or by simple arguments based on interference of the relaxations produced by the individual adatoms (cf. Fig. 11.4.). Later, Tiersten et al. (1991) consider Si(100)–O, finding generally similar qualitative features, but with larger magnitudes, around 50 meV at 4 Å, but then falling quickly to less than 5 meV, then to less than a meV. In other words, when electronic interactions are present (on metals), they should dominate, but on semiconductors or ionic crystals, these could be the leading interaction.

Recently Rickman and Srolovitz (1993) present a very general Green's function

formalism for finding the elastic interaction between defects of spatial dimensionality D and multipole character m on a surface. Specifically, they tabulate results for four generic defects: a point force ($D = 0$, $m = 0$), an impurity adatom or island ($D = 0$, $m = 1$), a stress domain ($D = 1$, $m = 0$), and a step ($D = 1$, $m = 1$). Since defects in general involve more than the lowest-order multipole, the results apply for large lateral separation R. For point interactions ($D = 0$) between an m-pole and an n-pole, the interaction $E(R) \propto R^{-(m+n+1)}$, reproducing R^{-3} for the interaction between adatoms. For linear defects, $E(R) \propto R^{-(m+n)}$, or $C_1 \ln(R/a) + C_2$ for $m = n = 0$. Further comments related to steps are deferred to § 11.4.3.

The preceding discussion assumes that one can neatly distinguish between electronic and elastic interactions. Such a distinction is generally possible at moderate-to-large separations between adatoms, but fails in the "near" region: in computing carefully the electronic interaction between adsorbates (Feibelman, 1989a), relaxations can play an important role. There is clear experimental evidence that adsorption can distort the substrate in the vicinity of the binding site, although the precise nature of the deformation may be difficult to determine. For example, for Ni(111)p(2×2)–O Narusawa et al. (1982) measured, with high-energy ion scattering, outward displacements of about 0.15 Å of the three Ni's to which each adatom binds (i.e. substantial buckling and overall relaxation); from LEED analysis, Vu Grimsby et al. (1990) note, in addition, lateral "twist" displacements of about 0.07 Å. However, Schmidtke et al. (1994) find in a subsequent LEED analysis *no* twisting, minimal relaxation, but buckling of 0.09 Å. In a painstaking LEED survey of Ru(0001)–S, Pfnür's group finds progressively greater substrate distortions with structures of increasing coverage: for the p(2×2) there is slight buckling and outward relaxation, of ~0.03 Å (Jürgens et al., 1994). In the $(\sqrt{3}\times\sqrt{3})$ symmetry forbids such buckling; the relaxation is still comparably minimal (Jürgens et al., 1994). In the 1/2 ML c(4×2) phase, there is substantial (~0.2 Å) row buckling (Schwennicke et al., 1994), Ru atoms bonded to two S's relaxing more than those bonded to one S. (Moreover, the S atoms occupy fcc and hcp sites with equal probability, but are shifted laterally from the high-symmetry 3-fold position by ~0.16 Å!) Finally, in the $(\sqrt{7}\times\sqrt{7})$ at 0.57 ML, there is even stronger dependence of the Ru relaxation on the S coordination: surface atoms with 3 S's relax 0.39 Å more than those with a single S (although the overall relaxation is minimal) (Sklarek et al., 1995). (It is also noteworthy that in all cases the local chemistry is preserved in the sense that S–Ru bond lengths do not change by more than 0.05 Å!) Since these displacements are based on fits to data, accuracy depends on the insight and ingenuity of the experimentalist. Using Tensor LEED and scanning tunneling microscopy, Barbieri et al. (1994) investigate two of the four ordered overlayers of S on Re(0001) (Ogletree et al., 1991) and find a similar increase in surface distortions with increasing coverage.[1] Substantial displacements of surface atoms will certainly affect the electronic states nearby (and so the interaction energy) and

1 Einstein (1991) points out that several distinct trio interactions would be needed to account for these ordered phases; presumably some of these are related to the local distortions.

evidently can depend on the separation between the adatoms. It is a futile exercise to sort out which portion of the interaction is elastic. As more specific systems are carefully documented, it will be interesting and important to look for trends in the evolution of buckling with coverage.

11.2.6. Asymptotic form of the indirect interaction between atoms and between steps

In this section we present more information than in § 11.2.2 about the nature of the indirect interaction between widely separated adsorbates. Our intention is to stress the general features and underlying physics while skirting explicit formulas, which can become quite complicated (Einstein 1973, 1978, 1979a; Lau and Kohn, 1978; Flores et al., 1979; Roelofs, 1980). From Eq. (11.16) we see that the asymptotic behavior hinges on the behavior of $G_{on}(\varepsilon)$ at large $\boldsymbol{R}$, where $\boldsymbol{R}$ is the vector from site o to site n. While studying scattering in solids four decades ago, Koster (1954) recognized that with the competition of rapid oscillations, the solution required stationary-phase arguments. He uncovered much of the essence of our problem, finding that

$$G_{on}(\varepsilon) \propto R^{-1} \exp(i\,\boldsymbol{k}(\varepsilon) \cdot \boldsymbol{R}) \tag{11.25}$$

where $\boldsymbol{k}(\varepsilon)$ is that wavevector along a constant-energy surface at which the velocity (viz. $\vec{\nabla}_{\boldsymbol{k}}\varepsilon$) is parallel to $\boldsymbol{R}$, as illustrated in Fig. 11.5. Moreover, the proportionality constant varies inversely with the Gaussian curvature of the constant-energy surface at $\boldsymbol{k}$. More generally, if $G_{on}(\varepsilon) \propto k^{-1} R^{-m} \exp(ikR)$, then integration by parts (Grimley, 1967) leads to the important result

$$E_n \sim \frac{V^4}{R} \operatorname{Re}\,[\bar{G}^2_{aa}(\varepsilon_F)\, G^2_{on}(\varepsilon_F)] \tag{11.26}$$

and the interaction decays like $R^{-(2m+1)}$. For surfaces, one can show quite generally that $m = 2$, i.e. that $G_{on}(\varepsilon) \propto k^{-1} R^{-2} \exp(ikR)$ (cf. the discussion in the paragraph after Eq. (11.28)) and

$$E_n \sim R_n^{-5} \cos(2k_F R_n + \phi) \tag{11.27}$$

if the interaction is isotropic. The complex quantity $\bar{G}_{aa}$ is independent of the separation and so leads to the phase factor ϕ; from Eq. (11.14), this factor is given explicitly by (Joyce et al., 1987)

$$\phi = \arg(\bar{G}^2_{aa}) = 2 \arg\,[\varepsilon_F - \varepsilon_a - V^2\, G_{oo}(\varepsilon_F)]^{-1} \tag{11.28}$$

which vanishes when $V^2\pi\rho_0(\varepsilon_F) << \varepsilon_F - \varepsilon_a - V^2 \mathrm{Re} G_{00}(\varepsilon_F)$, e.g. when the coupling is weak or the adatom level is far from the Fermi energy. Gumhalter and Brenig (1995a) emphasize that the phase factor only appears in nonlinear theories.

In studying the static response function, Rudnick (1972) found essentially this result for jellium confined by an infinite barrier. He interpreted the sinusoidal

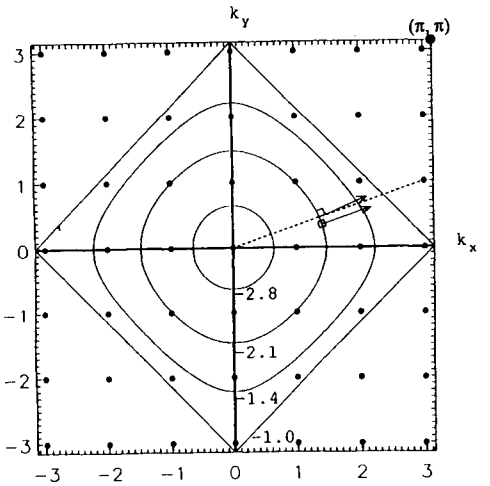

Fig. 11.5. Illustration of the wave vector which dominates the asymptotic interaction. The curves indicate constant-energy lines in the surface Brillouin zone, in the lower third of the band of a simple cubic crystal in the tight-binding model. The dots denote sites in *real* space. The dashed line shows the $\boldsymbol{R}$ connecting the origin with a particular site. For $\varepsilon = -2.1$, the arrows show the velocity $\nabla_{\boldsymbol{k}}\varepsilon$ of two candidates for this wave vector; it is not the $\boldsymbol{k}$ at which $\varepsilon(\boldsymbol{k})$ intersects $\boldsymbol{R}$, but rather the lower one at which $\nabla_{\boldsymbol{k}}\varepsilon$ is parallel to $\boldsymbol{R}$, which enters Eq. (11.25). For isotropic systems, the contours become circles (as near the bottom of the band, as depicted for $\varepsilon = -2.8$), and there is no distinction between the two candidates. When the Fermi curve lies on more than one "sheet", one must sum over the contributions from each $\boldsymbol{k}$ with $\nabla_{\boldsymbol{k}}\varepsilon$ parallel to $\boldsymbol{R}$.

variation as a Friedel oscillation of the screening charge around a point impurity. Similar behavior was also found by Moore (1976) and Flores et al. (1977a). The response at point n due to a disturbance at point o of the infinite-barrier system can be described in terms of the *bulk* responses from the disturbance at o and from a comparable disturbance at the mirror image of o, with the opposite sign to produce a node along the barrier (Flores et al., 1979). Then the leading R^{-1} contributions to G_{on} cancel, leaving the next order, with coefficient R^{-2}, to dominate.

Lau and Kohn (1978) verify that a similar asymptotic interaction occurs for a jellium substrate even if the barrier is finite. Treating the adatom–substrate interaction in second-order perturbation theory, they can separate the pair interaction energy from the adsorption energy of single atoms, analogous to what was done above for the tight-binding model. The $\boldsymbol{R}$ dependence of the pair interaction is given by

$$\int d^2 \boldsymbol{k}_{\parallel} \, e^{i\boldsymbol{k}_{\parallel} \cdot \boldsymbol{R}} \, \mathbf{G}(\boldsymbol{k}_{\parallel}), \tag{11.29}$$

where $\mathbf{G}(k_{\parallel})$ is a kernal which depends only on the substrate energy spectrum (here of the free electron form). After detailed analysis, they find that asymptotically the integral is dominated by a singularity in the *fourth* derivative of $\mathbf{G}\,(k_{\parallel})|_{2k_F}$ times a unit step function. Using the results for generalized functions given by Lighthill (1958), they reduce behavior to the form of Eq. (11.27).

Lighthill's formulas can be applied more generally to find the asymptotic form of the $G_{on}(\varepsilon)$, particularly in the tight-binding model; there is no need to assume 2D isotropy, weak coupling, or large separation between ε_F and ε_a, viz. ionic bonding (Einstein, 1973, 1978, 1979a). (From another approach with different expansions, Le Bossé et al. (1979) rederive most of Lau and Kohn's results without the latter restrictions.) The final expressions are rather cumbersome. An interesting qualitative aspect is that the use of surface rather than bulk Green's functions means that one must be somewhat cautious in applying Koster's approach. (Cf. Flores et al. (1979) for some details of the application to surfaces.) Only $\boldsymbol{k}_{\|}$ is a good quantum number (since the surface destroys crystal translation invariance in the $k_{\perp}$ direction), so we have a Fermi "loop" rather than a surface. For each $\boldsymbol{k}_{\|}$, however, the kernel of the surface Green's function can be rather simply related to those of bulk Green functions (Kalkstein and Soven, 1971). For the (100) face of a simple-cubic tight-binding model, it turns out that there are essentially two subbands, each with 2/3 the bulk bandwidth B and centered at $B/3$ from either band edge. Thus, in the central portion of the band, there are essentially two sheets to the Fermi surface, so that there are two special values of $\boldsymbol{k}_{\|}$ to be considered. For a more realistic model of the substrate, there might well be even more. On the other hand, near the bottom of the band, the tight-binding dispersion relation simplifies to the parabolic form; Lau and Kohn (1978) manipulate the Anderson model (in essence, applying the Schrieffer–Wolff (1966) transformation) to make contact between their free-electron calculations and the earlier tight-binding work. (See also Einstein (1978).)

An R^{-5} interaction at large separations is clearly of rather academic interest. However, in the infinite-barrier model, prompted by Hjelmberg's (1978) explicit numerical calculations, Johansson (1979) and Johansson and Hjelmberg (1979) notice that in addition to this "far asymptotic" region, there is a region with bulk R^{-3} interaction occurring for much smaller values of R, still larger than k_F^{-1} but smaller than the distance to the barrier, so that the image does not cancel the leading term due to the atomic charge. (Cf. comments after Eq. (11.28).) When R is a few lattice spacings (specific range dependent on the electronic charge density, i.e. k_F, of the jellium), there typically is a crossover region between the bulk-like and far asymptotic limits, with a decay exponent varying continuously from 3 to 5. Le Bossé et al. (1978) also find the R^{-3} decay, but do not report the transition or far asymptotic region and attribute (Le Bossé et al., 1979) the lack of R^{-5} decay to other factors.

Seemingly the latest word on this problem is Eguiluz and coworkers' numerical treatment (Equiluz et al., 1984), based on a Kohn–Sham self-consistent approach, of two charges in Al- and Na-like jellium. They recover Lau and Kohn's result (Lau and Kohn, 1978) as the dominant result for contributions to the response function from wavevectors at least $2k_F$, but their calculations show that this weak oscillatory term is masked by a much larger, monotonically-decaying attractive interaction due to smaller wavevectors. (The singularity in the integrand at $2k_F$ is numerically invisible.) When the charges are placed outside (inside) the jellium, the direct Coulomb repulsion overwhelms (roughly compensates) this attraction, which is presumably a manifestation of the polarization screening. In their range of study (which does not reach the "far asymptotic" regime), they also see the R^{-3} decay of

the envelope of the oscillatory part. The oscillations are observable in the total interaction only when the charges are inside the jellium, and are strongest when the charges are near the surface, with initial oscillation amplitudes somewhat larger than 10 meV (larger for "Na" than "Al"). Although for charges outside jellium there is no observable evidence of long-range oscillatory interactions due to polarization of the substrate electron gas, the authors carefully note that their model does not allow for electron exchange coupling to the substrate expressed in Eq. (11.5)

In the asymptotic regime, the lateral interaction may be analytically tractable but is generally insignificant. At short distances, the interaction is far more complicated, since it depends on all the occupied states and not just those at one point on the Fermi surface. By the distances that the asymptotic form dominates, the interaction is quite small and is often masked by other interactions decaying like R^{-3}. Thus, a particularly significant result of Lau and Kohn is: if the indirect interaction is mediated by a *surface state* (assumed to be circularly symmetric), the singular nature of expression (11.29) appears in the first derivative of $\mathbf{G}(k_{\|})$ at $2k_F$, and the prefactor of $\cos(2k_FR)$ in Eq. (11.27) becomes R^{-2}! Of course k_F is now associated with the cylindrical Fermi surface. The slower decay should in retrospect be not so surprising, since the curvature of the cylinder vanishes along the axis direction, so that the form derived by Koster would diverge. For the more general cases of a (2D) hexagonal or square tight-binding substrate, Volokitin (1979) and Braun and Medvedev (1989), respectively, also find asymptotic R^{-2} decay, the latter suggesting that such behavior might be seen on Re (0001). With the axis of the cylindrical Fermi surface parallel rather than perpendicular to the physical surface, as obtained by adsorption onto the edge of a semiinfinite square tight-binding net, Braun (1981) and Braun and Medvedev (1989) find R^{-4} and R^{-2} for the "surface" (edge) and "bulk" contributions, respectively, to the interaction energy; the physical analogue is Re $(10\bar{1}0)$ in the $[\bar{1}2\bar{1}0]$ direction.

Lau and Kohn (1978) also consider a model in which the Fermi surface is defined by two exactly parallel planes spaced Δk apart in the x direction; they find $E_x \propto x^{-1}\cos(\Delta k x)$. Braun (1981) and, more explicitly, Braun and Medvedev (1989) illustrate this decay for the case of a tight-binding chain as the substrate. In rederiving these asymptotic behaviors, Flores et al. (1979) also find a fractional exponent for a conical Fermi surface. Lau and Kohn's idea of mediation of interactions by quasi-one-dimensional states with consequent x^{-1} decay has captured the imagination of many for years but has only very recently been applied to a physical system: Ni(110)–H (Bertel and Bischler 1994; Gumhalter and Brenig 1995). This speculative recent work is discussed at the end of § 11.4.3.

Further analytic progress was achieved by Brodskii and Urbakh (1981). (For a more general theoretical review from their perspective, see Urbakh and Brodskii (1985).) They note that in the Lippmann–Schwinger integral equations underlying the formalism in § 11.2.2.2, behavior is dominated by poles in the Green's functions at the resonance energies of the closely-spaced and the infinitely-separated adatoms, as well as by the singularity in the energy spectrum of the substrate. Making a zero-range potential approximation, they recover the structure of the asymptotic form reported by Einstein (1978). They also obtain a somewhat similar expression

assuming a separable potential. More remarkably, they derive, with suitable approximations, analytic expressions for the "intermediate asymptote" regime, for smaller separations than the asymptotic regime. In trying to make contact with experiments, they consider both wide and narrow bulk bands, surface bands, and possibly different species of adatoms. Including the possibility of interactions between heterogeneous pairs, they produce a table with at least four different power-law decay exponents.

Apparently independent of all the above work, Ebina and Kaburagi (1991) apply methods of Brovman and Kagan (1974) for finite-temperature Green's functions to study interactions on jellium substrates. By approximating surface electrons as two-dimensional objects, they implicitly focus on interactions mediated by surface states. From a step-like anomaly in the second-order susceptibility, they find a trio interaction dominated by wave vector $k_F\sqrt{3}$. In their calculations, there is also a contribution from wavevector $2k_F$. Seemingly this competition in the asymptotic regime reflects the two interaction terms in Eq. (11.21).

While most of this chapter is devoted to individual adatoms on flat surfaces, it is worth mentioning some relevant results for vicinal surfaces, i.e. surfaces misoriented slightly from high symmetry directions. On semiconductors, the energetic interactions between steps, if noticeable, are repulsive. In contrast, on metals evidence is emerging that the interactions can be oscillatory in sign. We discuss this novel application further in the § 11.4.3.

11.3. Attempts to model real systems

11.3.1. Tight-binding, jellium, and asymptotic-ansatz

The philosophy behind the single-band tight-binding calculations of ES is that the d-band is primarily responsible for the lateral indirect interactions. Burke (1976) raised doubts about the adequacy of this idea, even for refractory transition metals like W, by performing more realistic tight-binding calculations with a five-fold degenerate substrate band. His goal was to reproduce the pair data for transition metals on transition metals, gleaned from experiments performed by Tsong and coworkers (1973, 1975), Bassett (1975), and Graham and Ehrlich (1974) using field ion microscopy. Generalizing ES, Burke first showed how five-fold degenerate adatoms may be incorporated into the formation starting with Eq. (11.9) by an orbital-peeling matrix procedure. The idea was (1) to focus on one of a pair of nearby adatoms, (2) to remove it from the system orbital by orbital, and (3) to replant it infinitely far away (as though there had been originally five single-level adatoms rather than one at each site of the pair). In this procedure, the bulk is unspecified. In actual calculations, the substrate was the (100) or (110) face of a semi-infinite bcc crystal, with adatoms imagined as the same element (viz. W) as the substrate and sitting in the otherwise vacant lattice sites above the surface. All diagonal matrix elements are set at the energy zero; the possibility of having to modify what amounts to $\varepsilon_a = 0$ is discussed and dismissed, thereby neglecting

self-consistency corrections completely. Overlap is also excluded. Slater-Koster (1954) matrix elements between nearest and next-nearest sites are calculated in terms of the two sets of 3 d-d tight-binding parameters. Alas, these six values are simply scaled up from narrow band values (Pettifor, 1969), ignoring any details of hybridization with s-p electrons. To compute the substrate Green's functions, Burke combines the continued fraction approach with a scheme counting poles and zeros on the real energy axis. When the adatoms are separated by just a (bulk) nearest or next-nearest neighbor distance, a direct interaction between them can (and should) also be included. With no direct interaction, the results look similar to those of ES: oscillatory in sign, peaking in strength when ε_F is near ε_a. Inclusion of the direct interaction makes a substantial difference for small interadatom separation, leading to an attraction at all ε_F due to the bonding between the adatoms themselves (Desjonquères and Spanjaard, 1993). Overall, Burke reconfirms that the pair interaction energy has roughly the same size as in ES and that it oscillates as a function of ε_F for fixed separation and as a function of R for fixed ε_F. In a rather cursory look at decay with separation, Burke finds much faster fall-off on the (110) face than the (100); there are no analytic results. Burke was disappointed to find the calculated pair binding of a nearest-neighbor dimer on the (110) surface to be nearly five times the experimental value of 0.3 eV (Tsong, 1973; Tsong et al., 1975; Bassett, 1975). Another difficulty is that subsequent work suggests that the adsorbed W sits in a "surface site" rather than a "vacant lattice site". Burke alleges this makes little difference but gives no supporting evidence; in light of the results of ES — cf. Table 11.1, especially the difference between the two bridge configurations — this insensitivity is surprising. Burke suggests a number of sources of error, but aside from adding a Coulomb counter term or massaging parameters, it is not clear how to improve matters. His dissatisfaction with this approach was heightened when he could not explain the ordered phases of Ni(100)–O (Holloway and Hudson, 1974; Demuth and Rhodin, 1974); in this case the computed strength is typically much too *small*, of order 1–10 meV, to account for disordering temperatures.

As discussed in § 11.2.6, Flores et al. (1977a), Lau and Kohn (1978), Le Bossé et al. (1978, 1979), Johansson (1979), Johansson and Hjelmberg (1979), and Eguiluz et al. (1984) show that with a jellium substrate there are also indirect interactions of substantial magnitude. The last group in fact explore the interaction between two protons on/in Al as a function of separation, for several distances from the surface. A major result of the latter four of these studies is that the ultimate $[R^{-5}\cos(2k_FR)]$ asymptotic regime is not reached till separations R so large that the interaction is negligible. At shorter spacings, the interaction goes first like $R^{-3}\cos(2k_FR)$, as in the bulk; for larger R, typically those of most interest, the decay exponent increases smoothly to the surface value of 5. Rogowska and Wojciechowski (1989, 1990) use these ideas to consider noble-metal adatoms on jellium, using the exponent 3 exclusively (for separations larger than suggested by Johansson and Hjelmberg (1979)), offering ways to compute the charge density, from which to get k_F. While this approach may be reasonable for free-electron-like substrates, the eventual application to a W(110) substrate (Rogowska and Kolaczkiewicz 1992) seems questionable.

Proposing an alternative to the cluster-based picture of H–H interaction of e.g. Grimley and Torrini (1973), Flores et al. (1977b) consider the system Pt(111)–H. From a variety of experimental evidence, they argue that the H atoms sit in regions of high electron density, viz. center sites. They then invoke (without justification and rather implausibly) the asymptotic form of the interaction, Eq. (2.27), for five structures involving separations between one and two Pt nearest-neighbor spacings. Taking into account the coverage of the ordered phase and the idea that the assumed potential form must have a minimum at the pair spacing of the ordered structure, they deduce this spacing and the associated graphitic (2×2) overlayer, found subsequently by LEED (Van Hove et al., 1978). Noting that for most of the structures there are at least two identical nets with the particular choice of neighbor spacing, they argue for the existence of two different binding states, consistent with experiment (Christmann et al., 1976). Consistent with experiment again, these become identical at monolayer coverage, when both nets are complete (Burch, 1980).

11.3.2. Embedded cluster model

Muscat (Muscat, 1985a; Muscat and Newns, 1981) was the first to allow explicitly for contributions of both free and d-like electrons in producing lateral interactions between adatoms, in his case H atoms. In his embedded cluster model, spheres are centered on the sites of the H adatoms as well as on several nearby metal atoms in the substrate. Within the latter muffin-tin spheres, he places self-consistent bulk band-structure potentials (Moruzzi et al., 1978). The spheres are then embedded in some model of a free-electron gas, usually infinite-barrier jellium. (In some later work, the jellium contribution is taken from effective medium theory (Nørskov, 1982; Nordlander and Holmström, 1985), discussed below.) The d-wave contribution comes from the $l = 2$ solutions. Again, interaction energies are calculated from changes in all the one-electron energies. The technique was applied to a wide variety of late-transition and noble metal substrates. Pair interactions generally have the correct sign and order of magnitude to corroborate the energies deduced from Monte Carlo simulations of the experimental phase diagram (but were often off by factors of very roughly 3). In these calculations the distance d between the H proton and the jellium edge (taken as a plane half-way between the surface atoms and what would have been the next plane above the surface (Muscat, 1986)) is the only explicit adjustable parameter. By quoting the results for a few values of d, Muscat gives some idea of an intrinsic uncertainty in this approach. While the variation is not negligible, the qualitative and usually semi-quantitative results are not overly sensitive.

More specifically, this method also evaluates interaction energies based on integrations over one-electron phase shifts. For a pair of adatoms, an explicit subtraction is required (in contrast to Eq. (2.15)). As an illustration, the phase shift for a single H muffin tin centered z_0 from the infinite barrier is

$$\eta(\varepsilon) = \tan^{-1} \frac{1 - j_0(2kz_0)}{\cot \delta_0 - n_0(2kz_0)}, \tag{11.30}$$

where δ_0 is the phase shift of a single muffin tin in a free-electron gas. For two H atoms, the spherical Bessel function $j_0(2kz_0)$ is replaced by $j_0(kR) - j_0(k\sqrt{R^2+4z_o^2})$, similarly for the spherical Neumann function $n_0(2kz_0)$, and there is a second $\tan^{-1}$ term in which these Bessel functions are added rather than subtracted. To calculate δ_0 one must stipulate the spherical potential in the muffin tin; Muscat and Newns (1981) choose a simple exponential with a prefactor set to produce a bound state just below the bottom of the *sp*-band of Ni. On jellium (at the separations of *C* sites on Ni(111), neglecting any difference between "fcc" and "hcp" sites), they then find $E_1 = 900$ meV, $E_2 = -70$ meV, and $E_3 = -35$ meV. Since $E_2 < E_3$, these interactions would lead to a (1×1) rather than the experimentally observed graphitic (2×2). Next, they add a (hexagonal) cluster of (seven) spheres at the appropriate positions to represent the top layer of Ni. The effect is calculated using standard multiple-scattering (KKR) techniques, using only the $l = 2$ component of the Ni-centered spheres. To the relatively simple argument of $\tan^{-1}$ above, one subtracts summations over products of scattering matrix elements. In this case, for $d = 0$, they now find $E_1 = 450$ meV, $E_2 = 2$ meV, and $E_3 = -9$ meV. (As a measure of sensitivity, for the largest $|d|$, $d = -0.4$, $E_2 = -10$ meV and $E_3 = -19$ meV. For Cu with $d = 0$, $E_1 = 600$ meV, $E_2 = -2$ meV, and $E_3 = 0$ meV.) To calibrate these numbers, Bartelt et al. (1983) show with Monte Carlo simulations that the transition temperature at the saturation coverage of the overlayer (i.e. the correct number of adatoms to form a defect-free overlayer) is below 100 K, far below the value of 270 K determined in LEED experiments by Christmann et al. (1979).

Extending earlier work (Muscat 1984b, 1985b), Muscat (1986) gives the most comprehensive results, treating the close-packed faces of seven substrates: Ti, Co, Ni, Cu, Ru, Rh, and Pd. He first shows that the fcc site is more favorable for H adsorption than the hcp site (by about 10 meV for Ni up to 137 meV for Ru), except for Cu. Most of this energy is due to one-electron contributions, computed as described with phase shifts. To assess Coulomb corrections due to changes in electron density at the adsite, an effective medium function is computed. This correction is roughly an order of magnitude smaller, around 10 meV. The principal goal was to evaluate the relative stabilities of the ground states of various possible ordered overlayers. In this regard, pairwise interactions alone, out to sixth neighbor (i.e. third neighbor for the Ni's or the *same* kind of 3-fold site), suffice. For Ni, Co, Ru, Rh, and Pd, the dominant interaction is an attractive *sixth* neighbor (producing (2×2) islands). An unsettling feature of the numbers is that the interactions do not tend to decay with increasing separation; these attractions have the largest magnitude, except for the very-short-range enormous E_1 repulsion.

For Pd(111)–H, Muscat confesses substantial problems in comparison with experiment: his interactions are quite small, dominated by $E_6 \equiv -10$ meV, which would produce a $p(2\times2)$ rather than the observed graphitic (2×2). He also notes in comparison with EAM calculations by Foiles and Daw (1985) that he does not obtain subsurface occupation, which they found to be crucial. On the other hand, in reexamining the system Ni(111)–H with larger clusters, he basically reproduces his earlier values for E_1, E_2, and E_3 but now cites small E_4 and E_5 repulsions and a remarkable attraction $E_6 = -18$ meV (at an H–H separation twice the substrate

nearest-neighbor distance). He claims "excellent agreement with experiment" (Christmann et al., 1979). This conclusion provides an opportunity to warn the reader that there are so many degrees of freedom in these systems that one can easily be tempted into unwarranted enthusiasm. In this case, Muscat obtains not only the correct ordered state, a graphitic (2×2), but even a good estimate of the disordering temperature for the saturation coverage. However, a more detailed look at the experiment reveals a fairly broad (2×2) region in the phase diagram which disorders continuously to a disordered state. In a Monte Carlo simulation using Muscat's interactions, Roelofs et al. (1986) find, in contrast, a very narrow pure (2×2) region surrounded by very broad coexistence ("island") regions produced by the anomalously strong 6th-neighbor attraction. Roelofs (1982) and Nagai (1984) both wrote down sets of interactions based on fits to the whole phase diagram rather than on any microscopic computation; their sets had relatively weaker E_6 interactions and stronger shorter-range repulsions.

Another problem with the embedded cluster model is that it is expensive to extend the clusters, since the number of spheres grows rapidly with number of shells. Reduced symmetry in the clusters severely complicates the calculation, making it taxing to include local distortions. In general, there is no unambiguous way to find the parameter d nor to assess the accuracy. It is not clear what would happen for a transition metal with wider d-bands or for a more complicated adsorbate. In spite of these criticisms, I hasten to add that these calculations were the state-of-the-art in their time. They made several clear predictions and usually produced energies with sensible magnitudes.

Special cautionary case Fe(110)–H

Muscat's (1984a) most extensive tabulation of trio energies is in his treatment of Fe(110)–H. Experimental determination of the adsorption site was problematic. Adsorption was first thought to occur in the long-bridge site (based on LEED (Imbihl et al., 1982)) and then in the short-bridge site (based on EELS (Baró et al., 1981)), a conclusion consistent with Muscat's calculations. The system has an interesting phase diagram with a phase transition that was thought to be highly unusual. Painstaking calculations (Kinzel et al., 1982; Selke et al., 1983) using lattice gas models were performed to elucidate the system. Eventually, however, they were supplanted by the conclusion from detailed LEED work (Moritz et al., 1985) that H sits in the quasi-three-fold site and that the ordered phases observed in LEED have different real-space symmetry.

11.3.3. Effective medium theory and embedded atom method — semiempiricism

The first of the semiempirical methods (Nørskov 1977), effective medium theory (EMT) begins with the self-consistent calculation of the function $E_{c,Z_i}(\bar{\rho})$ of an atom i, with nuclear charge Z_i, in a homogeneous electron gas of density $\bar{\rho}$. (This laborious calculation need be done only once. While this procedure to get $E_{c,Z_i}(\bar{\rho})$ is typical, Nørskov (e.g. 1993) mentions an alternative.) For non-noble-gas atoms, these functions have a simple shape with a single minimum at a value on the order

of 0.1 bohr^{-3}. In a solid each atom sits in the tails of the electronic charge density of its neighbors. The total energy of a solid is then approximated, to first order, by the sum of $E_{c,Z_i}(\bar{\rho})$ for all atoms i. Here $\bar{\rho}$ is the average over the atomic sphere. There are correction terms due to electrostatic effects (discussed in § 11.2.1) and to changes in one-electron energy sums, say between an adsorbed system and the same atoms before adsorption (essentially the topic of § 11.2.2). An early application was to adsorption on jellium (Nørskov and Lang, 1980), with later studies of transition metal substrates, reviewed by Nørskov (1994). Variants of this method are the quasi-atom approach (Stott and Zaremba, 1981) and the corrected effective medium theory (Raeker and DePristo, 1989, 1991).

Applications of EMT to adsorbate–adsorbate interactions has centered on the issue of poisoning and promoting by preadsorption (Nørskov 1993, 1994). Most of this interaction is electrostatic and was discussed earlier in § 11.2.1. From another perspective, the role of rehybridization, i.e. altering of the chemical nature of the adsorption bond, has been stressed by Feibelman and Hamann (1984) and by MacLaren et al. (1987). These calculations focus on the change in the local density of states around metal atoms due to preadsorbed electropositive or electronegative atoms. Part of this change is electrostatic, but the rest, in EMT language, must be attributed to one-electron effects, i.e. the sort of covalent aspects discussed in § 11.2.2.

There is a general result that emerges nicely in EMT (Nørskov 1993) that will be useful in later analyses. If one plots the cohesive energy of an fcc metal as a function of coordination number for fixed interatomic spacing, the curve does not decrease linearly as it would for a simple nearest-neighbor pair interaction model. Instead the decreasing curve has a positive second derivative. The effective pair interaction, defined as the derivative of this curve, is therefore enhanced for small coordination numbers (below 5) and diminished for larger such numbers (above 5 or 6), compared to (1/12) the bulk cohesive energy. Thus, interactions on surfaces should be considerably smaller than one would predict based on near-neighbor bond models gauged by bulk cohesive energy.

The semi-empirical embedded atom method (EAM) (Daw et al., 1984, 1993; Foiles et al., 1986) has offered a relatively easy way to contend with the low-symmetry problems. In this approach, the cohesive energy is written

$$E_{\text{coh}} = \sum_i F\left(\sum_j{}' \rho^a(R_{ij})\right) + \tfrac{1}{2}\sum_{ij} U(R_{ij}) \tag{11.31}$$

where the ρ^a's are spherically-averaged computed atomic electron densities, the prime on the summation indicates $j = i$ is excluded, and U is the electrostatic Coulomb repulsion $Z_iZ_je^2/|R_{ij}|$. The effective charge densities Z inserted into U are determined by the formula $Z(R) = Z_0(1 + \beta_z R)\exp(-\alpha_z R)$. The embedding energy can be determined numerically by embedding an atom in a homogeneous background, as in effective medium theory (Nørskov 1982, 1994) or by using the "universal" binding curve of Rose et al. (1984):

$$E(a) = -E_b(1 + a^*)\exp(-a^*),\ a^* \equiv (a - a_0)/\lambda \tag{11.32}$$

where a_0 is the equilibrium separation. Typically, the parameters are adjusted to fit the bulk properties such as lattice constant, cohesive energy, and elastic constants (e.g. λ can be obtained from the bulk modulus). For adsorption of one species on another, one can fit adsorption position and vibration frequencies (Voter, 1987). In the "glue model" (Ercolessi et al., 1986, 1988) (and for Voter-Chen (1987) potentials) one fits, in addition to F and U, the atomic density ρ (Tosatti and Ercolessi, 1991). The fact that fitting functions are not uniquely specified leaves the method vulnerable to criticism, but alternatively can be viewed as a strength in that one can tailor functions for specific applications and gauge uncertainties by use of different sets of functions. In contrast, in an earlier but similar scheme, Finnis and Sinclair (1984) took the functions F to be proportional to the negative square root (of ρ), as they would be in the lowest approximation to a tight-binding model.

Since the numbers produced by EAM and similar calculations can be tuned somewhat arbitrarily, they are most useful in identifying trends and rough magnitudes that do not depend on the detailed choices. For high-symmetry systems more exacting band-structure techniques become feasible and offer more reliable information. (However, the flexibility of EAM can often lead the practitioner to unexpected structural revelations that might elude someone calculating with a scheme that depends on human ingenuity to determine the likely choices for equilibrium sites. For example, for Pd(111)–H the existence of subsurface sites and their domination of the interactions needed to describe the phase diagram (Felter et al., 1986; Daw et al., 1987) were discovered "by accident" during dynamical simulations!) EAM is quite helpful in assessing the effects of coordination number on bonding. This theme underlies more exact work by Feibelman, to be discussed below. The driving program developed at Sandia-Livermore easily allows for substrate relaxations or for preventing the motion of any atom in any direction. On the other hand, since there is no Fermi surface in the method, EAM cannot describe any effect involving Friedel oscillations, such as the asymptotic form of lateral interactions.

In EAM calculations of Ni(111)–H and Pd(100)–H, Einstein et al. (1990) assessed the ability of EAM to predict lateral interactions. The origin of the interaction in this framework comes from the change in the argument of the embedding functions of the atoms in the cluster of atoms in the vicinity of the adatoms. Presuming the overlap of the adatoms is negligible and their atomic density decays fairly rapidly, the primary contribution to the interaction, in the EAM formulation, comes from substrate atoms "touching" both adatoms. Specifically, by expanding the embedding functions, we focus attention on the effect of a small increase in density due to a second adatom adding density to a substrate site (Foiles, 1985):

$$\Delta E_{\mathrm{coh}} \cong S \sum_j \left[F'_i(\bar{\rho}_i)\, \rho_j^a(R_{ij}) + F''_i(\bar{\rho}_i) \left\{ \rho_j^s(R_{ij}) \right\}^2 \right] \tag{11.33}$$

To lowest order, the positive curvature of $F(\rho)$ leads EAM to predict repulsive interactions, with their magnitude proportional to the number of shared substrate

nearest-neighbors (except at the shortest separations, when direct interactions can overwhelm the physics). We will find a similar result below in a second-moment, tight-binding picture (cf. Eq. (11.37)). In first-principles calculations Feibelman (1988b, 1989a) found such a repulsion for Al–S and Al–Te dimers on Al (100) and for H–S on Rh(001).

Furthermore, for trio interactions, EAM is rather insensitive to the configuration of the trimer: because the charge densities are spherical, the only dependence of the trio interaction on the angle (as opposed to the length of the legs) of the trimer comes from substrate relaxations. Such relaxations are particularly small for close-packed (111) fcc surfaces (cf. Wright et al. (1990), discussed near the end of § 11.3.5, for evidence that a (100) fcc surface can be expected to have significant relaxations.) Thus, for (111) fcc surfaces, in EAM one can to good approximation replace explicit treatment of trios (and higher-order multi-atom terms) by pair energies which depend on coordination (Fallis et al., 1995). While this approximation may be reasonable for the systems for which EAM works well, viz. late transition and noble metals, it is unlikely to be viable for most refractory transition-metal systems (even their closest-packed (110) bcc faces), since angle-dependent bonding is important; cf. § 11.3.5. On the other hand, when viable it can be very helpful when doing simulations, and it highlights the idea that high-coordination atoms bind less strongly to another atom than low-coordination atoms. In the bond-saturation model (BSM), one posits that the cohesive energy of each atom depends only on its (nearest-neighbor) coordination. For the particular case of Pt(111), Fallis et al. (1995) report that the bonding of adatoms can be characterized simply by a quadratic expression $A + Bz + Cz^2$. Here z, the coordination number within the adlayer, ranges from 1 to 6, $A = -961.423$ meV, $B = 97.5456$ meV, and $C = -4.86116$ meV. The positive value of B is a reflection of the positive curvature of the embedding function in EAM. The strength of the interaction between two adatoms with coordinations z_1 and z_2 is then the average $A + B(z_1 + z_2)/2 + C(z_1^2 + z_2^2)/2$. The same tactic can be applied more generally to problems in growth, where the total coordination rather than just that in the overlayer is considered. The dependence of bond strength on coordination was already discussed early in this section in the context of EMT and is reconsidered in § 11.3.6.

For Ni(111)–H only the first-, second-, and third-nearest neighbors are above 1 meV, since only these involve shared substrate atoms. Their magnitudes are comparable to those found by Muscat (1984b, 1985b, 1986) but all are positive, consistent with behavior deduced from Monte Carlo fits of the phase diagram (Roelofs et al., 1986). We find a tiny attractive trio interaction for the smallest equilateral triangle of adatoms in the same kind of three-fold site, comparable in size to that found by Muscat but of the opposite sign. Overall, the signs of the interactions seem more reliable than Muscat's, and there are no anomalous attractions, but since the second-neighbor repulsion is less than 3/2 of the third, a $p(2\times1)$ overlayer is predicted instead of the observed graphitic (2×2) (or (2×2)–2H) (Christmann et al., 1979). Truong et al. (1989) extend EAM to a procedure called EDIM (embedded diatomics-in-molecules); they obtain magnitudes for the lateral interactions more consistent with expectations from experiment, but with the same

sign as we found. There are a number of modifications, with no commentary on the effect of each. A likely possibility is the allowance, for Ni's in the top layer, of a different number of s-electrons from the bulk value.

Since EAM successfully treated alloying at surfaces and phase transitions of one noble metal on another (Foiles 1987), we expected (Einstein et al., 1990) that late transition metals adsorbed on each other would be more accurately described in EAM. Wright et al. (1990)'s studies of Pt, Pd, and Ni on Pt(100) bear out this belief. We defer this discussion, as well as comparisons between EAM and tight-binding results, until the end of § 11.3.5.

Another issue of concern for adsorbates is the large charge gradient near surfaces. For the reconstruction of Au(110), EAM predicts (Foiles 1987) a (1×3) pattern rather than the observed (1×2). To rectify this problem, Roelofs et al. (1990) include the leading correction from such gradients, using Daw's (1989) modification of EAM formalism. Moreover, to treat this system with Monte Carlo simulations, they decompose the interactions of Au atoms in the top layer, finding that not only are trios significant, so are "quartos" (i.e. the interaction energy of four surface atoms minus the constituent pairs and trios); even the close-packed "hexto" interaction has a strength −3.4 meV. To assess the role of the gradient contribution, I quote some numbers for pair interactions I computed in an early stage of this project before the corrections were implemented: for adatoms on neighboring rows, at the same position along the row or shifted by one unit (so somewhat diagonal), the interactions are −10 and +17.6 meV, respectively, without the gradient term vs. −2.6 and +12.3 meV with corrections. In short, the gradient corrections do not change the qualitative results but are important for quantitative assessments.

More recently, Haftel (1993) proposed that many of the problems in applying EAM to surfaces could be cured by increasing the curvature of the embedding functions $F(\rho)$, particularly on the low-density side of the bulk value. The impact of this procedure on pair interactions has not yet been explored.

11.3.4. Empirical schemes

To illustrate why EAM and related calculations are called semi-empirical rather than empirical, in spite of the several adjustable parameters, we present an example of a truly empirical scheme. To take advantage of the success of computationally intensive schemes such as FLAPW (Wimmer et al., 1981) to compute details of monolayer adsorption, Gollisch (1986) constructed an effective potential U_i, a generalization of the Morse form, with several parameters to be fit to the numerical "data":

$$U_i = \sum_{i \neq j} b_{ij} \left[Q_{ij}(\boldsymbol{r}_{ij})\right]^{s\mu\lambda_{ij}} - \left\{ \sum_{i \neq j} a_{ij} \left[Q_{ij}(\boldsymbol{r}_{ij})\right]^{\lambda_{ij}} \right\}^{\mu} \tag{11.34}$$

The two global parameters s and μ, on which the quality of the potential depends sensitively, adjust the exponents of competing terms. Three more parameters, a, b, and λ, adjust the scale and exponent of a separation-dependent interaction function Q, here a sum of two exponentials, introducing four more parameters. These seven

parameters, computed from bulk properties, are tabulated for each element of interest. The off-diagonal a, b, and λ (i.e. those for differing atoms) are computed as the geometric mean of those values for the two constituents.

As a test of the accuracy of the numbers produced by this scheme, Roelofs and Bellon (1989) compute the resultant phase diagrams, using transfer-matrix finite-size scaling, for Cu and Au on W(110). In both cases the pair interactions for the three shortest separations are all attractive, indicating the formation at low temperatures of coexistence between a low-coverage lattice "gas" and a high-coverage lattice "liquid", both with (1×1) symmetry. Accepting Gollisch's pair values, they try to fit the experimentally determined phase boundary by tuning the multisite interactions. For W(110)–Cu the "quarto" interaction is negligible while they estimate that the (repulsive) trios underestimate the actual values by about a factor of two. For W(110)–Au they find that if they include the repulsive trio interactions computed by Gollisch (as well as the attractive pairs) then to fit the temperature-coverage phase boundary would require a *repulsive* rather than the computed attractive quarto (with a magnitude at least a third smaller).

11.3.5. Field-ion microscopy, modern tight-binding, and more on semiempiricism

While field ion microscopy (FIM) has long been arguably the most direct and convincing way to see atoms on surfaces, only in the last decade or so have technological advances made it possible to accumulate enough data to contribute detailed quantitative information about the interaction between adsorbates. In the earlier years of this work, it was necessary to azimuthally average data in order to obtain tolerable statistics (Tsong, 1973). Casanova and Tsong (1980, 1982) plotted the pair interaction energy of Ir–Ir, of Ir–W, and of Si–Si on W(110) as a function solely of separation; hence the oscillating curve added to guide the eye actually misleads it: this plotting strategy might be satisfactory for physisorbed atoms (which are not amenable to FIM), but it obscures the anisotropy that we have seen to be ubiquitous and significant. Moreover, Watanabe and Ehrlich (1991) comment that such a plotting scheme could mislead one into thinking that a diffusing adatom could get trapped between two radial barriers in the potential, when in fact the adatom can skirt the repulsive sites because of the strong anisotropy of the interactions.

In recent years it has become possible to accumulate enough data to assess interactions between pairs of adatoms at dozens of distinct separations, as best illustrated by an intensive set of experiments by Watanabe and Ehrlich (1989, 1991, 1992), Ehrlich and Watanabe (1991). This process can be eased by using two different atoms, one of which bonds more strongly than the other, so that one can study equilibration at a temperature at which only the more weakly bonded atom is mobile.[1] An additional advantage is that the stationary atom can be set near the

---

1 This idea dates back at least to 1977, when Cowan and Tsong (1977) studied the interaction between a W adatom and a substitutional Re atom on W(110). Without benefit of a PC image digitizer, they found strong deviations in the site distribution from random (viz. the same measurement with no Re atom substituted).

center of a facet, minimizing the number of "snapshots" with an adatom near the edge of the terrace, where fringe fields make the data questionable. Accordingly, Watanabe and Ehrlich (1989, 1991) fix a W or a Re atom near the center of a W(110) plane on a FIM tip and monitored the distribution of a mobile Pd atom. They observe that Pd is most frequently found at the nearest-neighbor position of the fixed adatom, but the nearby second and third neighbor sites are not populated. From 1638 observations of a Re-Pd pair equilibrated at 205 K, they deduce $E_1 = -36.8 \pm 1.0$ meV, $E_2 \gtrsim 45$ meV, $E_3 \gtrsim 45$ meV; from 1288 observations of a W–Pd pair equilibrated at 225 K, they find, rather similarly, $E_1 = -50.4 \pm 8.0$ meV, $E_2 \gtrsim 40$ meV, $E_3 \gtrsim 40$ meV. (Actually, these are free energies rather than energies; we neglect the distinction in quoting numbers. See § 11.4.2 for more comments on the analysis.) Along the close-packed [1$\bar{1}$1] the interactions are attractive out to ~10 Å. The decay in strength is monotonic except for the second site (E_4), which is considerably smaller, giving an oscillatory appearance to the decay vs. R. Along the [001] direction the interactions tend to be repulsive, along the [110] beyond one spacing, they tend to be weakly attractive, in both cases with some exceptions. Overall, then, the interaction is highly anisotropic and oscillatory in sign, extending to large separations, with no simple pattern, i.e. consistent with the general picture presented in § 11.2.2.

With further work they were able to observe pairs of identical adatoms, Ir–Ir (Watanabe and Ehrlich, 1989, 1992) and Re–Re (Watanabe and Ehrlich 1992) on W(110). From 2232 observations of the Ir pair equilibrated at 375 K, they find qualitatively similar behavior to the two heteropairs: $E_1 = -86 \pm 2$ meV, E_2, $E_3 \approx 70 \pm 30$ meV. In all directions there are oscillations in sign and non-monotonic decay in amplitude (see Fig. 11.6). From 3145 observations of the Re pair equilibrated at 390 K, they find different behavior in that the interaction is repulsive at all close spacings: $E_1 = +21.5 \pm 9.3$ meV, E_2, $E_3 > 70$ meV. At larger R, the interactions again become attractive and are dependent on the orientation of the pair on the surface; the interaction is oscillatory and anisotropic. Watanabe and Ehrlich (1992) also try to assess the trio interaction. It is not feasible to measure this interaction directly because at the temperatures at which trimers dissociate, the liberated adatoms quickly move to the edge. From an Arrhenius plot of lifetimes of linear (straight) trimers, they deduce a dissociation energy, from which they subtract the diffusion barrier E_d to find the trimer binding energy. From this they subtract the pair energies of the three legs of the trimer to obtain an attractive trio interaction of -130 ± 70 meV for the linear (L) configuration. On (110) bcc surfaces there are two other trimer configurations with two nearest-neighbor pairs (i.e. legs in the [111] direction): nearly equilateral (P for "pointed"), and H_2O-like (O for "open" or bent). For Re the trio interaction is even more dramatic, stabilizing L and O trimers in spite of the short-range repulsions, with energies of –240 meV and –210 meV, respectively (Fink and Ehrlich 1984b), suggesting trio attractions of –340 meV and at least –380 meV, respectively; the P trimer is unstable, so has a quite different trio energy. In both cases the adatoms are at neighboring sites and are comparable in size to the substrate atoms, so that direct interactions undoubtedly play a dominant role in these interactions, which are much stronger (relative to the constituent pairs) than expected from § 11.2.3.1.

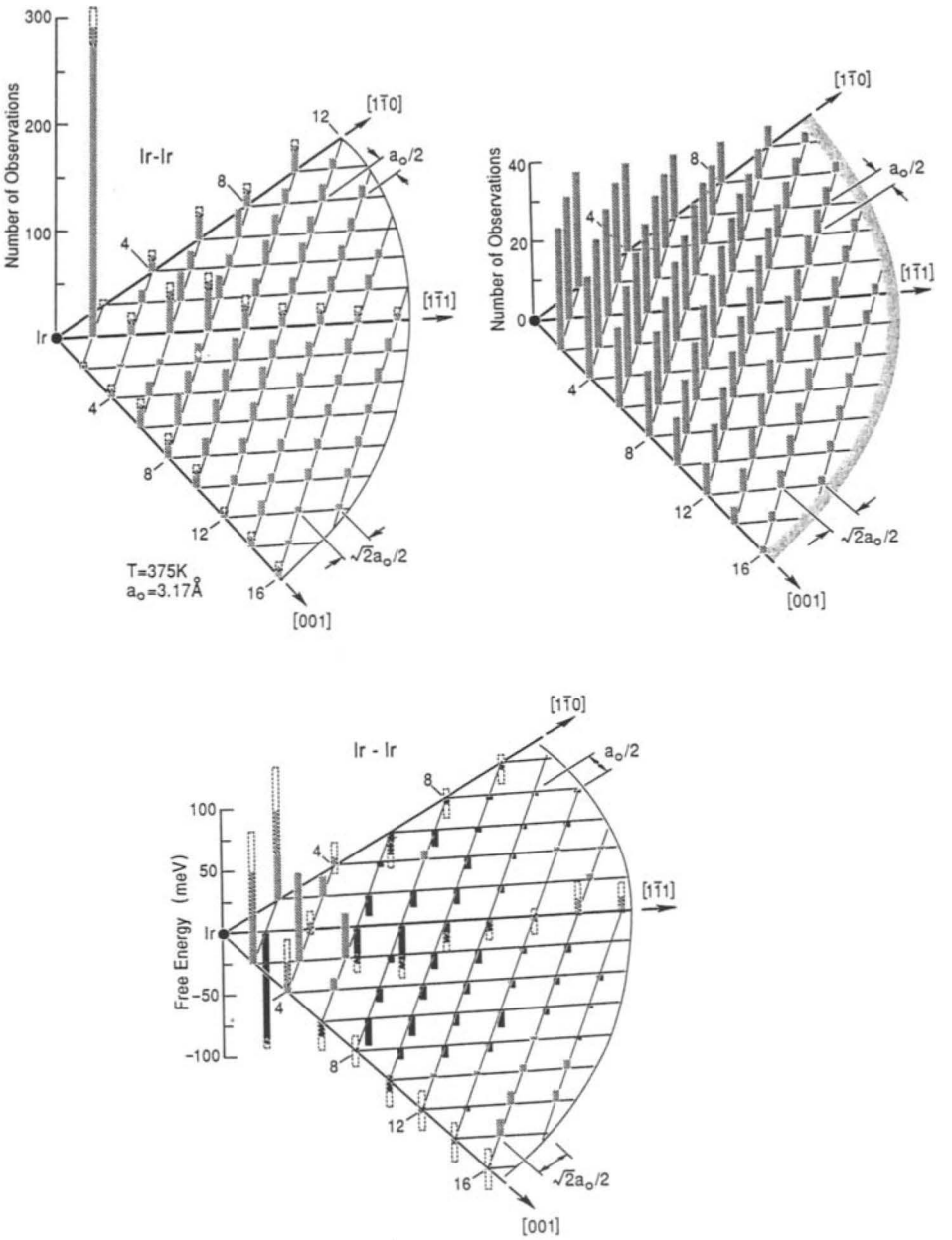

Fig. 11.6. (a) Distribution of separations between two Ir atoms on W(110) at 375 K. Observations over the entire surface have been folded into a quadrant, and distant separations not plotted. (Along the bounding axes the number of observations is doubled.) (b) Distribution of separations between two noninteracting identical atoms on W(110). (c) From the ratio of these two distributions, the (free) energy of interaction between the Ir pair is computed and plotted as bars vs. $\boldsymbol{R}$. Gray bars indicate repulsions, black bars attractions. Standard errors are shown at a few locations, based on statistical uncertainty. From Watanabe and Ehrlich (1992), with permission.

Unfortunately, many kinds of atoms cannot be probed with FIM: FIM is largely limited to refractory transition metals. Scanning tunneling microscopy (STM) does not share this restriction; it has been used to examine a breathtaking range of systems (Güntherodt and Wiesendanger, 1992). On the other hand, one cannot quench a whole (STM) sample nearly so quickly as one can an FIM tip[1] to get "snapshots" of rapidly evolving configurations, even if one has a low-temperature STM. If the STM scan time is not fast compared to the hop rate of the adatoms, the analysis is considerably more difficult. (Cf. Giesen-Seibert et al., 1993.)

Much of the theoretical work in the 1980s on pair interactions was spurred by earlier FIM measurements of transition metals on (other) transition metals. In examining the dimer attraction for the 5-d series on W(110), Bassett (1975) measured a striking minimum for Re, with a rapid linear increase in attraction for lower Z and a slower increase for heavier Z. This observation was particularly intriguing because the adsorption energy and activation energies where largest in the middle of the series and so motivated Desjonquères and Spanjaard (1993) and coworkers to undertake several theoretical studies. Bourdin et al. (1985) propose a very simple analytical model. They claim that Burke's excessively large energies were due to his neglect of both core-core repulsions and electronic correlations (but cf. § 11.2.4), which they compute to second order in U/w, where U is the Hubbard-like intraatomic Coulomb repulsion and w the bandwidth. Bourdin et al. consider linear trimers at nearest-neighbor separation. They make several simplifying assumptions: (1) The substrate is rigid and the adatoms sit exactly at high-symmetry sites. (2) The core–core repulsion is the same for all the adsorbates. (3) The one-electron, "band" contribution comes solely from broadening of the adsorbate levels. Thus, the dominant interaction is directly between adsorbates rather than through the substrate. This ansatz is only reasonable at short spacings. (ES explicitly neglected these direct effects in their tight-binding calculations.) (4) The local density of states increases with coordination number (as one would expect from tight-binding theory) and is taken to be constant over an energy range (as for a 2D band). (5) The Coulomb integral U is the same for adatom, dimer, or trimer and independent of N_a, the number of d-electrons on the adatom. The band contribution to the dimer interaction energy E_1 is

$$E_1^{\text{band}} = -10(N_a/10)\,(1 - N_a/10)\,(w_1 - w_\infty) \tag{11.35}$$

where $w_1 - w_\infty$ is the increase in the width of the rectangular local density of states due to bringing the adatoms to neighboring sites. This contribution alone would produce the expected but incorrect result of maximum binding at $N_a = 5$. The additional contribution from correlation,

$$E_1^{\text{cor}} = -90U^2(w_1^{-1} - w_\infty^{-1})\,[(N_a/10)\,(1 - N_a/10)]^2 \tag{11.36}$$

---

1 Watanabe and Ehrlich (1991) note that FIM tips can be cooled from a high equilibration temperature of 350 K to the imaging temperature of 80 K in under 5 seconds.

is positive and tends to destabilize the dimer. They also consider trimer energies, adjusting U first to produce the experimental dimer pair energy. The estimated trio energies are (with a small exception) attractive and range from the same magnitude as the pair energy down to below an order of magnitude smaller. Olès et al. (1988) consider the magnetic contribution, which they find to be repulsive by a similar amount because the magnetic moment on the Re atoms decreases considerably when the dimer forms. Bourdin et al. (1987) find that on more open bcc surfaces (viz. W(211) and Ta(211)), on which the adatoms can increase their coordination number by additional bonding to subsurface atoms, the repulsive contributions decrease or disappear, and the maximum bonding of 5d dimers occurs near half filling. In this study the local density of states for the calculation of the band contribution comes from a continued-fraction expansion of the Green's function. Desjonquères et al. (1988) also apply their approach to compute potential energy curves for adsorption of gas dimers on bcc substrates.

Desjonquères and Spanjaard (1993) present an appealing, simple argument stemming from this work that predicts that a repulsive interaction between adatoms close enough to share N common substrate bonding partners but too far apart to interact directly. When the (z-coordinated) adatoms are far apart, there are $2z$ substrate atoms which gain an extra bond to an adatom; their band energy is proportional to $-(\mu + \beta^2)^{1/2}$, where μ is the centered second moment of the density of states of an atom on the clean surface and $\beta \propto V$. When adatoms share N host atoms, their band energy $\propto -(\mu + 2\beta^2)^{1/2}$ while the energy of the other $2(z-N)$ substrate atoms is unchanged. Finally, at close range only $2z-N$ surface atoms are coupled to adatoms, N fewer than at large separation. Hence, in this second-moment picture, the pair energy $E_{(N)}$

$$\begin{aligned} E_{(N)} &\propto -N\sqrt{\mu + 2\beta^2} - 2(z-N)\sqrt{\mu + \beta^2} - N\sqrt{\mu} + 2z\sqrt{\mu + \beta^2} \\ &\propto N(2\sqrt{\mu + \beta^2} - \sqrt{\mu + 2\beta^2} - \sqrt{\mu}) \geq 0 \end{aligned} \tag{11.37}$$

This generic result was noted above for EAM in conjunction with Eq. (11.31).

In a more sophisticated study, Dreyssé et al. (1986) find similar results for W(110)–Re. Also considering only d-electrons, they consider the same three contributions, treating the one-electron energy using 5-fold degenerate tight-binding bands, the correlation energy using second-order perturbation theory (but with local atomic densities computed from their Green's functions), and the repulsion using Born-Mayer interactions. They also take some account of self-consistency by shifting atomic levels (cf. § 11.2.4.) They compute interaction energies for the three trimer configurations, L, P, and O, as well as the six shortest-separation pairs. For the pairs, including correlation energy with intra-atomic Coulomb integral $U = 1.6$ eV has a considerable effect, in most cases reversing the sign of the interaction; U is taken as just big enough to make the nearest-neighbor pair interaction repulsive, to reproduce experiment. Making use of an effective coordination number, they obtain for Re on W(110) the nearest-neighbor pair interaction

$$E_1 = -(2\sqrt{2.8 + \zeta} - 3.35)\, E_{coh}^{bulk} \sqrt{10.4} \tag{11.38}$$

and for the L trimer interaction (lamentably called "trio"), i.e. trio plus 3 constituent pairs

$$E(\mathrm{L}) = -(2\sqrt{2.8 + \zeta} + \sqrt{2.8 + 2\zeta} - 5.04)\, E_{coh}^{bulk} \sqrt{10.4} \tag{11.39}$$

Here ζ is related to the square of the interadatom hopping. With no direct interactions ($\zeta = 0$), both energies vanish. With direct interactions ($\zeta = 1$), they estimate $E_1 = -1.5$ eV and $E(\mathrm{L}) = -2.9$ eV. Additional correlation effects (since some are seemingly included in the total energies leading to the formulas) counteract these unphysically large numbers. The correlation contribution is about 10% of the band contribution and is most important for the half-filled band. If local charge neutrality is invoked (Bourdin et al., 1985), the P-trimer is favored, inconsistent with experiment (Fink and Ehrlich 1984a,b). This configuration is destabilized by correlation energies computed in first-order perturbation theory, stemming from charge transfer.

Very recently Xu and Adams (1994, 1995) have developed a semiempirical scheme for treating bcc transition metals with minimal non-d bonding (i.e. with about half-filled d-bands). In the spirit of the Finnis-Sinclair (1984) method discussed after Eq. (11.32), they seek to approximate a tight-binding model. However, rather than using just a second moment (so square root) approximation to describe the d-band width, they follow Carlsson's (1991) approach and also include third and fourth moments to describe the band shape, in particular three- and four-site contributions. (Recall that the nth moment of a nearest-neighbor tight-binding model counts paths that return to the origin after n nearest-neighbor steps.) For each metal (W, Mo, and V were studied), the model contains 10 adjustable parameters: one to weight each of three computed moment terms, five to characterize the pair potential (i.e. the $U(R_{ij})$ of Eq. (11.31)), and a pair of radial cut-offs for the pair potential and for the moment terms. These are determined by fitting to 12 *bulk* properties, 2 calculated energy differences with other lattice structures and 10 measured properties: sublimation energy, lattice constant, relaxed vacancy formation energy, 3 elastic constants, and 4 zone-edge phonon frequencies. The model differs from a similar one by Foiles (1992) by including the third-moment term and by using different fitting criteria, demanding in particular that W(100) and Mo(100) reconstruct. To test the model, Xu and Adams compute surface properties. The relaxations agree well with experiments and larger-scale computations, and the surface energies do not suffer the great underestimation well known to occur for EAM. On the other hand, the calculations require two orders of magnitude more CPU time than EAM.

Xu and Adams (1995) recently applied their model to the pair interaction between W atoms on W(110). As observed in some previous studies of bcc (110) substrates (cf., e.g., Williams et al. (1978), Roelofs and Bellon (1989)), the pair of quasi-three-fold sites have lower energy (in this study by a mere 8.8 meV) than the bridge site between them, where the next layer would grow. The main findings are that the interactions are strongly anisotropic (consistent with the highly anisotropic

band structure) and oscillatory in any particular direction. At large separations, the interaction is slightly repulsive. The authors attribute this effect to strain fields, which might well mask electronic effects at large separations; this notion could be confirmed with a calculation of interactions with the strains prohibited by hand ("frozen out"). In comparing with Watanabe and Ehrlich's (1989) data for Ir pairs on this surface, the authors find general agreement, particularly when one allows for the experimental error bars. A detailed comparison between calculated W pairs and measured Ir pairs seems risky, since Re pairs differ notably from Ir pairs on this substrate, and Re is closer to W on the periodic table. The authors fret that their computed interaction for nearest-neighbor W pairs along the ⟨111⟩ direction is too strongly attractive at –2.633 eV, while for Ir the measured attraction is just –0.082 eV. Recalling Burke's (1976) result that the strong attraction between neighboring W's is due to *direct* interaction, one would expect the Ir attraction to be at least somewhat weaker since Ir atoms are smaller than W's. Xu and Adams present a discussion of the signs of short-range interactions in terms of bond coordination numbers and changes in bond strength with bond length (again, with no frozen-lattice calculations to quantify the effects); such effects are discussed at length in the next subsection.

For Pd(100)–H EAM calculations (Einstein et al., 1990) find that the minimum for H atoms to be slightly below the top Pd plane rather than slightly above. The magnitudes of the lateral interactions are more consistent with experiment, viz. 87 [94], 54, and –9 meV for the first-, second-, and third-neighbor interactions, E_1, E_2, and E_3, respectively. (The bracketed value for E_1 is obtained from analysis of ordered overlayers. By symmetry, local distortions that plague the isolated pair are removed.) However, since E_2 is more than E_1, a $p(2\times1)$ ordering is predicted rather than the $c(2\times2)$ observed by Behm et al. (1980). (This problem as well as the too-low binding site may be due to use of rather primitive EAM functions which were readily available for Pd.) The smallest-area right-triangle configuration has a trio energy $E_{RT} = -25$ meV; it plays no role in the balance between these two ordered states but does affect the phase diagram, as we will see shortly. It may not be a coincidence that the placing of H lower into the surface than in reality leads to more realistic binding energies: for Pd(111)–H (Felter et al., 1986; Daw et al., 1987) as noted above, the interactions producing the ordering come from the *subsurface* H's; those on top of the surface have little interaction, as for Ni(111).

For comparison, Stauffer et al. (1990) have used a state-of-the-art tight-binding approach to present a wealth of information on H atoms near Pd(100). The H atoms are only allowed to sit in lattice planes of the substrate lattice, so the results for the center site of the top layer are the ones of most interest. Then E_1, E_2, and E_3 are +14, –182, and +41 meV, respectively. Removing the constituent pair interactions from their tabulated trimer energies, I find that $E_{RT} = -32$ meV and the "linear-triangle" configuration $E_{LT} = -72$ meV. It would be interesting to know how these numbers would change if the H's were moved slightly above the surface; since the dependence on layer index is not monotonic, there is no obvious interpolation. In comparison with our EAM numbers, the tight-binding E_{RT} is quite similar but E_{LT} is much bigger than expected even in crude calculations and certainly in EAM. Moreover,

the pair interactions are starkly different. While their pair energies do lead to the observed $c(2\times2)$ ordered phase, the enormous size of E_2/E_1 would produce a broad coexistence region of $c(2\times2)$ + "gas" that persists to a temperature close to T_c of the pure $c(2\times2)$ phase (Roelofs et al., 1986). Binder and Landau (1981) had in fact conjectured such regions (of more modest size) on the basis of Monte Carlo simulations. Such a stable coexistence region would presumably have been observed in experiment (Behm et al., 1980). It is my understanding that subsequent experimental investigation of the low-T, low-coverage region produced no evidence of islands, and so nothing was published. On the other hand, it is conceivable that the islands could be the stable phase at so low a temperature that the adatoms cannot diffuse adequately to achieve the equilibrium configuration.

Motivated by FIM measurements, Wright et al. (1990) applied EAM to Pt, Pd, and Ni on (center sites of unreconstructed) Pt(001). Their main goal was to study whether, for small clusters of adatoms, linear chains or compact islands were more stable by computing the cluster binding energy, i.e. the difference between the total energy of the slab plus cluster of adatoms and the same number of adatoms isolated from each other. For Pt clusters, chains are preferable for clusters of 3 and 5 atoms; otherwise (up to 9 atoms) compact islands are favored, by a small but ever greater amount as size increases. These preferences are consistent with experiments by Schwoebel et al. (1989). For Pd the results are nearly the same (except for 5-atom clusters); in sharp contrast, for Ni the compact configurations of the clusters are usually not bound, so chains are favored by a considerable amount. (Presumably relatedly, Chen and Tsong (1991) find with FIM that Ir trimers form chains on Ir(100) but clusters on Ir(111).) Wright et al. (1990) find that substrate relaxation is a key factor in these interactions. On a frozen slab, compact islands are always preferable for Pt and Pd, and by a more substantial margin for larger clusters; even for Ni, the compact shape is favored for several sizes. For each type of adatom and each size, the relaxation contribution (the difference between total energy and that with a rigid substrate) favors the island configuration. The essence of this difference is that most of the relaxation occurs in the top layer along the circumference of the cluster, which for given size is clearly longer for the chain shape. Specifically, around an isolated Pt adatom, the four substrates relax laterally outward by 0.18 Å and upward by 0.08 Å. For an atom next to the center of a 4-atom chain, these numbers roughly double to 0.39 Å and 0.13 Å, respectively, while for an atom at the side of a 4-atom square, they scarcely increase, rising to 0.23 Å and 0.09 Å, respectively. Furthermore, the substrate atom at the center of the square cannot (by symmetry) relax laterally and sinks inward by 0.21 Å. There is no discussion of the heights of the adatoms when close together compared to when isolated.

If one allows for these relaxations, it becomes difficult to define the sorts of lateral interactions we have been discussing. Nearest neighbors near the center of a chain will have a different E_1 from those near the end; moreover, the size of these interactions will depend on the length of the chain. Except for Ni, the energies associated with the relaxations are smaller by a factor of about 1/2 or 1/4 than the energies for a frozen substrate. While the relaxation issue becomes crucial when we try to distinguish between configurations, it may not be paramount for other

properties such as phase boundaries. For *frozen* Pt (100), Wright et al. (1990) tabulate the E_1 to be –299, –263, and –64 meV for Pt, Pd, and Ni adatoms; E_2 to be +59, +4, and +97 meV, respectively, for the three kinds of adatoms; and E_{RT} to be –76, –12, and –40 meV, respectively. Thus, the sign of the interaction does not depend on the kind of adatom. The small E_1 attraction and large E_2 repulsion for Ni are important factors in its preference for the chain configuration, in addition to the large relaxation difference between the two configurations.

For weaker adsorbates than transition metals, the substrate relaxations should be less dramatic or important. For example, for H on Ni(111), discussed above, Einstein et al. (1990) found a negligible contribution from substrate relaxations: Ni atoms moved by roughly 0.01 Å or less, and contributed 1/2 meV per adatom in a test calculation. Furthermore, when the adatoms are in the intermediate (and certainly in the asymptotic range), there should be little "cluster" shape dependence on the lateral energies or on the off-diagonal Green's function G_{on}. On the other hand, presumably the local coupling parameter would need to be recalibrated to take such effects into account, unless it were obtained semi-empirical from fits to adsorption energies of low-density clusters. More generally, for stronger adsorbates one must worry seriously about this problem, as discussed at the end of § 11.2.5.

11.3.6. Scattered-wave theory

Feibelman (1989a) notes that scattering-theory methods are designed to take advantage of the rapid screening by metallic-substrate electrons of the potential associated with defects, specifically adatoms. Because of the screening, the wavefunctions related to the adatoms can be described as solutions to a scattering problem involving incident and scattered Bloch waves of the clean surface. If N basis orbitals are needed to describe the spatial region where the potential is unscreened, then one must numerically solve $N \times N$ sets of linear equations. This focus on orbitals in the adsorption region has philosophical similarities to the tight-binding picture explored at the outset: one isolates the changes due to adsorption from the otherwise perfect, semi-infinite substrate. However, here both the background substrate and the adsorption area are described with far greater sophistication, without recourse to simple model parameters. To date, though, only pairs of adatoms in the near region have been investigated, and there is no attempt to focus on G_{on}, i.e. a propagator between the adsorption sites. Both adatoms are part of the same cluster, and the heritage is from cluster methods. Here, though, the adsorbate region is not so much a cluster to be embedded into an indented substrate but a scattering zone that perturbs the substrate Bloch states.

Specifically, this approach builds on the local-density-approximation (LDA) description of surface electronic structure (Lundqvist and March 1983), solving the Kohn-Sham (1965) energy-minimization problem, and uses state-of-the-art expressions for exchange-correlation potentials and (norm-conserving) pseudopotentials. The equations are solved self-consistently: from a guessed scattering potential, the electronic density is obtained from Dyson's equation, and an iteration–relaxation scheme (Johnson, 1988) is invoked.

Feibelman (1987a,b, 1988a,b, 1989a, 1990) applied this self-consistent, matrix Green's-function (MGF) scattering theory (Williams et al., 1982; Feibelman, 1987a) extensively to adsorption on Al (001). Most of these papers involved single adatoms, but Feibelman (1987b, 1988a,b) discusses Al–Al, Al–S, and Al–Te dimers. For Al dimers, Feibelman (1987b) finds that because of the direct bond between the adatoms, their bonds to the substrate weaken, consistent with Pauling's (1960) bond-order–bond-length correlation, and so they sit farther (by 0.16 Å) from the substrate than a single Al. (The most dramatic consequence is that the diffusion barrier for dimers is lower than for monomers!) From naive counting of bonds, the strength of which are deduced from the bulk coherence energy, one might guess that $E_1 \approx -0.556$ eV. From the EAM work cited earlier, and more directly from our summary of Nørskov's (1993) discussion of cohesive energy vs. coordination number, we would already guess this estimate to be much too high. Careful calculation shows the interaction to be just –0.07 eV. In addition to the vertical relaxation, this result includes lateral relaxation of each Al toward each other by 0.05 Å from the center site. If the separated Al adatoms are not allowed to relax back toward the substrate, their pair attraction would be –0.18 eV. Feibelman does not specify how much the attraction would decrease if the neighboring adatoms were fixed in the high-symmetry positions, with lateral relaxation forbidden. Note also that the relaxations are of the *adatoms* relative to their isolated-adsorption positions. There is no discussion of any distortion of the substrate neighbors on this fcc (100) surface, which we just saw plays a major role in the EAM study of Ni, Pd, and Pt on Pt(100). (However, since Feibelman (1990) later shows that Al diffuses by an exchange mechanism on Al(100), such distortions presumably do occur.) In later papers, perhaps to keep computations manageable, Feibelman (1988a, 1989a) fixes adatoms at their ideal "isolated" positions and just computes the force acting on each member of the dimer, in addition to the pair energy, to monitor the sort of corrections which would enter if the second-order relaxations were allowed. Recapping, Feibelman's (1987b, 1989a) key physical idea is that E_1 is small because, as pairs of Al adatoms are separated, the rupturing of their direct interaction is partially compensated by an increase in their bonding to the substrate. This viewpoint provides a fuller picture than the usually reliable insight (Desjonquères, 1980), cited in a footnote, that the (fractional) "disposition of adatoms toward lateral interaction" (i.e. $|E_{aa}/E_{as}|$, presumably) decreases as the strength of their bonds to the substrate increases.

Stumpf (1993) finds rather similar results for Al(111) using a different self-consistent total-energy calculation. His slab is 5 layers thick, with the top two (and adatoms) allowed to relax. He finds for Al dimers on hcp sites that $E_1 = -0.58$ eV, attractive again because of the low coordination of the separated adatoms; the Al adatoms again relaxed toward each other. Similarly, if one Al is replaced by Si, $E_1 = -0.56$ eV. Motivated by the discovery of Na-induced vacancy structures (Schmalz et al., 1991), and bearing on the preadsorption problem, he finds that there is an attraction (–0.21 eV) between an Al adsorbate and an Na in a surface vacancy. On the other hand, if the Na were in a step vacancy, there is a repulsion of 0.06 eV; this change is attributed to the stronger binding of the Na and especially the Al at the step, so that they are more stable in their isolated configuration.

Motivated by evidence of surface poisoning by chalcogens, Feibelman (1988) next considers the interaction of an Al adatom with an S or Te adatom, again at adjacent center sites on Al(001). The E_1 repulsions are 0.25 eV and 0.22 eV, respectively. From the force calculation, he finds that the pairs would relax outward as for Al dimers, but away from each other. (With such relaxations, the repulsions would decrease somewhat.) He shows that these interactions cannot come from hard-core or charge-transfer (dipolar) mechanisms and describes his numerical findings in terms of bond-order–bond-length ideas. Feibelman (1988, 1989a) focuses on the two substrate Al's to which both adatoms bind. The bond to each adatom weakens when the other adatom is adjacent. Feibelman asks how the electrons rehybridize to optimize their energy. The chalcogens, with valence two, can simply shift away and strengthen their bond with the two farther substrate atoms; the Al dimer, each with valence three, shift toward each other to form a direct bond, achieving an attraction rather than a repulsion. The situation is reminiscent of the simple argument sketched in the preceding section in Eq. (11.37), but the behavior of the Al dimer would require an extension to include the direct coupling. To distinguish these cases *a priori*, without the reliable numerical output, would be a formidable task. The simple chemical arguments are really compelling only when joined with solid numerical evidence, as Feibelman often remarks.

Feibelman (1991) reports the first application to dimer (viz. H–H and H–S) adsorption on a *transition*-metal substrate, Rh(001). The adatoms are placed in nearest-neighbor center sites, sharing two Rh neighbors, at the positions they would take if widely separated. Since the H atoms sit close to the surface (0.65 Å above the outer Rh plane), they are well screened and there is scant interaction between them. This result is consistent with the observation by Richter and Ho (1987) that the desorption energy of H from Rh(001) is independent of coverage up to 0.8 monolayers. In contrast, the S sits much farther out (at 1.47 Å) and so is less well screened. Consequently there is an H–S E_1 repulsion of 0.17 eV, consistent with the observation by Brand et al. (1988) that H on Rh(001) avoids regions where S has been preadsorbed.

To make progress on surface problems, improved scattering theories are being developed. Feibelman (1992) notes that the MGF approach requires that the number of equations N that must be solved simultaneously is larger than one would suspect solely from the size of the scattering length, because the kinetic-energy component of the adsorption coupling is not limited by screening but depends of the choice of basis. Accordingly, Scheffler et al.(1991) have developed an alternative scheme in which they include the full kinetic energy in the initial description of the electronic wavefunctions, but must consequently perform a taxing real-space integration. Feibelman (1992), in turn, has found a way to simplify the MGF method, eliminating much of the extra computation due to the kinetic-energy matrix.

It is now becoming possible to compute total energies using scattering theories to assess interactions. In the *bulk*, Dederichs et al. (1991) use a KKR approach to study vacancy-vacancy interactions at nearest neighbor, and in some cases next nearest neighbor, sites in Cu, Ni, Ag, and Pd. (Vacancy–vacancy interactions are essentially the same problem as adatom–adatom interactions, but with fewer parameters. Yaniv (1981) approached the problem using an approach identical to that

in ES. Feibelman (1989a) remarks that these are all examples of problems involving point defects.) The calculations are rather demanding, requiring, e.g., that they forgo the usual muffin tin description of charge density. This approach is being extended toward surface problems involving spin interactions (Dederichs et al., 1993). (Note that the indirect interaction between spin impurities via hyperfine coupling to the conduction electrons had earlier been considered: with an infinite-barrier jellium substrate, Gumbs and Glasser (1986) generalize the results of Lau and Kohn (1978). Zheng and Lin (1987) start from Kalkstein and Soven's (1971) tight-binding substrate, similar to § 11.2.2, and apply second-order perturbation theory.)

11.4. Implications of pair interactions

11.4.1. Ordered overlayers and their phase boundaries

As noted late in the introduction and discussed in more detail in Chapter 13, the lateral interactions we have been discussing can lead to the formation of ordered superlattices of adatoms. Such ordered structure can be measured readily by diffraction techniques, especially LEED, and much of a temperature vs. coverage phase diagram can be mapped out. There are typically problems at low temperatures due to slow equilibration and at high coverages due to breakdown of the lattice-gas approximation. Also it is not readily possible to measure the phase boundary between a pure phase and an adjacent island phase (e.g. a coexistence regime of the pure phase and the (1×1) gas phase). It is generally very difficult to deduce *uniquely* lateral interactions by fitting to phase diagrams. The typical approach is to choose the minimum number of interactions necessary to produce the correct topography of the phase diagram, and then to adjust their sizes to mimic optimally the available boundaries; such boundaries can be computed accurately using Metropolis (equilibrium) Monte Carlo methods (Roelofs, 1980, 1982, 1995; Binder and Landau, 1989) or transfer-matrix finite-size scaling (Kogut, 1979; Kinzel and Schick, 1981; Rikvold et al., 1984; Bartelt et al., 1986; Roelofs et al., 1986; Rikvold et al., 1988; Roelofs and Bellon, 1989; Nightingale, 1990; Myshlyavtsev and Zhdanov, 1993). Other methods, particularly mean field, but also quasi-chemical and cluster-variation, are ill suited for two-dimensional computations, for which fluctuations play a far greater role than in three-dimensional systems.

In fitting a phase diagram, it is important to consider the entire range of coverages, not just the saturation coverage of the ordered structure. This point was illustrated for Ni(111)–H near the end of § 11.3.2 and for Pd(100)–H in § 11.3.3. In the simple case of a $c(2\times2)$ one can get some idea of the effect of additional interactions from the case study of Ag(100)–Cl by Hwang et al. (1988). In an earlier paper Taylor et al. (1985) found that the phase diagram of this system is rather well approximated by the hard-square model: a square lattice gas with nearest-neighbor exclusion ($E_1 = +\infty$). However, the critical coverage for ordering at 300 K was measured (by LEED) as 0.394 ± 0.007 ML, higher than the 0.368 ML of the simple hard-square model. They concluded that a second-neighbor repulsion E_2 in the range 20–26 meV could account for the experimental result. Hwang et al. (1988)

found that this critical coverage θ_c did not change even if the sample temperature was increased to as much as 600 K. With only E_2 (and infinite E_1) there should be substantial variation in θ_c. The simplest explanation was an additional small E_3 repulsion. A plot of possible values of E_2 and E_3 was produced: if $0.387 \leq \theta_c \leq 0.401$ ML, then $E_3 \approx 4$ meV if $E_2 \approx 20$ meV, and $E_3 \approx 3.5$ meV if $E_2 \approx 24$ meV. If $0.386 \leq \theta_c \leq -0.401$ ML, the range of possible interactions more than doubles for both E_2 and E_3.

Near the other limit of complexity are studies of ordering of multiple phases on close-packed surfaces, with adsorption in both kinds of center sites. Such models invoking up to 5 pair interactions, are applied to Ni(111)–O (Roelofs 1982), Ru(0001)–O (Piercy et al., 1992), Ru(0001)–H (Sandhoff et al., 1993), and Ru(0001)–S (Sandhoff, 1994). In the latter cases, trio energies are also included (3 distinct ones for Ru–O!). Nonetheless, the fit of Ru–S is not fully satisfactory in that (1) the disordering temperature of the $(\sqrt{3}\times\sqrt{3})$ was comparable to that of the $c(2\times4)$, rather than nearly twice as high, the experimental result (Sokolowski and Pfnür, 1995); (2) no hint of the observed complex defect structure on the high-cover side of the $(\sqrt{3}\times\sqrt{3})$ is found.

For the problem of catalytic poisoning on Pt(111), Collins et al. (1989) apply transfer-matrix and Monte Carlo techniques to a two-species (H and S) lattice gas model. They use successively more sophisticated models and are able to account for the dependence of the H coverage on S coverage for several temperatures.

The role of trio interactions is included in a review of them not long ago by Einstein (1991); see also Roelofs (Chapter 13). The presence of such an interaction in a lattice gas Hamiltonian will break up-down symmetry in the associated Ising model. Accordingly, it is widely expected that such interactions will *ipso facto* produce gross asymmetries in the phase diagram. For a single trio interaction, this expectation is often misguided. The crucial aspect is not whether there is an asymmetry in the ground state energy but rather whether there is an asymmetry in the (lowest) excitation energy from the ground state, which leads to disordering and so determines the phase boundary. If there are several distinct trio interactions, however, asymmetry in the phase boundary is usually unavoidable. A second key idea is that if one wishes to gauge the size of the trio interaction from a fit to the skewed phase boundary, it is important that one include all such interactions of comparable magnitude in the fit, or else one is likely to strongly overestimate the physical size of this multisite interaction. This problem is discussed in the context of W(110)–O by Einstein (1979b).

11.4.2. Local correlations and effects on chemical potential

Until recently, most experimental probes of ordering on surfaces provided only statistical averages of correlation functions, convoluted with some instrument response function. In diffraction measurements, one can measure (subject to deconvoluting this response function) the long-range order parameter below the transition and its fluctuations above it, or in a different limit, an ill-defined sum over short-range correlation functions (Bartelt et al., 1985). Vibrational probes similarly give information about long-range order parameter, but with a far shorter range instrument response. Only in the FIM experiments cited earlier is use made of a

sequence of real-space atomic-scale images. In those experiments, there are typically just two adatoms, so that it is not hard to find the degeneracy (or configurational entropy) of each possible energy state and so to work backwards to the interaction energies, as noted by Meyer (1992). For STM "snapshots" there are too many adatoms for analytic insertion of degeneracies and regression to interaction energies. Instead, one must tune estimated values of these energies until the configurations generated in Monte Carlo simulations adequately reproduce the STM images, as he illustrates for Cu(110)–O (Kuk et al., 1990); similarly, Schuster et al. (1991) estimate values for seven distinct lateral interactions for Cu(110)–K.

The full power of STM and FIM as quantitative probes of atomic positions is that they allow experimental observation of specific (not just combinations of) short-range correlation functions. Meyer (1992) was the first to publish a way to exploit this potentiality by measuring correlation functions at two (or more) different temperatures. As in most methods, one must still posit at the outset which interactions to include. Then, he shows how to extract directly from a large number of snapshots the interaction energy associated with a particular correlation; the error varies as $C^{-1/2}$, where C is the adlayer specific heat. He further discusses how best to choose the difference between the two temperatures: too close and there will not be enough difference; too far apart, and there will be inadequate relationship between the two correlation functions. Meyer (1993) subsequently proposes a way to extract the interaction energy directly from a set of STM "snapshots" without collateral Monte Carlo simulations: the presumed energy (in terms of a model Hamiltonian) is evaluated for each configuration and for other configurations created by moving each adatom in turn according to allowed kinetics. The interaction energies are obtained by best satisfying a steady-state criterion. Neither of these schemes have yet been applied to actual experimental data.

Adsorption or desorption data is another more indirect way to look at lateral interactions. For example, Urbakh and Brodskii (1984, 1985) apply their ATA expression for $\Delta\rho(\varepsilon)$ (cf. § 11.2.3.2) to data for the isosteric heat of adsorption (and the change in work function) for Pt(111)–H, achieving good agreement with experiments (Christmann et al., 1976; Norton et al., 1982). Braun et al. (1980) compute these quantities for a system in which charge transfer dominates the interaction, W–Cs, and find good agreement with experiment (Bol'shov et al., 1977), at least until the coverage at which metallization occurs. More generally, the adsorption/desorption rate depends intimately on the overlayer chemical potential μ, which in turn depends subtly on the interactions as the coverage varies. In considering the effect of lattice–gas repulsions on temperature-programmed desorption spectra, Payne et al. (1991) consider just this issue. Starting with the relation

$$q(\theta,T) = \frac{5}{2} k_B T + k_B T^2 \left.\frac{\partial \mu/k_B T}{\partial T}\right|_{\theta} \tag{11.40}$$

for the isosteric heat of adsorption q, they conclude that computations using transfer matrices do not show the anomalous behavior found in calculations using approximate techniques. In recent years Kevan's group has devoted considerable effort to trying to extract interaction energies from adsorption and desorption data, as reviewed by

Wei et al. (1994,1995). While some of this work uses the virial expansion or the quasi-chemical method, they, too, recognize transfer matrices as the method of choice. For example, they consider the desorption of CO, measured by time-resolved EELS (electron energy loss spectroscopy), from the three principal facets of Cu. On Cu(100) Wei et al. (1995) find a strong repulsive E_1, $E_2 = -2.8$ meV, and $E_3 = +1.1$ meV (or $E_2 = -1.3$ meV and $E_3 = -0.9$ meV in their first report (Wei et al., 1994): E_2 and E_3 are correlated, and both pairs give comparable fits; both energies are much below k_BT, impeding greater precision). On the other two faces E_1 is also strongly repulsive ($>> k_BT$); on (110) $E_2 = -10.3$ meV and $E_3 = +8.2$ meV, while on (111) $E_2 = +9.2$ meV, $E_4 = +13.4$ meV, but, surprisingly, $E_3 > 69$ meV. On Pt(111), the interactions between CO's (in atop sites) are purely repulsive, with E_1 again effectively an exclusion and non-monotonic decay since $E_2 < E_3$ (Skelton et al., 1994). In order to produce sensible strengths, they must also include E_4 ($< E_3$); they discuss consequent difficulties in extracting three interactions from fits to isotherms and the inability to do transfer matrix computations that include all the E_4 interactions.

Applying the random-phase approximation (RPA) in a tight-binding formalism to EELS, Brenig (1993) shows that for high-symmetry, low-mass-adsorbate overlayers the single-particle dispersion and the phonon dispersion decouple: one first determines the band structure of the excited vibrational states (assuming a localized, zero-bandwidth ground state) and then finds the vibrational frequencies using standard lattice dynamics. The scattering intensity is proportional to the resulting RPA susceptibility. As a corollary, he notes that when indirect couplings are strong, then translation invariance of the interadatom interactions is likely to be lost, causing the zone-center wave vector to vary with adsorbate concentration. Applying this formalism to EELS data (Voigtländer et al., 1989) of high-coverage (1.5 ML) H on Ni(110), he analyzes the two low-lying optical modes with in-plane polarization using up to third-neighbor force constants. He finds that the lateral interaction between H atoms at the three shortest separations differs strongly from the "bare" [direct] interaction and has a [local] maximum near the H–H second-neighbor separation (viz. the Ni nearest-neighbor spacing). While he can deduce much information about the interactions, e.g. evidence of multi-site interactions, he discusses the non-uniqueness of his fit and the consequences of various assumptions about the tight-binding-like force constants. Unfortunately (cf. first paragraph of § 11.3.5), the potential — assumed to be isotropic — is plotted as a continuous function of R.

Kang and Weinberg (1994) review the kinetic modeling of surface rate processes in terms of four levels of sophistication: (1) In the Langmuir picture of adsorption and desorption, adatoms are assumed to be randomly distributed. (2) Neglecting lateral interactions, one can approach precursor-mediated adsorption and desorption from kinetic and statistical perspectives. (3) Lateral interactions (typically just nearest neighbors) can be included in Langmuirian and precursor-mediated processes using a quasi-chemical approximation. (4) For reliable results, one must, as noted repeatedly above, turn to a more exact method, in this case Monte Carlo simulations rather than transfer matrices; the review describes several applications, mostly with the generic lateral interactions as arbitrary input parameters.

The effect of lateral interactions on diffusion has generated interest for quite

some time (Bowker and King, 1978). Excellent reviews of adsorbate diffusion by Naumovets and Vedula (1985) and by Gomer (1990) provide a wealth of information. The dependence of diffusion on these interactions also comes through the chemical potential; specifically, the ratio of the chemical diffusion coefficient D to the jump diffusion D_j is the "thermodynamic driving force" (Gomer, 1994) $\partial(\mu/kT)/\partial\theta|_T$, where D_j is a complicated average that is essentially a frequency factor times an Arrhenius factor and is generally similar to the tracer diffusion D^* of single adatoms. (Note that jump rates ought also to depend on lateral interactions, although this complication is typically neglected.) Using Monte Carlo simulations, Uebing and Gomer (1991) study the effects on the three diffusion constants of several generic sets of lateral interactions on a square lattice. Except for a case with $E_1 < 0$ and $E_2 > 0$, the fluctuation method and the Kubo–Green approach give similar results. Using the transfer-matrix technique to calculate μ, Myshlyavtsev and Zhdanov (1993) consider similar problems on a rectangular lattice with anisotropic interactions. Tringides and Gomer (1992) show that lateral interactions could produce anomalous behavior in diffusion constants measured by laser-induced diffusion compared with those from fluctuations around equilibrium, in contrast to their similar behavior in the absence of such interactions.

11.4.3. Surface states on vicinal and reconstructed fcc(110) surfaces

The same mechanisms which underlie the interaction between atoms chemisorbed on flat surfaces should also play a role in the interactions between steps on vicinal surfaces. For most semiconductors the interaction potential between steps, $U(l)$, is repulsive and decays as l^{-2}, where l denotes the distance between steps, as reviewed by Bartelt and Williams (Chapter 2). This form describes energetic interactions expected from both dipole–dipole (Voronkov, 1968) and elastic effects (Marchenko and Parshin, 1980). As noted in § 11.2.5, this result can be argued from a very general Green's function perspective (Rickman and Srolovitz, 1993). Poon et al. (1990) found such behavior in a study of steps on Si(100) using the Stillinger–Weber (1985) interatomic potential. Using EAM to study vicinal Au (100) and (110), Wolf and Jaszczak (1992) assess how well Marchenko and Parshin's expression for two interacting steps (or another expression (Srolovitz and Hirth, 1991) for a periodic array of steps, which differs by just a numerical factor of order one) accounts for the computed step–step repulsion. They find first that the amplitude G_{el} of the l^{-2} decay, which depends on Poisson's ratio, Young's modulus, and components of the linear force densities or stress factors, is nearly independent of l for large l. The G_{el}'s for steps on the two surfaces are 50% and 70% of the value deduced directly from the orientational dependence of the surface free energy. The discrepancy is attributed to: (1) the fact that the expression for G_{el} assumes isotropic continuum-elasticity theory, while the environment near the step is highly anisotropic; (2) the bulk elastic moduli in the formula should be replaced by local responses near the surface, which have not been computed; (3) the treatment should be based on a fully relaxed flat surface with unrelaxed steps, i.e., doing the calculation correctly would require Gordian unraveling reminiscent of the comments near the end of § 11.2.5. Extending EAM calculations to six of the late

transition/noble fcc metals, Najafabadi and Srolovitz (1994) also found l^{-2} repulsions for $l > 3a_0$; inclusion of a higher-order l^{-3} term improved the χ^2 of the fit by over an order of magnitude. Simple continuum elastic theory is thus deemed to fail at small l because it neglects the discrete atomistic nature of steps and surfaces and because the elastic field of a step cannot be adequately described by a surface force dipole alone. Detailed comparison shows that modeling steps as in-surface-plane dipole line forces in an isotropic elastic medium predicts elastic fields qualitatively different from those simulated. In both studies, it is important to remember that the EAM calculations are incapable, *ipso facto*, of including long-range electronic interactions since there is no Fermi-surface singularity.

Recently, microscopic probes of surface structure, particularly the scanning tunneling microscope (STM) and reflection electron microscope, have permitted detailed measurements of the configuration of steps on single crystal surfaces. Specifically, the terrace-width distribution function $P(l)$ provides a sensitive probe of step–step interactions. The simple l^{-2}potential describes inadequately the terrace-width distributions which Frohn et al. (1991) have measured on vicinal Cu(100) surfaces: Although $P(l)$ for Cu(1,1,7) has the shape expected for a simple repulsive potential, the width and asymmetry of $P(l)$ for Cu(1,1,19) suggests attractive interactions between steps. Similarly, Pai et al. (1994) have recently reported STM measurements of vicinal Ag(110) surfaces in which steps appear noninteracting for $\langle l \rangle = 22$ Å, repulsive for $\langle l \rangle = 30$ Å, and attractive for $\langle l \rangle = 40$ Å.

While attractive interactions may result from surface stress relaxation in the vicinity of steps (Jayaprakash et al., 1984) or from dipole–dipole interactions (Wolf and Villain, 1990) (if dominated by the in-plane orientation), the most likely explanation is an indirect interaction between steps mediated by substrate electron states which can produce attractions at some step separations (Frohn et al., 1991; Redfield and Zangwill, 1992). In terms of the formalism in § 11.2.2.2, we can imagine the relaxation of each atom along the step edge as producing a localized perturbation on the substrate analogous to the chemisorption bond. In this perspective, we view the l^{-2} repulsion as arising from a naive integration along one of the steps of an r^{-3} point–point repulsion, thereby approximating the steps as lines of independent points (Redfield and Zangwill, 1992), although the result is more general.

At small separations, the $\boldsymbol{r}$-dependence of indirect interactions is usually quite complicated; however, for the nearest-neighbor tight-binding model, the asymptotic regime for indirect interactions via *bulk* states is reached in ~4 lattice spacings (Einstein, 1978). In this asymptotic limit, we saw in § 11.2.6 (cf. Eq. (11.27)) that the indirect interaction reduces to $r^{-p}\cos(2k_F r)$, where k_F is the Fermi wavevector with velocity pointing in the $\hat{r}$ direction, $p = 5$ for mediation by bulk states near a surface, and we have assumed the phase factor ϕ is negligible. The integration along the step edge is complicated by the oscillatory factor.[1] Redfield and Zangwill (1992) point out that, given site–site interactions of the form $r^{-p}\cos(\kappa r)$, the interrow

1 Redfield and Zangwill (1992) point out that this summation procedure is strictly valid only in the (weak) limit, when the local perturbation due to each site is independent of its neighbors.

interaction has the form $r^{-m}\cos(\kappa r+\delta)$, with $m = p - 1/2$ and $\delta = \pi/4$.[1] For bulk electronic states, $p = 5$, so $m = 9/2$. As noted in § 11.2.6, when mediated by [2D-isotropic] surface states, Lau and Kohn (1978) showed that the interaction decays like r^{-2} leading similarly to $m = 3/2$.

To decide which case is appropriate for a particular substrate, one obviously must know something about the electronic structure of the surface. On the highly anisotropic (110) faces of noble metals, there apparently are surface states that are promising candidates to mediate interactions in the [001] direction. However, these states[2] exist only (in a gap) near $\bar{Y}$, (the intersection of the [001] direction and the surface Brillouin zone boundary), which would suggest $m = 2$ rather than $m = 3/2$. In Monte Carlo (MC) simulations relying on a terrace-step-kink (TSK) model of surface structure, Pai et al. (1994) use a rather *ad hoc* potential embodying these ideas: it contains an oscillatory term at $l > 6$ lattice spacings and a repulsive l^{-2}-like form at smaller step separations. While there is insufficient data to warrant confidence in the specific potential, it is nonetheless noteworthy that this potential, with reasonable parameters, can account for the distributions measured at three different $\langle l \rangle$.

In summary, vicinal Ag(110) provides the first evidence of an indirect interaction mediated by a surface state. It also illustrates that when such effects occur, the long-range interaction is by no means negligible.

We also note that Xu et al. (1996) are applying their method using a modified fourth moment approximation to tight binding, discussed in the latter part of § 11.3.5, to consider step interactions. They fit their results to the form of a monotonic inverse-square law repulsion plus an oscillatory term as discussed above, including ϕ, and obtain a remarkably consistent, if curious, set of results.

Very recently, Gumhalter and Brenig (1995) studied the screening properties of quasi-one-dimensional states, such as may arise in the troughs of reconstructed (110) fcc metals such as Ni and Cu (but not Ag) and considered how such states might mediate the indirect interaction between H atoms. They derive analytic

---

1 The essence of the derivation is taking the leading term of $\int_0^\infty (x^2+y^2)^{-p/2}\cos(\kappa\sqrt{x^2+y^2})\,dy$ to be $\int_0^x x^{-p}\cos(\kappa(x+y^2/2x))\,dx = x^{-(p-1/2)}f(\kappa x)$, where $f(\kappa,x)$ contains products of trigonometric functions and Fresnel integrals but has a simple asymptotic limit $\propto \cos\left(\kappa x+\frac{\pi}{4}\right)$.

2 One state has been observed often for (110) late-transition/noble fcc metals, about 2 eV above E_F (Bischler and Bertel, 1994). These states are probably too far from E_F to play an important role. However, Liu et al. (1984) calculated on Au(110) a second surface state just below E_F, over a narrower range near $\bar{Y}$, and there is some calculational evidence of a similar state on Ag (K.-M. Ho, private communication). Courths et al. (1984) reported such a state in an angle-resolved photoemission (ARUPS) study of Ag: it was found to be dispersionless at 0.1 eV below E_F and sharply peaked in intensity at $\bar{Y}$, seemingly vanishing by 20% of the distance to $\bar{\Gamma}$. While the effect of steps and disorder are unclear, it is plausible that this state could be broadened or shifted to cross E_F in some small region near $\bar{Y}$.

expressions for the consequent indirect interaction first from second-order perturbation theory (as in Lau and Kohn (1978)) and then with non-linear screening as in § 11.2.2, but with overlap included, both explicitly (Anderson and McMillan, 1967) and as a proportionality factor for the adatom-substrate eigenstate coupling (Gumhalter and Zlatić, 1980). The proportionality constant for the adatom–substrate coupling and the adatom energy ε_a are related by the Friedel sum rule (cf. § 11.2.4). The surface states in question run along the localized chain states in the close-packed troughs of (H-induced reconstructed) Ni and along the step edges of similar metals. When trying to parametrize the indirect interaction, the authors find that unless they assume a very slow decay corresponding to R^{-1} in Eq. (11.27), the coupling parameter is unreasonably large. However, the specific fit to the potential in Brenig (1993) (cf. § 11.4.2) is unconvincing since that potential is: (1) represented as isotropic (while the interaction is manifestly highly anisotropic); (2) interpolated from interactions at three separations, all less than two lattice constants (and so far from the asymptotic regime); and (3) indicative of the total lateral interaction, including the direct contribution (which is likely non-negligible at the shortest separation). They and Bischler and Bertel (1993) (also Bertel and Bischler (1994)) suggest that this chain state is similar to the state seen in inverse photoemission by the latter pair. However, this particular state $S_{\bar{X}}$ is 6 eV above the Fermi energy, so presumably completely empty and hence inactive. [1]

11.5. Discussion and conclusions

Two decades ago at a Nobel Symposium (Lundqvist and Lundqvist, 1973) papers were presented on both the Kondo problem and the pair interaction, both cloaked in the Anderson model. In the conference summary, Anderson quotes Harry Suhl as saying "Like South America, the Kondo problem will always have a great future." Not only are such statements no longer "politically correct", in the meantime the Kondo model was instrumental in the formulation of the renormalization group (Wilson, 1975) and was solved exactly by Bethe ansatz methods (Andrei et al., 1983); even the two-impurity problem has been solved (Jones et al., 1989; Affleck and Ludwig, 1992).

In contrast, consider what we have learned about the pair interaction. The only exact results relate to the asymptotic regime. Until recent evidence on vicinal Ag (110) of indirect interactions via surface states, these results proved of purely academic interest. There have also been exciting observations recently of standing

1 The main import of Bertel and Bischler's (1994) work is to show that a one-dimensional *sp*-derived state can exist on the surface. It is curious that the dispersion of the state is flat in the direction (in k-space) parallel to the chain (where one would expect considerable dispersion); Bertel (private communication) points out that this behavior arises because the state is antibonding in the top layer of Ni but bonding in the second layer (cf. the LCAO discussion in Bertel (1994)). Unfortunately, experimental complications have so far prevented measurements in the perpendicular direction (along which the dispersion should be flat if the states are in fact quasi-one-dimensional along the close-packed direction).

waves on surfaces (Crommie et al., 1993; Hasegawa and Avouris, 1993); there may be some relationship between them and the propagator which transmits the indirect interaction. The Anderson picture developed earlier at length does provide a convenient way to conceptualize the physics of the interaction. The earlier model work gives a general feeling for the relative size of the interactions associated with adatoms in various configurations. On the other hand, it has been difficult to improve the model or to achieve quantitative accounting of actual experiments, although there certainly have been several attempts in this direction (Sulston et al., 1986; Dai et al., 1987; Zhang et al., 1990; Cong, 1994; Sun et al., 1994). The model seems more limited in dealing with the adsorption of single adatoms than in the subsequent interactions between pairs. Perhaps if there were a compelling way to evaluate adjustable parameters for the single-adatom case, one might make progress in this direction.

Models leave out many important pieces of physics which are particularly important in the "near" regime. Local distortions, changes in bond strength with coordination, and rehybridization subtleties have been seen to play a vital role in this regime. With scattering theory methods, compelling results have been obtained in a few simple cases. At present, progress seems to be computationally limited. It seems that in the foreseeable future, advances will come from improvements in the code rather than more powerful computers. In this regime, which is certainly the most important from a practical or chemical perspective, it is not necessary or perhaps even fruitful to concentrate on the Green's function carrying the disturbance produced by one adatom to the site of the second. Once the adatoms separate sufficiently so that they neither couple directly nor interact strongly with the same substrate atoms, the perspective stressing the propagation of disturbances should be the most appropriate.

The pair interactions of remarkably few physical systems have been computed successfully. More strikingly, in many cases where two different methods have been applied, inconsistent results are found. The case of Pd(100)–H was discussed above. Consider now the case of Pt(111)–CO, not an ideal prototypical adsorbate from a theory viewpoint due to the two active orbitals of CO and the complicated adsorption mechanism. (It is also an intermediate case energetically, with a heat of adsorption of 1–1½ eV (Toyoshima and Somorjai, 1979) so neither in the perturbative regime nor in the strong-adsorption regime of, say, H, which has an adsorption bond strength 1–2 eV greater (Christmann, 1988) and forms bonding and antibonding states during adsorption (Einstein et al., 1980). Persson (1989) (also Persson et al. (1990)) assumes that pair interactions depend only on separation R. Explicitly, his pair interaction consists of a Pauli (hard-core) (contributing 262 meV to E_1 and negligible for larger R) and an indirect term which is also repulsive and decays (isotropically and rapidly) monotonically: (1.3 eV) $\exp[-(0.8\ \text{Å}^{-1})\cdot R]$. The two constants are chosen so that (1) the binding energy at half coverage is 0.25 eV less than that at zero coverage, and (2) the frequency of the frustrated translation at the atop site (preferred by 60 meV over bridge) increases from 49 to 60 cm^{-1}. With this model potential he performs (off-lattice) Monte Carlo simulations which apparently do well at accounting for the experimental phase diagram. Joyce et al.

(1987) present a strikingly different picture, but also achieve good agreement with different experimental data! They separate the interactions into direct, indirect, and site (atop vs. bridge, high-symmetry positions only) contributions. The direct part is formulated in terms of gas-phase Lennard–Jones potentials. The indirect part is assumed to come from sp electrons and expressed in terms of the asymptotic form, even at short range! They believe that the adatom–substrate coupling occurs via the $2\pi^*$ orbital (3 eV above ε_F) rather than the 5σ orbital (7 eV below). Their interaction is not purely repulsive, but oscillates in sign. Nonetheless, the results apparently fit desorption energies at four different fractional coverages ranging from 1/3 to 2/3. Wong and Hoffmann (1991) applied extended Hückel theory to CO on Ni, Pd, and Pt(111). Unfortunately, they only report results for two coverages (1/3 and 1/2), so it is unclear what the size and the sign of the pair interactions are. Very recently Jennison et al. (1995b), using a promising technique described below, found that the CO–CO interaction on Pt(111) is repulsive and decays monotonically (to at least 3 lattice spacings), similar to Persson's (1989) result. However, their admolecules are placed only on bridge (not atop) sites (favored by ~0.1 eV); while the decay is sensibly less rapid, their repulsions are somewhat too strong: $E_3 = 25$ meV vs. $E_3 = 16$ meV for Persson's experimentally-calibrated potential. Finally, both sets of interactions differ from the non-monotonic repulsive decay deduced by (Skelton et al., 1994) (cf. § 11.4.2).

Until pair interactions can be computed readily and reliably, our general picture and its evolution provide a useful template with which to confront indeterminate interactions needed to begin Monte Carlo simulations. We have a good idea of which configurations should have comparable size (Einstein, 1979b). We can use phase boundaries to estimate interactions. When subtleties exist (Bartelt et al., 1989), they may provide particularly valuable insight into the size of small interactions. In some cases semiempirical methods can help in gauging interactions, but these usually only give significant interactions in the near region and certainly fail by the asymptotic limit, since they lack Fermi surfaces; they are best for late-transition and noble metals. Generalized tight-binding models, including d-band degeneracy and correlation effects, have been useful for mid-transition metals. Very recently Cohen et al. (1994) proposed a general tight-binding total-energy scheme that improves on previous similar schemes by adjusting the arbitrary zero of energy to eliminate the need for pair potentials; like EAM, it is in a sense an elaborate interpolation scheme, since parameters are fit using first-principles calculations. It has many times as many fitting parameters as the fourth-moment approximation method discussed earlier (Xu and Adams, 1994). It has done better than EAM in accounting for surface energies of late-transition and noble metals. Perhaps it or a related method will allow calculation of far more accurate Green's functions and, ultimately, interaction energies.

As this chapter was in its final stage, Jennison et al. (1995) communicated noteworthy advances in computational capabilities. With a new Gaussian-based local-density-approximation code for massively parallel computers that uses Feibelman's LCAO method discussed in § 11.3.6, they can treat systems (large clusters, molecules) and elements (transition metals, oxygen) that pose difficulties

for plane-wave methods. With a three-layer 91-atom cluster of Pt, they reproduce well the details of ammonia adsorption on a seven-layer slab of Pt(111). The top layer is a hexagon 7 atoms across. Like the CO molecules mentioned above, pairs of ammonia repel each other at the close and intermediate separations that can be computed on this cluster, decaying roughly like R^{-3}; the magnitude is somewhat greater. Specifically, they find for a pair of NH_3's that $E_3 = 85$ meV, which is much greater than the "through-space" dipolar repulsion, which they calculate to be 15 meV for two isolated ammonias. Multisite terms are relatively small: by comparing a compact cluster of seven molecules to a hexagonal ring of six, they find the effective E_3 drops to 75 meV, suggesting an attractive trio energy (for the associated equilateral triangles) of −10 meV. For the coadsorption case of CO at bridge sites and NO at hcp sites, there is a weak attraction at the largest computable separations. For both CO–CO and CO–NO (but not NH_3–NH_3) the LDA is expected to overestimate the adsorption energies and so the interactions, consistent with the above-noted difference from Persson's results; gradient corrections (Becke, 1988; Perdew et al., 1992) are expected (Jennison et al., 1995a) to temper this overestimate.

All this work considers adatoms at or near stable sites in the holding potential. The effects of interactions on diffusion barriers, i.e. with one of the adatoms near a saddle point in the holding potential, has not yet been approached systematically. Typically some unconvincing assertion is made about this contribution, which in some cases may significantly affect the kinetics.

The generic problem we have considered has broad ramifications. There are obvious extensions to defect interactions. Many analogous features occur in adsorption in electrochemical cells (Rikvold and Wieckowski, 1992). A more novel related situation is the oscillating interaction of magnetic sandwiches of varying thickness (Herman and Schrieffer, 1992; Stiles, 1993). Hopefully synergistic progress, lacking to date, will permit results from one of these problems to impact on others.

In summary, there has been decent progress in understanding the general principles of lateral interactions but limited progress in achieving detailed quantitative understanding. Interest has been rekindled recently in looking for long-range effects mediated by surface or even quasi-one-dimensional states. After a decade's work, issues of correlations and self-consistency that seemed particularly troublesome earlier (Einstein, 1979a) can be dealt with, at least in simple systems in the near regime (Feibelman, 1989a). The major issue today is the role of local relaxations and hybridizing effects. In the *near* regime, we may well be on the verge of significant progress. In contrast, it seems that advances in treatment of the *intermediate* regime will require some imaginative way to incorporate the results of careful calculations of the clean-surface (for the propagator) and single-adatom (for the coupling) problems into a general framework that recognizes that the interaction will perturb the single-adatom solution weakly at most.

Acknowledgements

My work has been supported by NSF-MRG Grant DMR 91-03031. In the later stages I also benefitted from the hospitality of the IGV, Forschungszentrum Jülich

and the support of a Humboldt Foundation U.S. Senior Scientist Award. I have been truly fortunate to have had enlightening conversations with a large fraction of the authors, both theorists and experimentalists, cited in the references. I thank N.C. Bartelt and H. Pfnür for critical readings of drafts of the manuscript. J.B. Adams, L.W. Bruch, A.G. Eguiluz, M.C. Fallis, D.R. Jennison, S.D. Kevan, J.K. Nørskov, and B.N.J. Persson provided comments on specific passages. I am particularly indebted to J.R. Schrieffer for having proposed a thesis problem of such enduring interest.

References

Affleck, I. and A.W.W. Ludwig, 1992, Phys. Rev. Lett. **68**, 1046.
Allan, G., 1970, Ann. Phys. (Paris) **5**, 169, Bruneel, C. and G. Allan, 1973, Surface Sci. **39**, 385.
Allan, G., 1994, Surface Sci. **299/300**, 319.
Allan, G. and P. Lenglart, 1972, Surface Sci. **30**, 641.
Anderson, P.W., 1961, Phys. Rev. **124**, 41.
Anderson, P.W. and W.L. McMillan, 1967, Theory of Magnetism in Transition Metals, ed. W. Marshall. Proc. International School of Physics "Enrico Fermi", Course 37. Academic, New York), p. 50.
Andrei, N., K. Furuya and J. Lowenstein, 1983, Rev. Mod. Phys. **55**, 331.
Appelbaum, J.A. and D.R. Hamann, 1976, Rev. Mod. Phys. **48**, 479, and extensive references therein; 1976, CRC Crit. Rev. Solid State Sci. **6**, 359.
Axilrod, B.M. and E. Teller, 1943, J. Chem. Phys. **11**, 299.
Barbieri, A., D. Jentz, N. Materer, G. Held, J. Dunphy, D.F. Ogletree, P. Sautet, M. Salmeron, M.A. Van Hove and G.A. Somorjai, 1994, Surface Sci. **312**, 10.
Barker, J.A. and C.T. Rettner, 1992, J. Chem. Phys. **97**, 5844.
Baró, A.M. and W. Erley, 1981, Surface Sci. **112**, L759.
Bartelt, N.C., T.L. Einstein and L.D. Roelofs, 1983, J. Vac. Sci. Technol. A **1**, 1217.
Bartelt, N.C., T.L. Einstein and L.D. Roelofs, 1985, Surface Sci. **149**, L47; Phys. Rev. B **32**, 2993.
Bartelt, N.C., T.L. Einstein and L.D. Roelofs, 1986, Phys. Rev. B **34**, 1616.
Bartelt, N.C., L.D. Roelofs and T.L. Einstein, 1989, Surface Sci. **221**, L750.
Bassett, D.W., 1975, Surface Sci. **53**, 74.
Bauer, E., 1984, in: The Chemical Physics of Solid Surfaces and Heterogeneous Catalysis, Vol. 3: Chemisorption Systems, eds. D.A. King and D.P. Woodruff. Elsevier, Amsterdam, p. 1.
Becke, A.D., 1988, Phys. Rev. A **38**, 3098.
Behm, R.J., K. Christmann and G. Ertl, G. 1980, Surface Sci. **99**, 320.
Bertel, E., 1994, Phys. Rev. B **50**, 4925.
Bertel, E. and U. Bischler, 1994, Surface Sci. **307-9**, 947.
Binder, K. and D.P. Landau, 1981, Surface Sci. **108**, 503.
Binder, K. and D.P. Landau, 1989, in: Molecule Surface Interactions, ed. K.P. Lawley. Advances in Chemical Physics, 76. Wiley, New York, p. 91.
Birkhoff, G. and S. MacLane, 1965, A Brief Survey of Modern Algebra, 2nd edn. Macmillan, New York.
Bischler, U. and E. Bertel, 1993, Phys. Rev. Lett. **71**, 2296.
Bol'shov, L.A., A.P. Napartovich, A.G. Naumovets and A.G. Fedorus, 1977, Sov. Phys. Usp. **20**, 432 (Usp. Fiz. Nauk **122**, 125).
Bourdin, J.P., M.C. Desjonquères, D. Spanjaard and J. Friedel, 1985, Surface Sci. **157**, L345.
Bourdin, J.P., M.C. Desjonquères, J.P. Ganachaud and D. Spanjaard, 1987, Surface Sci. **179**, L77.
Bowker, M. and D.A. King, 1978, Surface Sci. **71**, 583; **72**, 208.

Brand, J.L., A.A. Deckert and S.M. George, 1988, Surface Sci. **194**, 457.
Braun, O.M., 1981, Sov. Phys. Solid State **23**, 1626 (Fiz. Tverd. Tela **23**, 2779).
Braun, O.M., L.G. Il'chenko and E.A. Pashitskii, 1980, Sov. Phys. Solid State **22**, 963 (Fiz. Tverd. Tela **22**, 1649).
Braun, O.M. and V.K. Medvedev, 1989, Sov. Phys. Usp. **32**, 328 (Usp. Fiz. Nauk **157**, 631).
Brenig, W., 1993, Surface Sci. **291**, 207.
Brodskii, A.M. and M.I. Urbakh, 1981, Surface Sci. **105**, 196.
Bruch, L.W., 1983, Surface Sci. **125**, 194.
Bruch, L.W. and J.M. Phillips, 1980, Surface Sci. **91**, 1.
Burch, R., 1980, Chemical Physics of Solid and Their Surfaces, Spec. Per. Rep. of Roy. Soc. Chem. **8**, 1.
Burdett, J.K. and T.F. Fässler, 1990, Inorg. Chem. **29**, 4595.
Burke, N., 1976, Surface Sci. **58**, 349.
Burke, N., Ph.D. dissertation, Cambridge University, cited by Gallagher and Haydock (1979).
Carlsson, A.E., 1991, Phys. Rev. B **44**, 6590.
Casanova, R. and T.T. Tsong, 1980, Phys. Rev. B **22**, 5590.
Casanova, R. and T.T. Tsong, 1982, Thin Sol. Films **93**, 41.
Chen, C.-L. and T.T. Tsong, 1991, in: The Structure of Surfaces III, eds. M.A. Van Hove, S.Y. Tong, K. Takayanagi and X. Xie.(Springer, Berlin, p. 312; 1991, J. Vac. Sci. Technol. B **9**, 312.
Ching, W.Y., D.L. Huber, M.G. Lagally and G.-C. Wang, 1978, Surface Sci. **77**, 550.
Christmann, K., 1988, Surface Sci. Rept. **9**, 1.
Christmann, K., G. Ertl and T. Pignet, 1976, Surface Sci. **54**, 365.
Christmann, K., R.J. Behm, G. Ertl, M.A. Van Hove and W.H. Weinberg, 1979, J. Chem. Phys. **70**, 4168.
Christmann, K., G. Ertl and T. Pignet, 1976, Surface Sci. **54**, 365.
Cohen, R.E., M.J. Mehl and D.A. Papaconstantopoulos, 1994, Phys. Rev. B **50**, 14694.
Collins, J. B., P. Sacramento, P.A. Rikvold and J.D. Gunton, 1989, Surface Sci. **221**, 277.
Cong, S., 1994, Surface Sci. **320**, 55.
Courths, R., H. Wern, U. Hau, B. Cord, V. Bachelier and S. Hüfner, 1984, J. Phys. F **14**, 1559.
Cowan, P.L. and T.T. Tsong, 1977, Surface Sci. **67**, 158..
Cremaschi, P.L. and J.L. Whitten, 1981, Surface Sci. **112**, 343.
Crommie, M.F., C.P. Lutz and D.M. Eigler, 1993, Nature (Letters) 363, 524.
Cunningham, S.L., L. Dobrzynski and A.A. Maradudin, 1973, Phys. Rev. B **7**, 4643; 1973, Vide (France) **28**, 171.
Dai, X.Q., W.C. Lu, M. Wang, T. Zhang, W.-K. Liu, 1987, Prog. Surface Sci. **25**, 307.
Davison, S.G. and M. Steslicka, 1992, Basic Theory of Surface States. Clarendon Press, Oxford.
Davydov, S. Yu., 1978, Sov. Phys. Solid State **20**, 1013 (Fiz. Tverd. Tela **20**, 1752).
Daw, M.S. 1989, Phys. Rev. B **39**, 7441.
Daw, M.S. and M.I. Baskes, 1984, Phys. Rev. B **29**, 6443.
Daw, M.S., S.M. Foiles and M.I. Baskes, 1993, Mater. Sci. Rep. **9**, 251.
Dederichs, P.H., T. Hoshino, B. Drittler, K. Abraham and R. Zeller, 1991, Physica B **172**, 203.
Dederichs, P.H., P. Lang, K. Willenborg, R. Zeller, N. Papanikolaou and N. Stefanou, 1993, Hyperfine Interactions **78**, 341.
Demuth, J.E. and T.N. Rhodin, 1974, Surface Sci. **45**, 249.
Desjonquères, M.C., 1980, J. Phys. (Paris) Colloq. **41**, C3-243.
Desjonquères, M.C., J.P. Jardin and D. Spanjaard, 1988, Surface Sci. **204**, 247.
Desjonquères, M.C. and D. Spanjaard, 1993, Concepts in Surface Physics. Springer, Berlin.
Dobrzynski, L. and A.A. Maradudin, 1976, Phys. Rev. B **14**, 2200.
Dreyssé, H., and R. Riedinger, 1983, Phys. Rev. B **28**, 5669.
Dreyssé, H., D. Tománek and K.H. Bennemann, 1986, Surface Sci. **173**, 538.
Ebina, K. and M. Kaburagi, 1991, Surface Sci. **242**, 124.

Economou, E.N., 1979, Green's Functions in Quantum Physics. Springer, Berlin, p. 80.
Eguiluz, A.G., D.A. Campbell, A..A. Maradudin and R.F. Wallis, 1984, Phys. Rev. B **30**, 5449.
Ehrenreich, H. and L.M. Schwartz, 1976, in: Solid State Physics, Vol. 31, eds. H. Ehrenreich, F. Seitz and D. Turnbull. Academic, New York, p. 149.
Ehrlich, G. and F. Watanabe, 1991, Langmuir **7**, 2555.
Einstein, T.L., 1973, Ph.D. dissertation, University of Pennsylvania, unpublished.
Einstein, T.L., 1975, Phys. Rev. B **12**, 1262. The referee forced a considerable reduction of the critique from the original manuscript, which is available on request.
Einstein, T.L., 1977, Phys. Rev. B **16**, 3411.
Einstein, T.L., 1978, Surface Sci. **75**, L161.
Einstein, T.L., 1979a, in: Chemistry and Physics of Solid Surfaces II, ed. R. Vanselow. CRC Press, Boca Raton, FL, p 261.
Einstein, T.L., 1979b, Surface Sci. **84**, L497.
Einstein, T.L. and J.R. Schrieffer, 1973, Phys. Rev. B **7**, 3629.
Einstein, T.L., M.S. Daw and S.M. Foiles, 1990, Surface Sci. **227**, 114.
Einstein, T.L., J.A. Hertz and J.R. Schrieffer, 1980, in: Theory of Chemisorption, ed. J.R. Smith. Springer, Berlin, p. 183.
Einstein, T.L., 1991, Langmuir **7**, 2520.
Ercolessi, F., E. Tosatti and M. Parrinello, 1986, Phys.Rev. Lett. **57**, 719; Surface Sci. **177**, 314.
Ercolessi, F., M. Parrinello and E. Tosatti, 1988, Philos. Mag. A**58**, 213.
Fallis, M.C., M.S. Daw and C.Y. Fong, 1995, Phys. Rev. B **51**, 7817.
Feibelman, P.J., 1987a, Phys. Rev. B **35**, 2626.
Feibelman, P.J., 1987b, Phys. Rev. Lett. **58**, 2766.
Feibelman, P.J., 1988a, Phys. Rev. B **38**, 12133.
Feibelman, P.J., 1988b, Mat. Res. Soc. Symp. Proc. **111**, 71.
Feibelman, P.J., 1989a, Annu. Rev. Phys. Chem. **40**, 261.
Feibelman, P.J., 1989b, Phys. Rev. Lett. **63**, 2488.
Feibelman, P.J., 1990, Phys. Rev. Lett. **65**, 729.
Feibelman, P.J., 1992, Phys. Rev. B **46**, 15416.
Feibelman, P.J. and D. Hamann, 1984, Phys. Rev. Lett. **52**, 61.
Felter, T.E., S.M. Foiles, M.S. Daw and R.H. Stulen, 1986, Surface Sci. **171**, L379; Daw, M.S. and S.M. Foiles, 1987, Phys. Rev. B **35**, 2128
Fink, H.-W. and G. Ehrlich, 1984a, Phys. Rev. Lett. **52**, 1532.
Fink, H.-W. and G. Ehrlich, 1984b, J. Chem. Phys. **81**, 4657.
Finnis, M.W. and J.E. Sinclair, 1984, Phil. Mag. A **56**, 45.
Flores, F., N.H. March and I.D. Moore, 1977a, Surface Sci. **69**, 133.
Flores, F., N.H. March, Y. Ohmura and A.M. Stoneham, 1979, J. Phys. Chem. Solids **40**, 531.
Flores, F., N.H. March and C.J. Wright, 1977b, Phys. Lett. **64A**, 231.
Foiles, S.M., 1985, Phys. Rev. B **32**, 3409.
Foiles, S.M., 1987, Surface Sci. **191**, 329.
Foiles, S.M., 1987, Surface Sci. **191**, L779.
Foiles, S.M. and M.S. Daw, 1985, J. Vac. Sci. Technol. A **3**, 1565.
Foiles, S.M., M.I. Baskes and M.S. Daw, 1986, Phys. Rev. B **33**, 7983.
Freeman, D.L., 1975, J. Chem. Phys. **62**, 4300.
Friedel, J., 1958, Nuovo Cimento Supplemento **7**, 287
Frohn, J., M. Giesen, M. Poensgen, J.F. Wolf and H. Ibach, 1991, Phys. Rev. Lett. **67**, 3543.
Gallagher, J. and R. Haydock, 1979, Surface Sci. **83**, 117.
Gavrilenko, G.M., R. Cardenas and V.K. Fedyanin, 1989, Surface Sci. **217**, 468.
Giesen-Seibert, M., R. Jentjens, M. Poensgen and H. Ibach, 1993, Phys. Rev. Lett. **71**, 3521.

Girard, C. and C. Girardet, 1988, Surface Sci. **195**, 173.
Gollisch, H. 1986, Surface Sci. **175**, 249; **166**, 87.
Gomer, R., 1990, Rep. Prog. Phys. **53**, 917.
Gomer, R., 1994, Surface Sci. **299/300**, 129.
Gordon, R.G. and Y.S. Kim, 1972, J. Chem. Phys. **56**, 3122.
Gottfried, K., 1966, Quantum Mechanics. Vol. 1: Fundamentals. Benjamin, New York. Section 49.2, p. 382, citing Baker, M., 1958, Ann. of Phys. **4**, 27.
Gottlieb, J.M. and L.W. Bruch, 1991, Phys. Rev. B **44**, 5759.
Grimley, T.B., 1967, Proc. Phys. Soc. (London) **90**, 751; **92**, 776.
Grimley, T.B., 1974, in: Dynamic Aspects of Surface Physics, ed. F.O. Goodman. Editrice Composition, Bologna.
Grimley, T.B., 1976, CRC Crit. Rev. in Solid State Sci. **6**, 239.
Grimley, T.B. and C. Pisani, 1974, J. Phys. C. (Solid State Phys.) **7**, 2831.
Grimley, T.B. and M. Torrini, 1973, J. Phys. C **6**, 868.
Grimley, T.B. and S.M. Walker, 1969, Surface Sci. **14**, 395.
Gumhalter, B. and V. Zlatić, 1980, J. Phys. C **13**, 1679.
Gumhalter, B. and W. Brenig, 1995, a) Prog. Surface Sci. **48**, 39; b) Surface Sci. **336**, 326.
Güntherodt, H.-J. and R. Wiesendanger, eds., 1992, Scanning Tunneling Microscopy I. Springer, Berlin.
Gumbs, G. and M.L. Glasser, 1986, Phys. Rev. B **33**, 6739.
Haftel, M.I., 1993, Phys. Rev. B **48**, 2611.
Hasegawa, Y. and Ph. Avouris, 1993, Phys. Rev. Lett. **71**, 1071.
Herman, F. and R. Schrieffer, 1992, Phys. Rev. B **46**, 5806.
Hirschfelder, J.O., C.F. Curtiss and R.B. Bird, 1954, Molecular Theory of Gases and Liquids. Wiley, New York.
Hjelmberg, H., 1978, Phys. Scripta **18**, 481.
Hoffmann, R., 1963, J. Chem. Phys. **39**, 1397; **40**, 2474; **40**, 2480.
Hoffmann, R., 1988, Solids and Surfaces: a Chemist's View of Extended Bonding. VCH Publishers, New York, esp. pp. 65–68.
Holloway, P.H. and J.B. Hudson, 1974, Surface Sci. **43**, 123.
Hwang, R.Q., E.D. Williams, N.C. Bartelt and R.L. Park, 1988, Phys. Rev. B **37**, 5870.
Imbihl, R., R.J. Behm, K. Christman, G. Ertl and T. Matsushima, 1982, Surface Sci. **117**, 257.
Jayaprakash, C., C. Rottman and W.F. Saam, 1984, Phys. Rev. B **30**, 6549.
Jennison, D.R., E.B. Stechel, A.R. Burns and Y.S. Li, 1995a, Nucl. Inst. Meth. Phys. Res. B **101**, 22.
Jennison, D.R., P.A. Schultz and M.P. Sears, 1995b, Proc. 55th Annual Conference on Physical Electronics. Flagstaff, AZ. (unpublished), private communication and to be published.
Johansson, P.K. 1979, Solid State Commun. **31**, 591.
Johansson, P.K. and H. Hjelmberg, 1979, Surface Sci. **80**, 171.
Johnson, D.D., 1988, Phys. Rev. B **38**, 12807.
Jones, B.A., B.G. Kotliar and A.J. Millis, 1989, Phys. Rev. B **39**, 3415.
Joyce, K., A. Martin-Rodero, F. Flores, P.J. Grout and N.H. March, 1987, J. Phys. C **20**, 3381.
Jürgens, D., G. Held and H. Pfnür, 1994, Surface Sci. **303**, 77.
Kaburagi, M., 1978, J. Phys. Soc. Jpn. **44**, 54; **44**, 394.
Kaburagi, M. and J. Kanamori, 1974, Jpn. J. Appl. Phys. Suppl. **2**, P2, 145; 1978, J. Phys. Soc. Jpn. **44**, 718.
Kalkstein, D. and P. Soven, 1971, Surface Sci. **26**, 85.
Kang, H.C. and W.H. Weinberg, 1994, Surface Sci. **299/300**, 755.
Kappus, W., 1978, Z. Phys. B **29**, 239.
Kappus, W., 1980, Z. Phys. B **38**, 263.
Kappus, W., 1981, Z. Phys. B **45**, 113.
Khare, S.V. and T.L. Einstein, 1994, Surface Sci. **314**, L857.

Kinzel, W.and M. Schick, 1981, Phys. Rev. B **24**, 324.
Kinzel, W., W. Selke and K. Binder, 1982, Surface Sci. **121**, 13.
Klein, J.R., L.W. Bruch and M.W. Cole, 1986, Surface Sci. **173**, 555.
Kogut, J.B., 1979, Rev. Mod. Phys. **51**, 659.
Kohn, W. and K.H. Lau, 1976, Sol. State Commun. **18**, 553.
Kohn, W. and L.J. Sham, 1965, Phys. Rev. A **140**, 1133.
Korringa, J., 1958, J. Phys. Chem. Solids **7**, 252.
Koster, G.F., 1954, Phys. Rev. **95**, 1436.
Koutecký, J., 1958,. Trans. Faraday Soc. **54**, 1038.
Kuk, Y., F.M. Chua, P.J. Silverman and J.A. Meyer, 1990, Phys. Rev. B **41**, 12 393.
Lang, N.D. and A.R. Williams, 1975, Phys. Rev. Lett. **34**, 531.
Lau, K.H., 1978, Sol. State Commun. **28**, 757.
Lau, K.H. and W. Kohn, 1977, Surface Sci. **65**, 607.
Lau, K.H. and W. Kohn, 1978, Surface Sci. **75**, 69.
Le Bossé, J.C., J. Lopez and J. Rousseau-Violet, 1978, Surface Sci. **72**, 125.
Le Bossé, J.C., J. Lopez and J. Rousseau-Violet, 1979, Surface Sci. **81**, L329.
Leynaud, M. and G. Allan, 1975, Surface Sci. **53**, 359,
Liebsch, A., 1978, Phys. Rev. B **17**, 1653.
Lighthill, M.J., 1958, Introduction to Fourier Analysis and Generalized Functions. Cambridge University Press, Cambridge, p. 7.
Liu, S.H., C. Hinnen, C.N. van Huong, N.R. de Tacconi and K.-M. Ho, 1984, J. Electroanal. Chem. **176**, 325.
Liu, W.-K. and S.G. Davison, 1988, Theor. Chim. **74**, 251.
Lopez, J. and G. Allan, 1981, Surface Sci. 103, 456.
Löwdin, P.O., 1950, J. Chem. Phys. **18**, 365.
Lundqvist, B. and S. Lundqvist, 1973, Collective Properties of Physical Systems, Proc. 24th Nobel Symposium. Academic, New York.
Lundqvist, S. and N.H. March, eds., 1983, The Theory of the Inhomogeneous Electron Gas. Plenum, New York.
McLachlan, A.D., 1964, Mol. Phys. **7**, 381.
MacLaren, J.M., D.D. Vvedensky, J.B. Pendry and R.W. Joyner, 1987, J. Chem. Soc., Faraday Trans. I **83**, 1945.
MacRury, T. B. and B. Linder, 1971, J. Chem. Phys. **54**, 2056.
Madhavan, P. and J.L. Whitten, 1982, J. Chem. Phys. **77**, 2673.
Mahanty, J. and N.H. March, 1976, J.Phys. C **9**, 2905.
Maradudin, A.A. and R.F. Wallis, 1980, Surface Sci. **91**, 423.
March, N.H., 1987, Prog. Surface Sci. **25**, 229.
March, N.H., 1990, in: Interaction of Atoms and Molecules with Solid Surfaces, eds. V. Bortolani, N.H. March and M.P. Tosi. Plenum, New York, p. 1.
Marchenko, V.I. and A.Ya. Parshin, 1980, JETP Lett. **52**, 129; Zh. Eksp. Teor. Fiz. **79**, 257 (Sov. Phys. JETP **52** (1981) 129).
Meyer, J.A., 1992, Phys. Rev. Lett. **69**, 784.
Meyer, J.A., 1993, Surface Sci. **284**, L416.
Moore, I.D., 1976, J. Phys. F **6**, L71.
Moritz, W., R. Imbihl, R.J. Behm, G. Ertl and T. Matsushima, 1985, J. Chem. Phys. **83**, 1959.
Moruzzi, V.L., J.L. Janak and A.R. Williams, 1978, Calculated Electronic Properties of Metals. Pergamon, New York.
Müller, J.E., 1990, Phys. Rev. Lett. **65**, 3021.
Müller, K., G. Besold and K. Heinz, 1989, in: Physics and Chemistry of Alkali Adsorption, eds. H.P. Bonzel, A.M. Bradshaw and G. Ertl. Elsevier, Amsterdam, p. 65.

Muscat, J.-P., 1984a, Surface Sci. **139**, 491.
Muscat, J.-P., 1984b, Surface Sci. **148**, 237.
Muscat, J.-P., 1985, Prog. Surface Sci. **18**, 59.
Muscat, J.-P., 1985, Surface Sci. **152/153**, 684.
Muscat, J.-P., 1985a, Prog. Surface Sci. **18**, 59.
Muscat, J.-P., 1986, Phys. Rev. B **33**, 8136.
Muscat, J.-P., 1987, Prog. Surface Sci. **25**, 211.
Muto, Y., 1943, Proc. Phys. Math. Soc. Jpn. **17**, 629.
Myshlyavtsev, A.V. and V.P. Zhdanov, 1993, Surface Sci. **291**, 145.
Najafabadi, R. and D.J Srolovitz, 1994, Surface Sci. **317**, 221.
Narusawa, T., W.M. Gibson and E. Törnqvist, Surface Sci. **114**, 331.
Naumovets, A.G. and Yu.S. Vedula, 1985, Surface Sci. Rept. **4**, 365.
Nightingale, M.P., 1990, in: Finite Size Scaling and Numerical Simulation of Statistical Systems, ed. V. Privman. World Scientific, Singapore, p. 287.
Nordlander, P. and S. Holmström, 1985, Surface Sci. **159**, 443.
Nørskov, J.K., 1977, Solid State Commun. **24**, 691.
Nørskov, J.K., 1982, Phys. Rev. B **26**, 2875.
Nørskov, J.K., 1993, in: The Chemical Physics of Solid Surfaces, vol. 6: Coadsorption, Promoters and Poisons, eds. D.A. King and D.P. Woodruff. Elsevier, Amsterdam, p. 1.
Nørskov, J.K., 1994, Surface Sci. **299/300**, 690.
Nørskov, J.K. and N.D. Lang, 1980, Phys. Rev. B **21**, 2131.
Nørskov, J.K., S. Holloway and N.D. Lang, 1984, Surface Sci. **137**, 65; 1985, ibid. **150**, 24.
Norton, P.R., J.A. Davies and T.E. Jackman, 1982, Surface Sci. **121**, 103.
Ogletree, D.F., R.Q. Hwang, D.M. Zeglinski, A. Lopez Vazquez-de-Parga, G.A. Somorjai and M. Salmeron, 1991, J. Vac. Sci. Technol. B **9**, 886.
Ohtani, H., C.-T. Kao, M.A. Van Hove and G.A. Somorjai, Prog. Surface Sci. **23**, 155.
Olès, A.M., M.C. Desjonquères, D. Spanjaard and G. Tréglia, 1988, J. Phys. (Paris) **49**, C8, 1637.
Pacchioni, G., P.S. Bagus and F. Parmigiani, eds., 1992, Cluster Models for Surface and Bulk Phenomena. Plenum, New York.
Pai, W.W., J.S. Ozcomert, N.C. Bartelt, T.L. Einstein and J.E. Reutt-Robey, 1994, Surface Sci. **307–309**, 747.
Pauling, L., 1960, The Nature of the Chemical Bond, 3rd edn. Cornell University Press, Ithaca, NY.
Payne, S.H., H.J. Kreuzer and L.D. Roelofs, 1991, Surface Sci. **259**, L781.
Perdew, J.P., J.A. Chevary, S.H. Vosko, K.A. Jackson, M.R. Pederson, D.J. Singh and C. Fiolhais, 1992, Phys. Rev. B **46**, 6671
Persson, B.N.J., 1989, Phys. Rev. B **40**, 7115.
Persson, B.N.J., M. Tüshaus and A.M. Bradshaw, 1990, J. Chem. Phys. **92**, 5034.
Persson, B.N.J., 1991, Surface Sci. **258**, 451 and references therein.
Persson, B.N.J., 1992, Surface Sci. Rept. **15**, 4.
Persson, B.N.J. and R. Ryberg, 1981, Phys. Rev. B **24**, 6954.
Piercy, P., K. De'Bell and H. Pfnür, 1992, Phys. Rev. B **45**, 1869.
Poon, T.W., S. Yip, P.S. Ho and F.F. Abraham, 1990, Phys. Rev. Lett. **65**, 2161.
Portz, K. and A.A. Maradudin, 1977, Phys. Rev. B **16**, 3535.
Raeker, T.J. and A.E. DePristo, 1989, Phys. Rev. B**39**, 9967; 1991, Int. Rev. Phys. Chem. **10**, 1 and references therein.
Redfield, A.C. and A. Zangwill, 1992, Phys. Rev. B**46**, 4289.
Richter, L.J. and W. Ho, 1987, J. Vac. Sci. Technol. A **5**, 453.
Rickman, J.M. and D.J. Srolovitz, 1993, Surface Sci. **284**, 211.
Rikvold, P. A. and A. Wieckowski, 1992, Physica Scripta **T44**, 71.

Rikvold, P.A., J.B. Collins, G.D. Hansen and J.D. Gunton, 1988, Surface Sci. **203**, 500.
Rikvold, P.A., K. Kaski, J.D. Gunton and M.C. Yalabik, 1984, Phys. Rev. B **29**, 6285.
Rodriguez, A.M., G. Bozzolo and J. Ferrante, 1993, Surface Sci. **289**, 100.
Roelofs, L.D., 1980, Ph.D. dissertation, U. of Maryland, unpublished.
Roelofs, L.D., 1982, in: Chemistry and Physics of Solid Surfaces IV, eds. R. Vanselow and R. Howe. Springer, Berlin, p. 219.
Roelofs, L.D., 1995, this volume, chap. 13.
Roelofs, L.D. and R.J. Bellon, 1989, Surface Sci. **223**, 585.
Roelofs, L.D. and E.I. Martir, 1991, in: The Structure of Surfaces III, eds. M.A. Van Hove, S.Y. Tong, K. Takayanagi and X. Xie. Springer, Berlin, p. 248.
Roelofs, L.D., T.L. Einstein, N.C. Bartelt and J.D. Shore, 1986, Surface Sci. **176**, 295.
Roelofs, L.D., S.M. Foiles, M.S. Daw and M.I. Baskes, 1990, Surface Sci. **234**, 63.
Rogowska, J.M. and J. Kolaczkiewicz, 1992, Acta Phys. Polonica A **81**, 101.
Rogowska, J.M. and K.F. Wojciechowski, 1989, Surface Sci. **213**, 422.
Rogowska, J.M. and K.F. Wojciechowski, 1990, Surface Sci. **231**, 110.
Rose, J.H., J.R. Smith, F. Guinea and J. Ferrante, 1984, Phys. Rev. B **29**, 2963 and references therein.
Ruderman, M.A. and C. Kittel, 1954, Phys. Rev. **96**, 99, Yosida, K., 1957, Phys. Rev. **106**, 893, VanVleck, J.H., 1962, Rev. Mod. Phys. **34**, 681.
Rudnick, J., 1972, Phys. Rev. B **5**, 2863.
Rudnick, J. and Stern, E.A., 1973, Phys. Rev. B **7**, 5062.
Sandhoff, M., 1994, Ph.D. dissertation, University of Hannover.
Sandhoff, M., H. Pfnür and H.-U. Everts, 1993, Surface Sci. **280**, 185.
Scheffler, M., 1979, Surface Sci. **81**, 562.
Scheffler, M., Ch. Droste, A. Fleszar, F. Máca, G. Wachutka and G. Barzel, 1991, Physica B **172**, 143.
Schmidtke, E., C. Schwennicke and H. Pfnür, 1994, Surface Sci. **312**, 301.
Schönhammer, K., 1975, Z. Physik B **21**, 389,
Schönhammer, K., V. Hartung and W. Brenig, 1975, Z. Phys. B **22**, 143.
Schrieffer, J.R. and P.A. Wolff, 1966, Phys. Rev. **149**, 491.
Schwennicke, C., D. Jürgens, G. Held and H. Pfnür, 1994, Surface Sci. **316**, 81.
Schwoebel, P.R., S.M. Foiles, C.M. Bisson and G.L. Kellogg, 1989, Phys. Rev. B **40**, 10639.
Selke, W., W. Kinzel and K. Binder, 1983, Surface Sci. **125**, 74.
Sinanoglu, 0. and K.S. Pitzer, 1960, J. Chem. Phys. **32**, 1279.
Schmalz, A., S. Aminpirooz, L. Becker, J. Haase, J. Neugebauer, M. Scheffler, D.R. Batchelor, D.L. Adams and E. Bøgh, 1991, Phys. Rev. Lett. **67**, 2163.
Schuster, R., J.V. Barth, G. Ertl and R.J. Behm, 1991, Phys. Rev. B **44**, 13 689.
Skelton, D.C., D.H. Wei and S.D. Kevan, 1994, Surface Sci. **320**, 77.
Sklarek, W., C. Schwennicke, D. Jürgens and H. Pfnür, 1995, Surface Sci. **330**, 11.
Sokolowski, M. and H. Pfnür, 1995, Phys. Rev. B **52**, 15742.
Smith, J.R., T. Perry, A. Banerjea, J. Ferrante and G. Bozzolo, 1991, Phys. Rev. B **44**, 6444.
Soven, P., 1966, Phys. Rev. **156**, 809.
Srolovitz, D.J. and J.P. Hirth, 1991, Surface Sci. **255**, 111.
Stauffer, L., R. Riedinger and H. Dreyssé, 1990, Surface Sci. **238**, 83.
Stiles, M.D., 1993, Phys. Rev. B **48**, 7238.
Stillinger, F. and T. Weber, 1985, Phys. Rev. B **31**, 5262.
Stoltze, P. and J. Nørskov, 1991, in: The Structure of Surfaces III, eds. M.A. Van Hove, S.Y. Tong, K. Takayanagi and X. Xie. Springer, Berlin, p. 19.
Stott, M. and E. Zaremba, 1980, Phys. Rev. B **22**, 1564.
Stoneham, A.M., 1977, Sol. State Commun. **24**, 425.
Stumpf, R., 1993, Ph.D. dissertation, Technical University of Berlin.

Stumpf, R. and M. Scheffler, 1994, Phys. Rev. Lett. **72**, 254; Comp. Phys. Commun. **79**, 447.
Sulston, K.W., S.G. Davison and W.K. Liu, 1986, Phys. Rev. B **33**, 2263.
Sun, Q., J. Xie and T. Zhang, 1994, Solid State Comm. **91**, 691.
Taylor, D.E., E.D. Williams, R.L. Park, N.C. Bartelt and T.L. Einstein, 1985, Phys. Rev. B **32**, 4653.
Theodorou, G., 1979, Surface Sci. **81**, 379.
Tiersten, S.C., T.L. Reinecke and S.C. Ying, 1989, Phys. Rev. B **39**, 12575.
Tiersten, S.C., T.L. Reinecke and S.C. Ying, 1991, Phys. Rev. B **43**, 12045.
Tománek, D., S.G. Louie and C.T. Chan, 1986, Phys. Rev. Lett. **57**, 2594.
Tosatti, E., 1976, in: Proc. 13th Int. Conf. Semiconductors, ed. F.G. Fumi. Marves-North-Holland, Rome, p. 21.
Tosatti, E. and F. Ercolessi, 1991, Mod. Phys. Lett. B **5**, 413.
Toyoshima, I. and G.A. Somorjai, 1979, Catal. Rev.-Sci. Eng. **19**, 105.
Tringides, M. and R. Gomer, 1992, Surface Sci. **265**, 283.
Truong, T.N. and D.G. Truhlar, 1990, J. Chem. Phys. **93**, 2125.
Truong, T.N., D.G. Truhlar and B.C. Garrett, 1989, J. Phys. Chem. **93**, 8227.
Tserbak, C., H.M. Polatoglou and G. Theodorou, 1992, Phys. Rev. B **45**, 4327.
Tsong, T.T., 1973, Phys. Rev. Lett. **31**, 1207; Phys. Rev. B. **7**, 4018..
Tsong, T.T., 1988, Rep. Prog. Phys. **51**, 759.
Tsong, T.T., 1988, Surface Sci. Rep. **8**, 127.
Tsong, T.T., P. Cowan and G. Kellog, 1975, Thin Sol. Films **25**, 97.
Ueba, H., 1980, Phys. Status Solidi(b) **99**, 763.
Uebing, C. and R. Gomer, 1991, J. Chem. Phys. **95**, 7626, 7636, 7641, 7648.
Urbakh, A.M. and M.I. Brodskii, 1984, Poverkhnost' **1**, 27.
Urbakh, A.M. and M.I. Brodskii, 1985, Russ. J. Phys. Chem. **59**, 671 (Zh. Fiz. Khim. **59**, 1152).
Van Hove, M.A., G. Ertl, K. Christmann, R.J. Behm and W.H. Weinberg, 1978, Sol. St. Commun. **28**, 373.
Van Hove, M.A., S.W. Wang, D.F. Ogletree and G.A. Somorjai, 1989, in: Advances in Quantum Chemistry, Vol. 20, ed. P.O. Löwdin. Academic, San Diego, p. 1.
Vidali, G. and M.W. Cole, 1980, Phys. Rev. B **22**, 4661; 1981, *ibid.* **23**, 5649 (E).
Vidali, G., G. Ihm, H.-Y. Kim and M.W. Cole, 1991, Surf. Sci. Rep. **12**, 133. Lifshitz, I.M., 1964, Usp. Fiz. Nauk 84, 617 [Sov. Phys. Usp. **7**, 549].
Voigtländer, B., S. Lehwald and H. Ibach, 1989, Surface Sci. **208**, 113.
Volokitin, A.I., 1979, Sov. Phys. Semicond. **13**, 960 (Fiz. Tekh. Poluprovodn. **13**, 1648).
Voronkov, V.V., 1968, Sov. Phys.-Crystallogr. **12**, 728.
Voter, A.F., 1987, in: Modeling of Optical Thin Films, ed. M.R. Jacobson, SPIE **821**, 214; Voter and Chen (1987) also fit data from dimers.
Voter, A.F. and S.P. Chen, 1987, Mater. Res. Soc. Symp. Proc. **82**, 175.
Vu Grimsby, D.T. Y.K. Wu and K.A.R. Mitchell, 1990, Surface Sci. **232**, 51.
Wang, G.-C., T.-M. Lu and M.G. Lagally, 1978, J. Chem. Phys. **69**, 479.
Watanabe, F. and G. Ehrlich, 1989, Phys. Rev. Lett. **62**, 1146.
Watanabe, F. and G. Ehrlich, 1991, J. Chem. Phys. **95**, 6075.
Watanabe, F. and G. Ehrlich, 1992, J. Chem. Phys. **96**, 3191.
Watson, P.R., 1987, J. Phys. Chem. Ref. Data **16**, 953.
Watson, P.R., 1990, J. Phys. Chem. Ref. Data **19**, 85.
Watson, P.R., 1992, J. Phys. Chem. Ref. Data **21**, 123.
Watson, P.R., M.A. Van Hove and K. Hermann, 1994, Atlas of Surface Structures, Vols. 1A, 1B (J. Phys. Chem. Ref. Data, Monograph 5, Am. Chem. Soc./Am. Inst. Phys., N.Y.)
Wei, D.H., D.C. Skelton and S.D. Kevan, 1994, J. Vac. Sci. Tech. A **12**, 2029.
Wei, D.H., D.C. Skelton and S.D. Kevan, 1995, Surface Sci. **326**, 167.
Whitten, J.L., 1993, Chem. Phys. **177**, 387.

Williams, A.R., P.J. Feibelman and N.D. Lang, 1982, Phys. Rev. B **26**, 5433.
Williams, E.D., S.L. Cunningham and W.H. Weinberg, 1978, J. Chem. Phys. **68**, 4688.
Wilson, K.G., 1975, Rev. Mod. Phys. **47**, 773.
Wimmer, E., H. Krakauer, M. Weinert and A.J. Freeman, 1981, Phys. Rev. B **24**, 864.
Wolf, D. and J.A. Jaszczak, 1992, Surface Sci. **277**, 301.
Wolf, D.E. and J. Villain, 1990, Phys. Rev. B **41**, 2434.
Wong, Y.-T. and R. Hoffmann, 1991, J. Phys. Chem. **95**, 859.
Wright, A.F., M.S. Daw and C.Y. Fong, 1990, Phys. Rev. B **42**, 9409.
Xu, W. and J.B. Adams, 1994, Surface Sci. **301**, 371.
Xu, W. and J.B. Adams, 1995, Surface Sci. **339**, 241.
Xu, W., J.B. Adams and T.L. Einstein, 1996, Phys. Rev. B. **54**, 2910.
Yaniv, A., 1981, Phys. Rev. B **24**, 7093 .
Zangwill, A., 1988, Physics at Surfaces. Cambridge University Press, Cambridge.
Zhang, T., M.C. Kang and W.C. Lu, 1990, Phys. Stat. Sol. (a) **120**, K41.
Zheng, H. and D.L. Lin, 1987, Phys. Rev. B **36**, 2204.

Wood notation 25
work function 115, 262, 365, 382, 442, 449, 462, 466, 470, 478, 633
work function change 114
work-function lowering 461
Wulff plots 69, 224
wurtzite 193, 202, 231, 239, 241, 246
wurtzite cleavage faces 262
wurtzite structure 220

X-ray diffraction 37
X-ray photoelectron diffraction *see* XPD
X-ray photoemission spectroscopy *see* XPS
X-ray diffraction 204, 453, 557, 729, 733, 742, 757, 758, 760
X-ray reflectivity 330, 342
X-ray resolution function 339
X-ray scattering 321, 358, 511, 543, 708, 755
X-rays, critical angle for 330
Xe 511, 516, 518, 520, 524, 525, 557, 566
XPD (X-ray photoelectron diffraction) 143
XPS (X-ray photoemission spectroscopy) 143, 448, 456, 457

XY model 750, 751, 753, 801
XY model with cubic anisotropy 747, 751, 758

$YBa_2Cu_3O_{7-x}$ 211
Young's modulus 94, 635

zero and one-phonon intensities 287
zero creep 56
zero force 113
zero-point energy 584
zigzag chains 440, 455, 481, 482
zigzag type displacement 118
zincblende 215, 220, 231, 239, 248, 256, 260
zincblende (110) cleavage faces 250
zincite 231
zirconia 212
ZnO 202, 203, 231, 249, 263
ZnS 249
ZnSe 249
ZnTe 249
ZrC 195, 213
ZrN 192, 218, 219
ZrO_2 212